FINAL REPORT:

Radiation Effects in MOS Devices

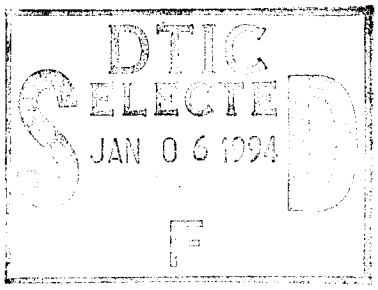

CONTRACT NUMBER: N00014-89-J-2022

CONTRACT PERIOD: June 1, 1989 - May 31, 1992

P.M. Lenahan

The Pennsylvania State University
University Park, Pennsylvania 16802

REPORT DOCUMENTATION PAGE

Form Approved
OMB No. 0704-0188

1. AGENCY USE ONLY *(Leave blank)*	2. REPORT DATE	3. REPORT TYPE AND DATES COVERED
	7/1/92	Technical

4. TITLE AND SUBTITLE
RADIATION EFFECTS IN MOS DEVICES

5. FUNDING NUMBERS
C - N00014-89-J-2022

6. AUTHOR(S)
P.M. Lenahan

7. PERFORMING ORGANIZATION NAME(S) AND ADDRESS(ES)
Pennsylvania State University
Department of Engineering Science & Mechanics
227 Hammond Building
University Park, PA 16802

8. PERFORMING ORGANIZATION REPORT NUMBER

9. SPONSORING/MONITORING AGENCY NAME(S) AND ADDRESS(ES)
Defense Nuclear Agency
6801 Telegraph Road
Alexandria, VA 22310-3398
RAEE/Cohn

10. SPONSORING/MONITORING AGENCY REPORT NUMBER

11. SUPPLEMENTARY NOTES

12a. DISTRIBUTION/AVAILABILITY STATEMENT

12b. DISTRIBUTION CODE

13. ABSTRACT *(Maximum 200 words)*

We have utilized electron spin resonance (ESR), including a new and much more sensitive ESR technique called spin dependent recombination (SDR), to study radiation damage in metal/oxide/silicon (MOS) field effect transistors (MOSFETS). Our study has led to a considerably greater understanding of the electronic properties of radiation induced interface state defect structure and the relationship of the atomic scale geometry of these defects to their electronic properties. We have also studied the role of atomic scale stress in the creation of E' centers in SiO_2. The E' center is the dominant deep hole trap in MOS oxides. In addition, we have used ESR to study the role of hydrogen in the MOS radiation damage process.

14. SUBJECT TERMS	15. NUMBER OF PAGES
Spin Dependent Recombination (SDR) Metal-Oxide-Semiconductor Field-Effect Transistors (MOSFET's)	16. PRICE CODE

17. SECURITY CLASSIFICATION OF REPORT	18. SECURITY CLASSIFICATION OF THIS PAGE	19. SECURITY CLASSIFICATION OF ABSTRACT	20. LIMITATION OF ABSTRACT
			SAR

CLASSIFIED BY

DECLASSIFY ON
N/A since Unclassified.

14. SUBJECT TERMS (Continued)

P_b Center
Electron Spin Resonance (ESR)

A-1

CONVERSION TABLE

Conversion factors for U.S. Customary to metric (SI) units of measurement

MULTIPLY TO GET	BY	TO GET DIVIDE
angstrom	1.000 000 X E -10	meters (m)
atmosphere (normal)	1.013 25 X E +2	kilo pascal (kPa)
bar	1.000 000 X E +2	kilo pascal (kPa)
barn	1.000 000 X E -28	meter^2 (m^2)
British thermal unit (thermochemical)	1.054 350 X E +3	joule (J)
calorie (thermochemical)	4.184 000	joule (J)
cal (thermochemical)/cm^2	4.184 000 X E -2	mega joule/m^2 (MJ/m^2)
curie	3.700 000 X E +1	*giga becquerel (GBq)
degree (angle)	1.745 329 X E -2	radian (rad)
degree Fahrenheit	$t_K = (t°f + 459.67)/1.8$	degree kelvin (K)
electron volt	1.602 19 X E -1^	joule (J)
erg	1.000 000 X E -7	joule (J)
erg/second	1.000 000 X E -7	watt (W)
foot	3.048 000 X E -1	meter (m)
foot-pound-force	1.355 818	joule (J)
gallon (U.S. liquid)	3.785 412 X E -3	meter^3 (m^3)
inch	2.540 000 X E -2	meter (m)
jerk	1.000 000 X E +9	joule (J)
joule/kilogram (J/kg) (radiation dose absorbed)	1.000 000	Gray (Gy)
kilotons	4.183	terajoules
kip (1000 lbf)	4.448 222 X E +3	newton (N)
kip/inch^2 (ksi)	6.894 757 X E +3	kilo pascal (kPa)
ktap	1.000 000 X E +2	newton-second/m^2 ($N-s/m^2$)
micron	1.000 000 X E -6	meter (m)
mil	2.540 000 X E -5	meter (m)
mile (international)	1.609 344 X E +3	meter (m)
ounce	2.834 952 X E -2	kilogram (kg)
pound-force (lbs avoirdupois)	4.448 222	newton (N)
pound-force inch	1.129 848 X E -1	newton-meter (N·m)
pound-force/inch	1.751 268 X E +2	newton/meter (N/m)
pound-force/foot^2	4.788 026 X E -2	kilo pascal (kPa)
pound-force/inch^2 (psi)	6.894 757	kilo pascal (kPa)
pound-mass (lbm avoirdupois)	4.535 924 X E -1	kilogram (kg)
pound-mass-foot^2 (moment of inertia)	4.214 011 X E -2	kilogram-meter^2 ($kg·m^2$)
pound-mass/foot^3	1.601 846 X E +1	kilogram/meter^3 (kg/m^3)
rad (radiation dose absorbed)	1.000 000 X E -2	**Gray (Gy)
roentgen	2.579 760 X E -4	coulomb/kilogram (C/kg)
shake	1.000 000 X E -8	second (s)
slug	1.459 390 X E +1	kilogram (kg)
torr (mm Hg, 0° C)	1.333 22 X E -1	kilo pascal (kPa)

*The becquerel (Bq) is the SI unit of radioactivity; 1 Bq = 1 event/s.
**The Gray (Gy) is the SI unit of absorbed radiation.

Table of Contents

Summary of Accomplishments

Introduction

Metal oxide silicon (MOS) field effect transistors (MOSFETs) are the fundamental building block of modern microelectronics technology. These devices are susceptible to damage from ionizing radiation and from the injection of hot carriers from the silicon substrate into the oxide. For several reasons, radiation and hot carrier damage are of substantial technological importance. MOS device technology in satellites utilized for defense applications, communications, weather forecasting etc. must be radiation hard. As the dimensions of ultra large scale integrated ULSI circuitry shrink to tenths of a micron, ionizing radiation plays an even more important role in device processing; hot carrier effects also become important in very small devices.

A fundamental understanding of radiation damage and the related hot carrier damage phenomena will permit device engineers and physicists to develop technology to mitigate the effects of ionizing radiation on MOSFETs. Our study has focused upon the development of a detailed atomic scale understanding of these phenomena. The study has utilized electron spin resonance (ESR) techniques in conjunction with a variety of irradiation sequences, charge injection techniques and electrical measurement on radiation and hot carrier damaged devices.

Organization Of This Report

This report has been organized into two segments, each with five parts. The opening summary of accomplishments segment briefly discusses progress which we have made in each of five subfields of investigation. The second segment of the report consists of our publications of the contract period organized in these subfields.

I. Spin Dependent Recombination

A. Bias Dependence of P_b Hyperfine Parameters

Our work on the bias dependence of P_b hyperfine parameters is discussed in M. A. Jupina and P. M. Lenahan "A^{29} Si Hyperfine Study of Radiation Induced P_b Centers at the Si/SiO_2 Interface," IEEE Trans. N.S. vol. 37, no. 6, p. 1650 (1990).

Our work has resulted in substantial progress in several areas. For some time, an area of controversy has involved the ESR observation that one kind of defect (P_b centers) [1-6] dominates radiation induced Si/SiO_2 interface state defects, but that rather different distributions of the density of states of this defect have been observed in electrical measurements. Several questions surround this controversy. How can one type of defect yield a variety of energy distributions? For that matter, how can one type of defect yield a very broad distribution of defect energy levels throughout the Si/SiO_2 band gap.

In the recent past one could answer these questions incompletely and in a manner which is not entirely satisfying. The standard ESR measurements are sufficiently precise to establish that most of the radiation induced interface states are due to P_b centers. However they have not been sufficiently precise to rule out the possibility of a relatively small fraction (~20%) of interface state defects with another structure. One could also argue that, in some way, the local environment of the P_b center affects the energy level of the defect. Since the Si/SiO_2 boundary is likely to exhibit a very high level of short range

disorder, this disorder might logically be taken to cause broadening of the P_b levels. Also, since the level of disorder might depend upon processing or the details of the irradiation process, one might attribute differences in the energy distributions of the interface states to differences in the disorder level at the interface. However, without any "atomic scale" data, however, these arguments are little more than idle speculation.

During this study we have been able to, at least in part, address these questions.

The SDR technique allows ESR measurements to be made on MOSFETs in integrated circuits. As such, it allows measurements to be made as a function of Si/SiO_2 surface potential. Due to SDR's sensitivity, it is possible to monitor the Si^{29} hyperfine spectra of the P_b centers as a function of surface potential. The Si^{29} hyperfine spectra allow measurement of the wave function of the P_b center's unpaired electron. We expect the unpaired electron to reside primarily on an sp hybridized orbital on the P_b central silicon atom. The hyperfine data allow us to calculate the percent s character and the percent p character of the electron wavefunction and also to calculate what percentage of the wavefunction is localized on the central silicon. These calculations are moderately precise, yielding numbers which are accurate to at least one significant figure but not quite two significant figures.

These wave function values may, at first glance, appear to be esoteric and irrelevant parameters. However, many years ago, Coulson [7] showed that the hyperfine results, the wavefunction hybridization numbers, could be used to calculate bonding angles. For the P_b centers, our measurements allow us to calculate the back bond angles of the centers for several values of surface potential. Our results show that the P_b center back bond angles vary by several degrees - P_b centers with energy levels in the lower part of the gap are "flattened" somewhat from a perfect tetrahedral geometry. P_b centers with levels in the middle and upper part of the gap have a more puckered geometry - a more nearly tetrahedral arrangement. (The results are summarized in figure 6 of the publication.)

The results show that we should not view the P_b centers in terms of a single distribution of energy levels but in terms of a distribution of energy levels which depends upon the local geometry - upon atomic scale stress.

B. Hot Carrier Damage in Short Channel MOSFETs

Our hot carrier damage SDR study is discussed in J. T. Krick, P. M. Lenahan, and G. J. Dunn, "Direct Observation Of Interfacial Point Defects Generated By Channel Hot Hole Injection In n-Channel Metal-oxide-Silicon Field Effect Transistors," Appl. Phys. Lett. vol. 59, p. 3437 (1991).

Another SDR investigation has involved hot carrier damage in short channel MOSFETs. Vulliame [8] and coworkers have argued that hot carrier damage at the Si/SiO_2 interface is not caused by the creation of P_b centers but by some other, possibly P_b like, centers. Since hot carrier damage takes place in a region only about $\approx 0.1\ \mu m$ wide near the drain of short channel MOSFETs, a conventional ESR study could not possibly address the validity of Vulliame's arguments. However the SDR systems we have constructed have sufficient sensitivity to detect Si/SiO_2 interface states in quite small samples. With SDR measurements we were able to clearly test the validity of Vulliame's arguments.

Working in collaboration with Greg Dunn of MIT Lincoln Labs and utilizing devices prepared by Brian Doyle of DEC, we hot carrier stressed short n-channel MOSFETs. The

MOSFETs had (100) silicon surface orientation. We found that the dominant interface state defect generated is the P_{bo} center. We earlier found that the P_{bo} center dominated radiation induced interface state defects in the (100) silicon surface system.[9] We argue that the P_{bo} defect may be the dominant generated interface state defect at (100) interfaces. Poindexter and coworkers consistently observe a second interface state defect, the P_{b1} center, in (100) Si/SiO_2 structures in which high interface state densities have been induced by high temperature processing.[10] The P_{bo} center is a silicon back bonded to three other silicons at the Si/SiO_2 interface. The structure of the P_{b1} is not yet established.

It is worth noting that the hot carrier experiment required unprecedented ESR/SDR sensitivity. We believe this work involves the most sensitive magnetic resonance experiment ever done in solids.

C. E' Center Hyperfine Parameters

In a third SDR investigation we have detected the ^{29}Si hyperfine lines of E' centers in irradiated MOSFETs. The signal to noise ratio in these observations is quite low, which severely limits our conclusions. However, two conclusions can be unequivocally drawn from the E' hyperfine results. (1) Two weak hyperfine lines appear with a separation of approximately 450 G. The combined intensity of these two lines is about ~ 5% of that of the center E' true which we observed in the same samples. The observation "proves" that the ESR/SDR signal is indeed due to a silicon back bonded to three oxygens in the oxide. (2) More importantly, the hyperfine line splitting is slightly greater (~ 10%) than that observed in ordinary bulk amorphous SiO_2. It is more nearly what is observed in "densified" amorphous SiO_2. The results show that the local environment of the E' centers near the Si/SiO_2 interface is not typical of ordinary amorphous SiO_2. The environment may be similar to that of "densified" SiO_2.

These, as yet unpublished, results are presented in Appendix A.

II. <u>Hydrogen's Role In Radiation Damage</u>

We have conducted several experiments to explore hydrogen's role in the radiation damage process. Many studies of the time temperature and electric field dependence of the radiation damage process have been interpreted in terms of radiation induced holes liberating a hydrogen specie in the oxide and the subsequent drift of that specie to the Si/SiO_2 interface. [11-13] At the interface, the hydrogen specie reacts to create silicon dangling bond centers.

A number of recent studies suggest that molecular hydrogen may somehow be involved in this process. [14-16] Several have proposed that hydrogen cracking events occur at hole trap sites, leading to the liberation of a hydrogen species, generally supposed to be a proton, and the subsequent field aided drift of the proton to the Si/SiO_2 interface. At the interface, the proton reacts to form P_b interface state defects.

We have conducted two studies to attempt to identify hydrogen's role in the damage process. One of the studies has lead in rather straightforward experimental results and conclusion. A second study lead to results which are more difficult for us to interpret.

A. Molecular Hydrogen and E' Centers

We have been able to generate extremely high (~ $10^{18}/cm^3$) densities of E' centers in separation by implanted oxygen (SIMOX) buried oxides by exposing the oxides to vacuum ultraviolet (VUV) light ($hc/\lambda \leq 10.2 eV$) from a 50 Watt deuterium lamp. We have generated essentially equal numbers of E' centers by exposing the oxides to approximately 210 Mrad of Co^{60} gamma irradiation.

After VUV or gamma irradiation, we expose the oxides to 10% H_2/90% N_2 forming gas at room temperature. Within a few minutes, 25 to 30% of the E' centers are transformed to hydrogen complexes. One complex ($O_2 = \dot{S}i$ - H) is associated with a 74G doublet ESR spectrum; we term this defect the 74 G doublet center.[17,18] A second complex ($O_2 = \dot{S}i$ - O - H) is associated with a 10.4 G doublet ESR spectrum; [18]we call it the 10.4 G doublet center. These results are illustrated in figures 3, 4, and 5 of the IEEE Transactions Manuscript.

Our results show that hydrogen "cracking" events can occur at room temperature at E' sites. The E' center is the dominant deep trap in thermal SiO_2. Preliminary experiments involving the injection of electrons and holes into the hydrogen soaked oxides shows that substantial structural changes - beyond the obvious hydrogen/silicon and hydrogen/oxygen bonding is taking place.

Our molecular hydrogen/E' Center work is discussed in J. F. Conley and P. M. Lenahan, "Room Temperature Reactions Involving Silicon Dangling Bond Centers and Molecular Hydrogen in Amorphous SiO_2 Thin Films on Silicon", IEEE Trans. N.S. Dec. 1992 and in a short letter form (same author and title, accepted by Applied Physics Letters).

We think that these observations may be useful in themselves since they demonstrate that a hydrogen molecule "cracking" event can be thermodynamically and kinetically favorable at room temperature at the dominant hole trap site in SiO_2. Recently, Shaneyfelt etal [19] proposed an extension of the McLean model[11] in which the proton is liberated into the oxide at hole trap sites. A recent model of Griscom proposes that the "cracking" of radiolytic molecular hydrogen at an oxide defect is an important step in the radiation induced interface state creation process. Our results involving molecular hydrogen and E' centers strongly suggest a connection between theses ideas, since E' is known to be the dominant hole capture site in the oxide.[4-6]. We think that these observations may eventually lead to an atomic scale understanding of the ways in which hydrogen affects radiation hardness.

B. A Search For Protons in Irradiated MOS Oxides.

Our work involving a search for protons is discussed in J. T. Krick, J. W. Gabrys, D. I. Semon, and P. M. Lenahan, "A Search For Protons in Irradiated MOS Oxides," Proceedings of the 1991 INFOS Conference, W. E. Eccleston and Millren editors Adam Hilger, Bristol, U.K. (1991) p. 299.

For quite some time evidence has been accumulating that proton drift to the Si/SiO_2 interface is an important, possibly rate limiting step, in the MOS radiation damage process. [11-13] However, nobody has ever directly demonstrated that protons are

generated by irradiating MOS devices. (Strong circumstantial evidence does exist, certainly, but in involves purely electronic measurements.)

We devised an experiment to search for protons in irradiated MOS oxides. The "inspiration" for our experiment came from the studies of the transient response of MOS devices to pulsed irradiation. [11-13] The pulsed irradiation studies generally involve exposing an MOS structure to a short intense irradiation from a linear accelerator (LINAC). After LINAC irradiation, the density of radiation induced interface states have been evaluated as functions of time, temperature, electric field magnitude and direction during and after irradiation. These studies of the time dependence of the radiation induced interface state buildup have provided strong but circumstantial evidence for proton drift models. These experiments show quite clearly that the radiation induced interface state generation process is thermally activated. The interface state generation process will proceed over a period of seconds to minutes at room temperature. If the temperature is dropped to ~ 250K, the process requires many hours.

We reasoned that, if proton drift to the interface is a requirement for interface state generation, and at $T \leq 250K$ the interface state generation process takes many hours, then the protons in the oxides must be stable for many hours.

Although protons cannot be observed in ESR measurements, atomic hydrogen can be observed very easily. It has a characteristic 503G doublet spectrum which is easy to identify and relatively easy to detect. We should be able to observe protons in SiO_2 by photoinjecting electrons into the oxide in question. The photoinjected electrons should be captured by the protons with large (coulombic) capture cross sections.

In our experiment we first built a small, marginally portable, ESR spectrometer. We equipped the spectrometer with a low temperature capability ($T \leq 100K$). The reason for the low temperature capability will be explained shortly. We transported the ESR spectrometer to Boeing's laboratory in Seattle, Washington. We then subjected some rather thick (~ 1000 A) and soft MOS oxides to heavy LINAC irradiation pulses (10 to 50 Mrad) at low temperature ($\equiv$ 225 to 250K).

If the proton drift models are correct, we would expect to have created large numbers of protons in these oxides. As mentioned earlier, since the radiation damage process takes many hours at this temperature, we assume that at this temperature the protons must be stable for many hours. Thus, we should be able to detect these protons by photoinjecting electrons into the oxide. The photoinjected electrons should be captured by the protons with very large capture cross section.

In order to detect the protons then, we photoinjected electrons into the oxide by exposing the oxides to rather intense ultraviolet illumination $(hc/\lambda \leq 5eV)$ from a focused mercury xenon lamp. Unfortunately atomic hydrogen in SiO_2 is unstable above 120K. Above 120K, the atomic hydrogen diffusion coefficient is so high that the hydrogen atoms collide with one another and form ESR inactive H_2 in seconds. In order to avoid the conversion of ESR active atomic hydrogen to ESR inactive H_2, we did the photoinjection at 77K.

After photoinjecting electrons into the oxide we transferred the structures to the ESR system which was, as mentioned, equipped with a cryogenic system to maintain the samples at 100K.

We determined the sensitivity of our ESR system to be $\cong 1 \times 10^{11}$ hydrogens/cm^2. Having subjected the soft, thick oxides to very heavy irradiation, we anticipated observing the characteristic atomic hydrogen ESR signal. However, in about 10 runs of the experiment we were unable to observe any atomic hydrogen. The result is illustrated in figure 1 of our paper.

Our tentative conclusion is that the irradiation did not create protons in our oxides. A possible problem with the experiment is that the oxides were irradiated unbiased. If a hole trapping event is required to trigger proton liberation we might not be doing the right experiment. The fact that our molecular hydrogen/E' measurements do indicate molecular hydrogen cracking at these sites tends to support this possibility. Other studies of molecular hydrogen ambients and radiation damage also tend to support this possibly.

(The molecular hydrogen results certainly don't prove this is what's happening!)

We hope to repeat this experiment within the coming year. Next time some of the oxides will be biased during irradiation.

III. Bond Strain and Radiation Damage

Our work involving bond strain is summarized in two publications, W. L. Warren, P. M. Lenahan, and C. J. Brinkes, "Relationship Between Strained Silicon Oxygen Bonds and Radiation Induced Paramagnetic Point Defects in Silicon Dioxide," Solid State Commun. 79, 49 (1991) and (same authors) "Experimental Evidence For Two Fundamentally Different E' Precursors in Amorphous Silicon Dioxide," J. Non. Cryst. Sol. 136, 151 (1991).

During much of the past decade, the "bond strain gradient" (BSG) model of Grunthaner [21] and coworkers was probably the most popular model to explain the radiation damage process at the Si/SiO_2 interface. Somewhat similar, though considerably less specific, ideas were proposed by the Princeton group [22]. The Grunthaner and Princeton group envision a radiation damage process which begins when holes are captured near the Si/SiO_2 interface. After hole capture, a complex irreversible rearrangement process occurs at the hole capture site. The process eventually leads to the creation of silicon dangling bonds at the Si/SiO_2 interface. In the Grunthaner model the process is caused by "strained bonds" in the SiO_2 near the Si/SiO_2 interface.

The Grunthaner and Princeton group ideas have fallen somewhat into disfavor due to a number of experimental observations which appear to be inconsistent with these ideas.[13,24,25] Nevertheless, the ideas still have some notably vigorous proponents.

We have conducted a series of experiments which we designed (1) to generally test the ideas that a complex structural rearrangement occurs with hole capture and (2) to test the idea that "bond strain" can play a role in hole capture - more specifically in E' generation.

A. Multiple Charge Cycling Experiments

If the Grunthaner and Princeton groups are correct, a complex irreversible structural change takes place at the hole capture site. If this is so the electronic properties of the hole trap site would necessarily be altered by the hole trapping event. In order to test whether or not this is so, we subjected MOS oxides to flooding with holes then electrons, then holes.... The process of alternating hole and electron injection was repeated many times. After each hole flooding sequence and each electron flooding sequence we made

CV and ESR measurements or the MOS devices. In each hole and electron flooding sequence we injected the same number of charge carriers. If a complex irreversible rearrangement process occurs we would not expect, for example, the third hole and electron flooding sequence to yield results identical to those we obtained in the first charge carrier flooding sequence.

We found that flooding the oxides with holes generated a substantial negative CV shift and a substantial E' signal. As expected, the number of E' centers closely matched the number of trapped holes. Injecting electrons into the oxide annihilates the trapped positive change as well as the E' centers. A second hole flooding sequence (after the electron injection) created a density of E' centers virtually identical to the density generated in the original hole injection process. A second electron injection sequence annihilates the E' centers, just as the first electron injection sequence annihilates the first set of E' centers. The electron injection sequence also annihilated the oxide positive charge. Repeated hole injection/electron injection sequences produced identical results. These results are clearly illustrated in figures 1 and 2 of our Journal of Non-Crystalline solids paper.

It is exceedingly difficult to reconcile these results with any model which involves complex irreversible structural changes at the hole capture site. Our results are thus not only totally inconsistent with the Grunthaner BSG Model, they are inconsistent with <u>any</u> other models which involve complex irreversible to structural changes at the hole capture site.

B. "Bond Strain" Experiments

In a related series of experiments, we decided to test the general idea that strained bonds can play a role in radiation damage. We did this work in collaboration with a glass chemist at Sandia National Laboratories, C. J. Brinker.

In earlier work Brinker had demonstrated that it was possible to synthesize SiO_2 with an extremely high level of strained bonds through sol gel processing. [19] Brinker and coworkers earlier showed that a very high density of highly strained three membered rings could be incorporated into a sol gel derived oxide under some circumstances.[19] They established this by identifying a strong D_2 Raman vibrational band (at 608 cm^{-1}) in these sol gel oxides and through magic angle spinning (MAS) nuclear magnetic resonance (NMR) measurements. Earlier work by Galeener[26,27] had convincingly established the link between the D_2 band and the strained rings. The MAS/NMR technique, which is sensitive to local bonding also indicates the presence of those rings.[19] The number of highly strained bonds could be varied by exposing the oxides to water vapor.

We found that, at high dose levels (~ 100 Mrad), the generation of E' centers and nonbridging oxygen centers was considerably enhanced in the samples with the high strained bond density. (The result is illustrated in figure 7 of our Journal of Non-crystalline Solids paper.) Our results suggest that bond strain may play some role in radiation hardness; however this role does not seem to correspond to the role proposed in the BSG model.

IV. Study of the Bias Dependence of P_b Paramagnetism in (III) Si Substrate Devices

During the early 1980's Lenahan and Dressendorfer reported first semiquantitative[2] and then a more quantitative [4] measurement of the amplitude of the P_b ESR signal in irradiated MOS devices with (III) silicon substrates. These semiquantitative and more quantitative studies were each reproduced by another group [20, 21], working with unirridated (III) structures about a year after the Lenahan/Dressendorfer publications. Several years later Gerardi etal repeated the measurements in unirradiated (100) Si Structures. [22] In 1988, Kim and Lenahan repeated these measurements in irradiated (100) Si device structures. [6]

The results of all of these studies are that the P_b amplitude is small when the Si/SiO_2 Fermi energy is near the valence band edge. The P_b amplitude grows to a maximum when the Fermi energy is moved from near the valence band edge to near mid gap. The P_b amplitude decreases to a small value when the Fermi energy moves from mid gap to near the valence band edge. This result was interpreted by Lenahan and Dressendorfer, and then by others, to mean that P_b centers are primarily positively charged and diamagnetic (ESR inactive) when the Fermi level is near the valence band edge. The P_b centers accept an electron and become neutral when the Fermi level moves to mid-gap. As the Fermi level moves from mid-gap towards the conduction band edge, the centers accept a second electron becoming diamagnetic and negatively charged.

On the basis at this interpretation, Lenahan and Dressendorfer argued that space charge in the oxide could be evaluated from CV shifts corresponding to a mid-gap Fermi level. With the Femi level at mid-gap, the P_b center interface states are electrically neutral and will not contribute to the CV shift. Since P_b centers dominate the radiation induced interface state defects, this shift should be due almost entirely to oxide space charge.

Suppose that this isn't right? Suppose that the P_b levels do not generally yield a neutral interface state charge with the Fermi level at mid-gap. Nelson Saks recently noted that some unirradiated devices on (111) Si substrates exhibit a distribution of interface stress which is very unsymetrically distributed about mid-gap. [23]

We have repeated the earlier P_b amplitude versus gate bias measurements on similar (111) Si structures supplied to us by N. Saks. Somewhat surprisingly, we find a very different distribution of P_b levels within the gap. In fact, we observe relatively little change in P_b amplitude as the Fermi levels moves through the middle half of the gap. However, if the Fermi level is near either valence or condition-band edge, the P_b amplitude is greatly diminished.

This study is still in progress. Our results strongly suggest that the P_b energy level distribution is not unique. We suspect that we will eventually be able to link these observations to atomic scale stress, since SDR/hyperfine results, discussed elsewhere in this report, strongly indicate that atomic scale stress has a large effect on P_b energy levels.

V. Related Studies

A. Radiation Effects in SIMOX Buried Oxides
B. Nitrided Oxides and Reoxidized Nitrided Oxides

We have made considerable progress in understanding the radiation responses of reoxidized nitrided oxides, nitrided oxides and separation by implanted oxygen (SIMOX)

buried oxides. The SIMOX work has been done in collaboration with Peter Roitman of NIST and the nitrided and reoxidized oxide work has been done in collaboration with Greg Dunn of MIT, Lincoln Labs.

A. SIMOX Buried Oxides

Our SIMOX results are summarized in three papers by J. F. Conley, P. M. Lenahan, and P. Roitman. "Electron Spin Resonance Study of Trapping Centers in SIMOX Buried Oxides," Proceedings of the 1991 INFOS Conference, W. E. Eccleston, editor, Adam Hilger, Bristol (1991) p. 259, "Electron Spin Resonance Study of E' Trapping Centers in SIMOX Buried Oxides," IEEE Trans NS-38, 1247 (1991), "Electron Spin Resonance of Separation By Implanted Oxygen Oxides: Evidence For Structural Change and a Deep Electron Trap," Appl. Phys. Lett. 60. 2889 (1992).

Several years ago we demonstrated that SIMOX buried oxides exhibit a very large ($\sim 10^{18}/cm^3$) density of E' precursors. We also showed that E' centers could be generated uniformly within the SIMOX oxides at high densitites without a corresponding net density of space charge. Similar results were soon produced by another group dealing with hydrogen treated SIMOX buried oxides.[28]

These initial results could be interpreted in several ways. One might assume that the SIMOX E' centers are electrically neutral or all of the E' centers were positive and compensated by negative charge.

We initially suggested that some of the SIMOX E' centers are probably positively charged and compensated. A second group proposed that the SIMOX E' centers are electrically neutral.

Recently, we have shown that our suggestion is correct. We find that the creation of high E' densities is accompanied by substantial electron trapping. This result is most clearly illustrated by figure 4 of our Applied Physics Letter. The SIMOX system is quite complex and although much work remains to be done, we can draw some conclusions. (1) Our work shows that E' centers play an extremely important role in buried oxide trapping. (2) A significant fraction of the E' centers are positively charged. (3) Some E' centers are compensated by negative charge.

B. Nitrided Oxides and Reoxidized Nitrided Oxides.

Our work on nitrided oxides and reoxidized nitrided oxides is summarized in two papers by I. A. Chaiyesena, P. M. Lenahan, and G. J. Dunn, "Identification of a Paramagnetic Nitrogen Dangling Bond Defect in Nitrided Silicon Dioxide Films on Silicon," Appl. Phys. Lett. 58, 2141 (1991) and "Electron Spin Resonance Investigation of the Trapping in Reoxidized Nitride and Silicon Dioxide," published in the Journal of Applied Physics, July 15, 1992.

When thermal oxides are nitrided their Si/dielectric interfaces become very radiation hard. Unfortunately, the nitridation has some seriously damaging side effects. The most important of these side effects is the creation of electron traps in the nitrided oxide. Reoxidation reduces but does not completely eliminate these electron traps. Reoxidation also introduces some hole traps in the region of the electric heat the gate/dielectric interface.

We have been engage in a joint (MIT/Penn State) ONR sponsored study to understand the effects of nitridation and reoxidaties of the radiation and hot carrier response of oxides. Our MIT collaborator has been Greg Dunn.

We have identified a bridging nitrogen defect which is created when oxides are nitrided. The defect's density is greatly reduced though not eliminated by a subsequent reoxidation. We find that the reoxidation creates a new defect - an overcoordinated nitrogen - near the gate dielectric interface. The fact that this defect is created by nitridation and mostly eliminated by reoxidation suggests it is linked to the nitroxidation induced electron trap.

We find that nitridation greatly reduces the density of E' centers generated by ionizing radiation. Reoxidation increases the E' density in irradiated oxides; however, these E' center appear near the gate dielectric interface. In conventional oxides, the E' centers are concentrated near the Si/SiO_2 interface, and can thus more strongly effect threshold voltage. Preliminary results also suggest that the E' centers in reoxidized nitroxided oxides are electrically neutral.

Although far more work remains to be done, we feel that we have begun to develop fundamental understanding of the radiation response of nitrided and reoxidized nitrided oxides.

VI. Summary of What We've Learned

We've made progress on several fronts during the past three years. We've learned to make evermore sensitive SDR measurements and are now making the most sensitive spin resonance work ever done in solids in our SDR studies of damaged MOSFETS. In our SDR experiments, we've worked out a basic understanding of the SDR response of MOS devices, a measure of "atomic scale stress" at the Si/SiO_2 interface, and some preliminary evidence that the oxide near the Si/SiO_2 interface is more dense than ordinary amorphous SiO_2.

We've made progress in identifying the "basic mechanisms" of MOS devices, identifying several molecular hydrogen/E' reactions which occur quickly at room temperature. We've also obtained some preliminary results indicating that protons are <u>not</u> created in the oxide directly by irradiation. We've demonstrated that a type of "bond strain" can enhance radiation damage in some oxides but have also provided further evidence contradicting the "bond strain gradient" model.

Our work has extended beyond gate oxides to include some newer dielectrics, buried oxides of silicon on insulator structures and nitruded and reoxidized nitrided oxides. We've made considerable progress in both areas. We identified oxygen deficient silicon defects as the dominant trapping centers in SIMOX buried oxides. We have found evidence linking a bridging nitrogen defect to electron traps induced by nitridation and find that the hole trap in reoxidized nitrided oxides is not the E' center.

VII. Future Work

We believe our work on the past contract has contributed significantly to our current understanding of MOS device instabilities caused by ionizing radiation as well as other technologically important factors. We hope to further contribute to this understanding by focusing upon several problems.

One of the last major issues to resolve is the precise role of hydrogen in the damage process. We intend to focus upon the role of both protons and molecular hydrogen in our

futurework. Our LINAC experiments strongly indicate that the ionizing radiation does not directly create the protons within the oxide. Our molecular hydrogen studies show that E' centers can reach with H_2 to create several H/E' complexes. It is clear that oxygen/silicon bonds are broken in these reactions. We plan to extend our H_2 studies to include a simultaneous comparison on P_b and E' H_2 reactions. We would hope to establish whether or not these E' reactions may be directly involved in interface state generation. We also hope to repeat our LINAC experiments, this time looking for hydrogen/E' complexes.

There is still a remarkable amount of controversy surrounding the identification of radiation and hot carrier damage defects at the (100) Si/SiO_2 interface. Early ESR studies focused upon the (111) Si/SiO_2 interface and pretty firmly established that the radiation damage involved a silicon back bonded to three other silicons at the Si/SiO_2 interface. During the past five or six years evidence has strongly indicated that the (100) Si/SiO_2 P_{bo} center plays the dominant role at that interface. According to Poindexter etal, the P_{bo} center of the (100) Si/SiO_2 interface is essentially identical to the well understood (111) Si/SiO_2 P_b center.

There are at least two problems with regard to the P_{bo} center. First, statics and Dori [ ] claim that the Poindexter etal identification is wrong! Secondly, different groups observe different distributions of interfaces state levels across the band gap. Could one defect five several densities of states?

We plan to make some measurements of P_{bo} centers on the well understood (111) Si/SiO_2 system in which the samples have been prepared under very different circumstances. We will establish whether the P_b center in this well understood system can yield several different densities of states.

We plan to look closely at the correspondence between (111) P_b and (100) P_{bo} [29] Si hyperfine spectra. The hyperfine spectra provide a very sensitive probe of P_b defect structure. If we can establish a close correspondence between (111) P_b and (100) P_{bo} hyperfine spectra we have a very strong argument that they are the same defect. If we find that significant differences exist between the (111) P_b and (100) P_{bo} hyperfine spectra our results would support the Stathis/Dori idea that the P_{bo} is a fundamentally different defect.

References

1. P.M. Lenahan, K.L. Brower, P.V. Dressendorfer, and W.C. Johnson, IEEE Trans. Nucl. Sci. 28, 4105 (1981)
2. P.M. Lenahan and P.V. Dressendorfer, Appl. Phys. Lett. 41, 542 (1982)
3. P.M. Lenahan and P.V. Dresendorfer, J. Appl. Phys. 54, 1457 (1983)
4. P.M. Lenahan and P.V. Dressendorfer, Appl. Phys. Lett. 44, 96 (1984)
5. P.M. Lenahan and P.V. Dressendorfer, J. Appl. Phys. 55, 3495 (1984)
6. Y.Y. Kim and P.M. Lenahan, J. Appl. Phys. 64, 3551 (1988)
7. C.A. Coulson, Valence (Oxford University, London, 203 (1961)
8. D. Vuillame, D. Goguenheim, and G. Vincent, Appl. Phys. Lett. 57, 1206 (1990)
9. M.A. Jupina and P.M. Lenahan, IEEE Trans. Nucl. Sci. 36, 1800 (1989)
10. E.H. Poindexter, P.J. Caplan, B.E. Deal, R.R. Razouk, J. Appl. Phys 52, 879 (1981)
11. F.B. McLean, IEEE Trans NS-27, 1651 (1980)
12. P.S. Winokur, H.E. Boesch, J.M. McGarrity, and F.B. McLean, J. Appl. Phys. 50, 3492 (1979)
13. N.S. Saks and D.B. Brown, IEEE Trans. NS - 37, 1624 (1990)
14. R.A. Kohler, R.A. Kushner, and K.H. Lee, IEEE Trans. NS - 35, 1492 (1988)
15. R.E. Stahlbush, B.J. Mrstik, and R.K. Lawrence, IEEE Trans NS - 37, 1641 (1990)
16. B.J. Mrstik and R.W. Rendell, IEEE Trans NS - 38, 1101 (1991)
17. F.J. Grunthaner, P.J. Grunthaner, and J. Maserjian, IEEE Trans, NS - 29, 462 (1982)
18. S.J. Wang, J.M. Sung and S.A. Lyon, Appl. Phys. Lett. 52, 1431 (1988)
19. C.J. Brinker, R.J. Kirkpatrick, D.R. Tellent, B.C. Bunker, and B. Montez, J. Non Cryst. Solids 99, 418 (1988)
20. N.M. Johnson, D.R. Biegelson, M.D. Moyer, S.T. Chaing, E.H. Poindexter and P.J. Caplan, Appl. Phys. Lett. 43, 563 (1983)
21. E.H. Poindexter, G.J. Gerardi, M.E. Ruechel, and P.J. Caplan, J. Appl. Phys. 56, 2844 (1984)
22. G.J. Gerardi, E.H. Poindexter, and P.J. Caplan Appl. Phys. Lett. 49, 348 (1986)
23. N.S. Saks, M.G. Ancona, and W. Chen, Appl. Phys. Lett. 60, 2261 (1992)

24. H.S. Witham and P.M. Lenahan, Appl. Phys. Lett., 51, 1007 (1987).

25. N.S. Saks, D.B. Brown, and R.W. Rendell, IEEE Trans NS-381, 1130 (1991).

26. F.L. Galeener, Sol. State Commun., 44, 1037 (1982).

27. F.L. Galeener, R.A. Barrion, E. Martinez, and R.J. Elliot, Phys. Rev. Lett. 53, 2429 (1984).

28. M.E. Zvanut, R.E. Stahlbush, W.E. Carlos, H.L. Hughes, R.K. Lawrence, R. Hevey, G.A. Brown, IEEE Trans NS-38, 1253 (1991).

29. J.H. Stathis and L. Dori, Appl. Phys. Lett., 58, 1641 (1991).

Publications

The work summarized in the preceding section resulted in a number of publications. All publications, in some or all respects, address the research topics of our contract (N00014-89-J-2022); however, several publications involved multiple sponsorship and two papers involving nitrided and reoxidized nitrided oxide were fully funded by another contract. These publications are reproduced in this section and are organized under the same format utilized in the opening section of this report.

Spin Dependent Recombination Publications
June 1, 1989 - May 31, 1992

M.A. Jupina and P.M. Lenahan "A Spin Dependent Recombination Study of Radiation Induced Defects at and Near the Si/SiO_2 interface," IEEE Trans. Nucl. Sci. NS 36, 1800 (1989)

M.A. Jupina and P.M. Lenahan "Spin Dependent Recombination: A^{29} Si Hyperfine Study of Radiation-Induced P_b Centers at the Si/SiO_2 Interface," IEEE Trans Nucl. Sci. 37, 1650 (1990)

J.T. Krick, P.M. Lenahan, and G.J. Dunn, "Direct Observation of Interfacial Point Defects Generated by Channel Hot Hole Injection in n-Channel Metal Oxide Silicon Field Effect Transistors", Appl. Phys. Lett. 59, 3437 (1991)

A SPIN DEPENDENT RECOMBINATION STUDY OF RADIATION INDUCED DEFECTS AT AND NEAR THE Si/SiO_2 INTERFACE

M. A. Jupina and P. M. Lenahan
Pennsylvania State University
University Park, PA 16802

ABSTRACT

A new electron spin resonance technique, spin dependent recombination (SDR) permits extremely rapid, high signal to noise ratio Electron Spin Resonance (ESR) measurements of electrically active radiation damage centers in (relatively) hard MOS transistors in integrated circuits.

Using SDR, we observe the radiation induced buildup of P_{bo} and E' centers at relatively low concentration in individual MOSFETs in integrated circuits with (100) silicon surface orientation. Earlier ESR studies of extremely large (~1 cm^2) capacitor structures have identified P_b and E' centers as the dominant radiation induced defects in MOS devices. Our results extend and confirm these earlier results and at least qualitatively answer objections to the earlier work related to the relevance of large capacitor studies to transistors in an integrated circuit.

INTRODUCTION

Since the mid-1960s when it was shown that metal-oxide-semiconductor (MOS) devices were sensitive to ionizing radiation [1], the radiation response of these devices has been an active research area. The radiation damage process results in the creation of interface states at the Si/SiO_2 interface and the capture of holes in deep traps near the Si/SiO_2 interface [2-6]. Combining electron spin resonance (ESR) and capacitance versus voltage (CV) measurements, Lenahan and Dressendorfer [7,8] showed that a trivalent silicon defect called the P_b center, which is located at the Si/SiO_2 interface, is the dominant radiation-induced interface state, while an oxygen deficient silicon defect in the oxide, termed the E' center, is the hole trap. Their studies used large area MOS capacitors (several cm^2) because standard ESR detection techniques available at that time were many orders of magnitude too insensitive to permit studies of individual metal-oxide-semiconductor field-effect transistors (MOSFETs).

In this study we use the electron spin resonance technique called spin dependent recombination (SDR). SDR has several advantages over standard ESR in the study of radiation damage in MOSFETs. It is many orders of magnitude more sensitive than standard ESR detection; it allows the rapid (a few minutes) detection of low densities (~$10^{11}/cm^2$) of radiation induced point defects in single MOSFETs in integrated circuits. We show that SDR is sensitive to both radiation induced P_b and E' centers. We provide a semiquantitative analysis of the P_b results; however we are able only to show that SDR is sensitive to the E' centers generated by radiation and that these E' centers are "close" to the Si/SiO_2 interface.

Our observations collectively confirm and extend earlier ESR studies of radiation damage that used large area capacitors. Our studies qualitatively answer objections to earlier ESR work related to the relevance of very large area capacitor ESR studies to MOSFETs in integrated circuits.

Our measurements involve relatively hard and relatively soft MOSFETs. The difference in hardness in the two sets of devices involved only a high temperature post oxidation anneal. Our results suggest that E' centers are, on average, closer to the interface in the harder device.

EARLIER ESR STUDIES INVOLVING MOS CAPACITORS

Our SDR results involve two point defects that earlier capacitor/standard ESR studies have shown to be the dominant radiation induced defects in MOS devices: P_b and E' centers.

The P_b center was discovered by Nishi [9]. Nishi and his coworkers studied unirradiated MOS structures. Nishi et al [9, 10] identified the P_b center as a trivalent silicon at or very near the Si/SiO_2 interface. They demonstrated [10] that high temperature processing steps that yield high Si/SiO_2 interface state density also yield high P_b density, and that high temperature processing steps that yield low interface state density, also yield low P_b density.

Nishi et al [10] established that the Hall mobility of inversion layer electrons at the Si/SiO_2 interface decreases with increasing P_b concentration. They showed that this correlation between processing induced P_b and electron mobility could be explained in terms of coulombic scattering from negatively charged P_b interface state centers at the Si/SiO_2 boundary. They also showed that the MOSFET's transconductance increases with decreasing P_b concentration, and furthermore, specifically noted that the dependence of P_b density on the partial pressure of water during oxidation is quite similar to that of the Si/SiO_2 interface state density. These observations convincingly established the strong correlation between interface states created by high temperature processing and P_b centers. Caplan et al [11] while studying unirradiated devices, later provided an ingenious proof that P_b is a silicon bonded to three other silicons at the Si/SiO_2

0018-9499/89/1200-1800$01.00 © 1989 IEEE

interface. Poindexter et al [12] additionally established that $P_b$spin-lattice relaxation time is strongly dependent upon gate bias, but they were unable to establish whether or not the P_b center charge state and spin state are bias dependent--that is whether or not the P_b levels are themselves interface states.

Lenahan and Dressendorfer [7,8,13] established that the P_b center is an amphoteric interface state defect with levels in the band gap matching the electronic density of interface states. Their ESR work indicates that when the Fermi level is at midgap there is approximately zero net charge in the P_b center interface state defects. They furthermore demonstrated that P_b centers and radiation induced interface states [14,15] are generated in approximately equal numbers and that they exhibit the same annealing characteristics [15]. Their work, however, was restricted to (111) substrate silicon devices. Kim and Lenahan have found quite similar results for P_b centers on (100) substrates [16].

More than 30 years ago, Weeks [17] discovered the E' center in irradiated crystalline SiO_2. He proposed that E' is an electron trap with an unpaired electron residing on a silicon atom [17]. Silsbee [18] and Feigl [19] et al refined Week's initial assessment of E' in crystalline quartz. Feigl et al argued that the E' center is essentially a hole trapped in an oxygen vacancy. An asymmetric relaxation of the silicons on either side of the vacancy occurs upon hole capture; the relaxation results in the unpaired spin residing almost entirely at one of the silicons.

Marquardt and Sigel [20] were apparently the first to observe E' centers in an irradiated MOS structure. They observed a weak narrow resonance with the appropriate g value in heavily irradiated (220 Mrad), rather thick (up to 11,000Å) oxides on silicon. Although they reported no results of electrical measurements on their devices, they suggested (correctly) that E' centers could be the trapped hole centers in the oxide.

Lenahan and Dressendorfer showed that the E' center is primarily responsible for the buildup of positive charge in irradiated oxides. They found that the densities of E' centers and holes trapped in the oxide are approximately equal, [8,16,21,22] that the E' centers and trapped holes have identical annealing characteristics, [8] and that the E' centers and trapped holes are identically distributed in the oxide [8]. Combining vacuum ultraviolet ($hc/\lambda \simeq 10.2$ eV) and ultraviolet ($hc/\lambda \simeq 5$ eV) illumination sequences with ESR and CV measurements, Witham and Lenahan [23,24] showed that the hole trapping process involving E' centers is entirely consistent with the simple oxygen vacancy model of Feigl et al [19].

Quite recent electron spin resonance studies of Takahashi et al [25] and Miki et al [26] also show a correspondence between E' centers and trapped holes in MOS oxides.

SPIN DEPENDENT RECOMBINATION

The technique of spin dependent recombination (SDR) was first demonstrated by Lepine [27] in 1972. It has been applied to unoxidized silicon surfaces [27], pn junction diodes [28], amorphous hydrogenated silicon thin films [29], silicon grain boundaries [30], and the MOS system [31-33]. Vranch et al [33] recently demonstrated SDR in a gate controlled diode; although Vranch and coworkers provided limited information, their diode was quite large (0.25 cm^2) and possessed an extremely high surface state density. Although the qualitative observations of Vranch et al did not explore the relationship between SDR signals, applied voltages, modulation frequencies, etc., it did, as does our study, provide confirmatory evidence that P_b centers play a dominant role in the radiation induced interface states at the Si/SiO_2 interface. (Unlike our study, the Vranch study was unable to detect the presence of E' centers in their SDR measurements).

THE TECHNIQUE

Just as in standard ESR, SDR detects the presence of paramagnetic point defects, that is, defects with an unpaired electron [27-36]. The technique exploits the fact that the capture cross-section of a paramagnetic trapping center is affected by its spin state. Several somewhat contradictory models [27,28,34-36] have been proposed to explain the spin dependent recombination process. Since a detailed description of these models is not appropriate for our discussion, we present only a qualitative rationalization of the phenomenon. If we apply a strong magnetic field to a semiconductor, the electron, hole, and trap spins will be polarized: they will tend to line up with the applied field. Only those electrons and holes whose spin states are anti-parallel to the spin state of the paramagnetic defect are trapped; those electrons and holes whose spin states are parallel to the spin state of the paramagnetic defect are not (or are very unlikely to be) trapped. Only electrons and holes trapped in singlet configuration at a paramagnetic center will recombine. The applied field increases the probability of triplet configurations and decreases the probability of singlet configurations. The field induced decrease in singlet configurations decreases the overall probability of capture events. The effect of the applied field is thus to decrease the capture cross-section of paramagnetic traps.

If in addition to the static field we add an oscillating (microwave frequency) field, we can flip the spins in the paramagnetic trap centers if the ESR condition is satisfied. (For a trap with $g = g_t$, $h\nu = g_t\beta H$, where h is Planck's constant, ν is the microwave frequency, β is the Bohr magneton, and H is the "static" field.) If the microwave intensity is high enough, we can completely randomize the spin orientations in the trap, significantly increasing the probability of singlet potential trapping events. The microwave radiation in turn increases the trap capture cross-section and thereby increases the recombination rate. In our experiments the microwave frequency is fixed by the resonance

frequency of our microwave cavity; the "static" field is slowly varied over tens or hundreds of seconds.

OUR EXPERIMENT

A. The Device

In these studies, a MOSFET is used as a gate-controlled diode [37-41] (source and drain shorted together) to study radiation-induced paramagnetic trapping centers. The p-n junction of the gated-diode is slightly forward biased ($V_J \leq 0.3$ V), so that changes in the recombination current associated with deep trap levels can be monitored while their spin resonance condition is satisfied. For low forward biases, with the surface under the gate in accumulation, only those centers that are within the depletion region of the p-n junction contribute to the recombination current and SDR. If the surface under the gate is inverted, centers within the depletion region of the field-induced junction between the inversion layer and the underlying substrate also contribute to the total recombination current and SDR (which are, therefore, larger than in accumulation). In depletion, interface states will provide another contribution to the total recombination current, resulting in a peak in the forward current versus gate voltage characteristic. It is the SDR spectra in depletion that we are primarily concerned with in this study.

The MOSFETs used in this study were p-channel with (100) substrate orientation. Oxides were grown in dry 0_2 at 1000 C to a thickness of 37 nm. Annealing these oxides in situ in N_2 at 1000 C for 25 minutes resulted in a radiation soft oxide while annealing in situ in N_2 at 900 C for 25 minutes resulted in a radiation hard oxide. The n-well doping was $1.5 \times 10^{16}/cm^3$ with a well depth of 6 μm. The gate area of the devices was $10^{-4}cm^2$ and the p^+ source and drain dopings were $3 \times 10^{19}/cm^3$.

Since this study is primarily concerned with radiation-induced centers at the Si/SiO_2 boundary, the Si/SiO_2 interface contribution to recombination is our major concern. In our analysis we assume that the quasi-Fermi levels for electrons (E_{Fn}) and holes (E_{Fp}) are approximately constant throughout the depletion region underneath the gate. This assumption has been used by others [37,38] but may not always be entirely valid [41]. The band diagram (for the cross-section AA) of a gated-diode with its gate area depleted and junction forward biased is shown in Figure 1. The spacing between the quasi-Fermi levels is determined by the forward bias V_J. The total band bending is described by the surface potential ψ_S (a function of gate bias, V_G). The difference between the (bulk) energy levels E_{Fn} and E_i (intrinsic Fermi level) is termed Φ_{Fn}. The rate of recombination depends on the number of interface states in the depleted surface region and on the density of carriers injected into this region under low forward bias [38,39]. The surface recombination rate will be largest when the sum of the electron and hole concentrations at the surface has its minimum value [38,39]. This happens when the concentrations are equal. The carrier concentrations are equal when the surface potential is [39]

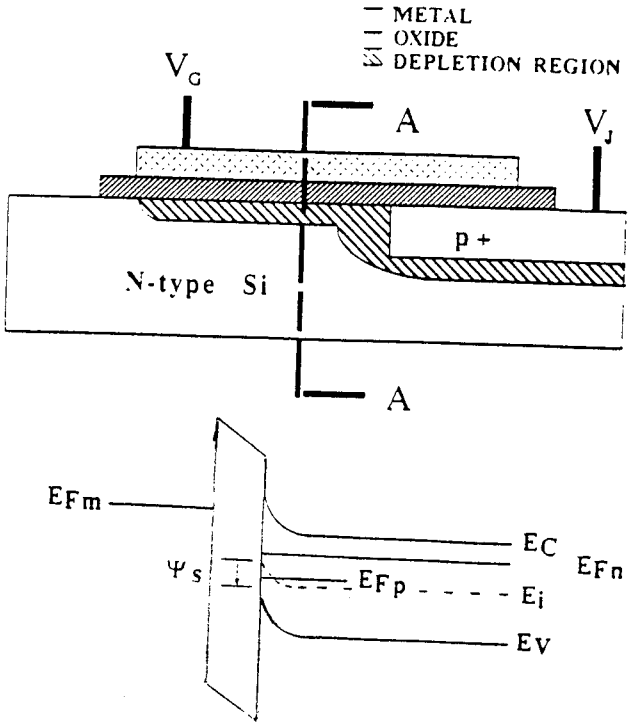

Figure 1 A gated diode (1a) forward biased and gate area depleted of carriers. An energy band diagram (1b) for the cross-section AA of the gated-diode.

$$\psi_S = \Phi_{Fn} - V_J/2 \tag{1}$$

$$n_S = p_S = n_i \exp(qV_J/2kT) \tag{2}$$

(where n_S and p_S are the electron and hole surface concentrations and n_i is the intrinsic carrier concentration).

From simple Shockley, Read [42], Hall Theory, the surface recombination current maximum of the resulting forward current is [38]

$$I_{rec,s} \simeq \left[\frac{2}{\pi} q s_o n_i \frac{q|V_J|}{2kT} \exp\left(\frac{q|V_J|}{2kT}\right)\right] A_G \tag{3}$$

for $V_J >> kT/q$, where $s_o = (\pi/2)\sigma v_{th} kTD_{it}$ and σ is taken to be the electron and hole capture cross-section, v_{th} is the thermal velocity of the charge carriers, k is the Boltzmann constant, T is the absolute temperature, D_{it} is the interface state density around the middle of the gap and A_G is the area under the gate. For $V_J >> kT/q$, only the interface states whose energy lie within a band $\sim qV_J/2$ centered around the middle of the forbidden gap contribute significantly to the surface recombination current [37,38]. (Grove and Fitzgerald have defined s_o as the surface recombination velocity of a depleted surface [37].)

B. Experimental Technique

The SDR spectrometer employed in this study is schematically illustrated in Figure 2. The gated-diode was mounted on a rectangular quartz rod and centered inside an X band TE_{102} microwave cavity with a resonant frequency of ~9.5 GHz. The (100) Si/SiO_2 interface of the device was perpendicular to the applied field. Care was taken to minimize the microwave electric field at the device, since the diode acts as a microwave detector generating an unwanted pick-up current. The loaded cavity had a Q of about 5000. The microwave source was a low noise 100 mW X-band solid state oscillator. The cavity was placed in an electromagnet (~3500 G), and Helmholtz coils were used for magnetic field modulation (audio frequencies and 4 G_{pp} amplitude). The microwave cavity, microwave generator, magnet, and controller were taken from a Micro-Now Model 8300 ESR spectrometer.

The gated-diode was biased at a fixed gate and junction voltage while spin dependent variations in the recombination current at resonance were monitored using a current-to-voltage pre-amplifier and lock-in amplifier (Ithaco Dynatrac Model 393). With continuous wave microwave exitation, the magnetic field was slowly ramped (~50 G in two minutes) while the SDR signal was cycled in and out resonance and monitored by the lock-in amplifier. The resulting spectra are approximately the first derivative of an "absorption-like" curve. For g-value determination of the paramagnetic recombination centers, a commercial NMR (nuclear magnetic resonance) gaussmeter (Micro-Now Model 515) was used in conjunction with a frequency meter.

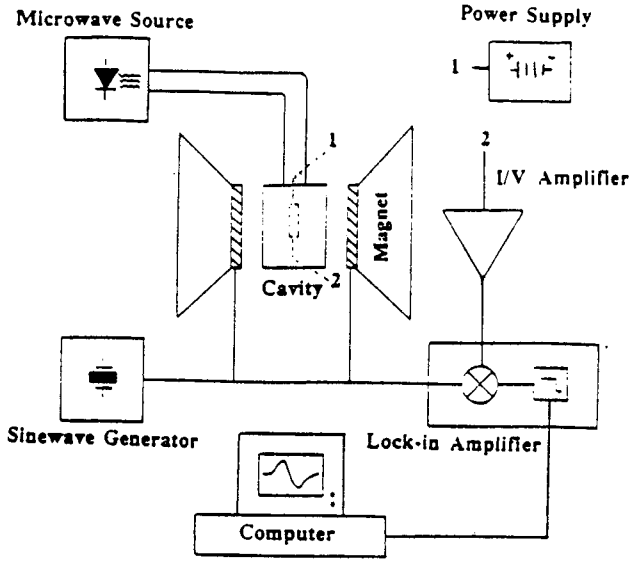

Figure 2 Block diagram of the SDR spectrometer.

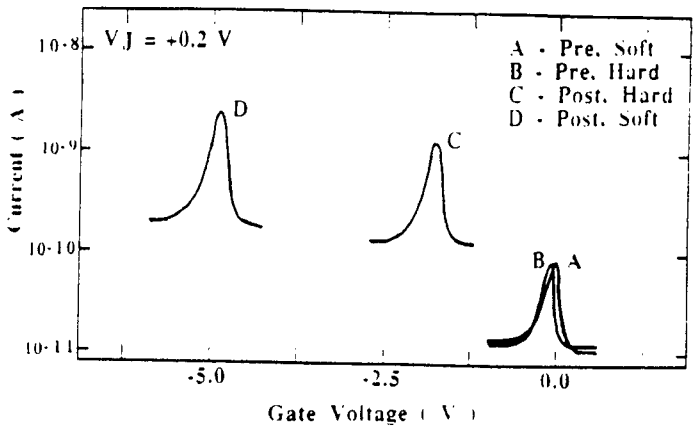

Figure 3 Pre- and post-irradiation IV curves for both hard and soft oxides.

	Pre irradiation		Post-irradiation	
	Hard	Soft	Hard	Soft
Midgap D_{it} ($10^{11}/cm^2eV$) from CV	0.3	0.2	2.0	3.5
s_o (cm/sec.)	2.0	2.0	45	51
Midgap D_{it} ($10^{11}/cm^2eV$) from s_o with $\sigma = 4 \times 10^{-16}$ cm^2	0.1	0.1	2.9	3.2
ΔV_{mg} (volts)	----	----	-1.6	-4.8

Table 1 Summary of electrical characteristics for pre- and post-irradiated devices.

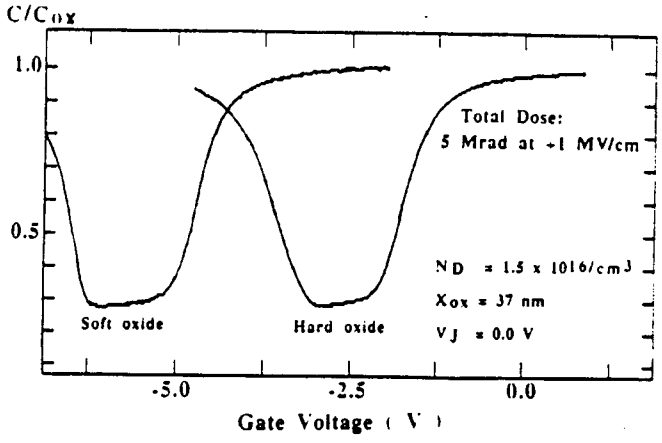

Figure 4 Post-irradiation HF CV curves for both hard and soft oxides.

Discussion and Results

Both the relatively hard and relatively soft devices were irradiated with Co^{60} γ-rays to a total dose of 5 Mrads. A gate bias of +5 volts was applied during irradiation. The effects of the radiation on the electrical characteristics of the devices are displayed in Figure 3 in the form of recombination current versus gate voltage for a given forward bias. Pre- and post-irradiation curves are shown for both the hard and soft devices. The radiation generated interface states in both hard and soft devices have increased the surface recombination current by about a factor of about twenty in both cases. The increase in trapped positive charge in the oxide has shifted the IV (current versus voltage) curves more negatively along the voltage axis. The MOSFETs' electrical characteristics, both before and after irradiation, are summarized in Table 1. Mid-gap interface state densities (D_{it}) before irradiation were determined by the High-Low CV (capacitance versus voltage) technique [43] on test capacitors fabricated with the same processing steps as the MOSFETs. Mid-gap D_{it} after irradiation was determined by the Terman technique [44] on the actual MOSFETs used in this study. The post-irradiation HF (high frequency) CV curves of the MOSFETs (source and drain shorted to substrate) are shown in Figure 4. The "stretch-out" of these curves was due entirely to interface states, and no LNUs (lateral charge nonuniformities) were present as determined by a test for LNUs in MOSFETs.[45] Surface recombination velocities (s_o) of the depleted surface both before and after irradiation, were determined from reverse bias IV curves, taking the generation current for a depleted surface as constant and given by $I_{gen,s} = qs_o n_i A_G$ [38]. The mid-gap interface state density was also determined from the s_o values obtained from the IV curves. (In the calculation, we took the square root of the product of electron and hole capture cross-sections $\sigma = (\sigma_n \sigma_p)^{1/2}$ to be 4×10^{-16} cm^2). Finally, the mid-gap voltage shifts are given.

In irradiated hard and soft gated diodes, we observe SDR spectra in accumulation, depletion, and inversion at low forward bias. (Attempts to observe SDR in either devices before irradiation failed. The limit of our detection was a variation ΔI in the recombination current at resonance of approximately 10^{-14} amps.) Spectra, qualitatively representative of both types of oxides, are displayed in Figure 5. In Figure 5a, the surface under the gate is in accumulation, so only those paramagnetic recombination centers in the depletion region of the p-n junction contribute to the SDR signal. This signal with a g-value of 2.0055 and a 10 G_{pp} width has been observed before by Solomon [28] in a depletion region of an ordinary p-n diode. In Figure 5b, the surface under the gate is in depletion, so the paramagnetic recombination centers at the Si/SiO_2 interface generate most of the SDR signal. In Figure 5b, both P_{bo} ($g = 2.006 \pm 0.0003$) and E' ($g = 2.0007 \pm 0.0003$) centers are visible as in previous ESR studies done by Kim and Lenahan [16] on radiation-induced defects in (100) MOS structures. Just as they reported, we find that the radiation-induced interface state buildup consists mostly of P_{bo} centers. On (100) surfaces with process-induced interface states, Poindexter et al [46] observed two P_b centers, termed P_{bo} and P_{b1}. The P_{bo} defect is a silicon bonded to three other silicons at the Si/SiO_2 interface; the structure of P_{b1} is not yet clearly established. Rotation of the device in the cavity revealed the P_{bo} spectra's anisotropy. In Figure 5c, the surface under the gate is in inversion, so the paramagnetic recombination centers within the depletion region of the field-induced junction between the inversion layer and the underlying substrate contribute to the SDR signal. This SDR signal (g = 2.0055 and 10 G_{pp} width) is very much like the resonance signal found in the depletion region of the p-n junction for accumulation.

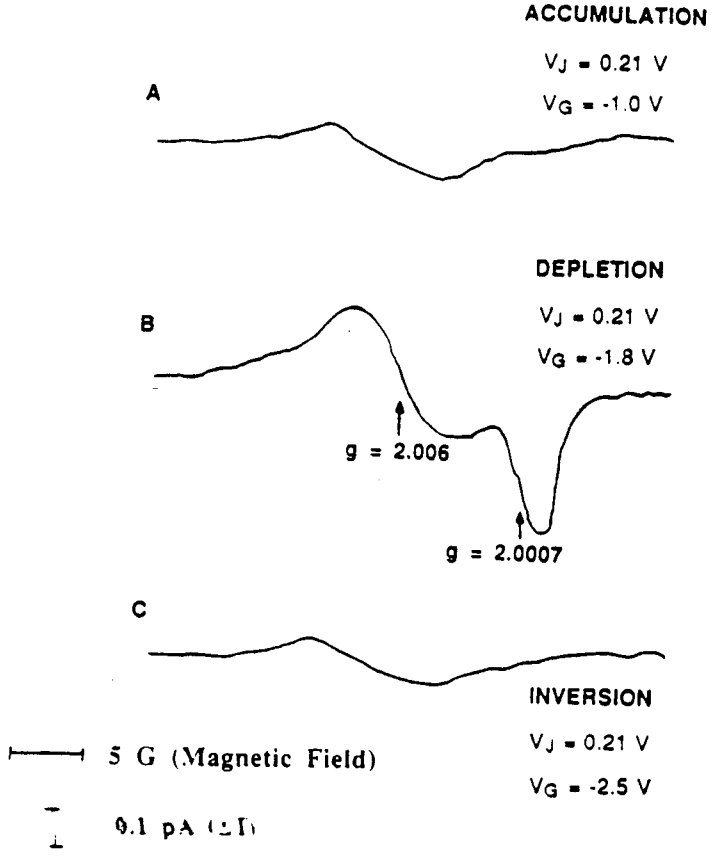

Figure 5 SDR spectra for the irradiated "hard" device in accumulation (A), depletion (B), inversion (C).

Semiquantitative Analysis of P_{bo} Results

Recombination current (I) and the peak-to-peak magnitude of the P_{bo} center's SDR signal (ΔI) versus gate bias are plotted in Figures 6 and 7 (hard oxide is 6 and soft oxide is 7) where the maximum $\Delta I/I = \sim 5 \times 10^{-4}$ in both plots. Shockley-Read statistics [42] for nonequilibrium predict that the recombination current peaks in the region between the quasi Fermi levels near mid-gap ($\psi_s = \Phi_{Fn} - V_J/2$). Qualitatively, the P_{bo} signals in both the hard and the soft oxides also peak in the gate bias regime where surface recombination dominates, as one would expect for interface defects with levels near mid-gap.

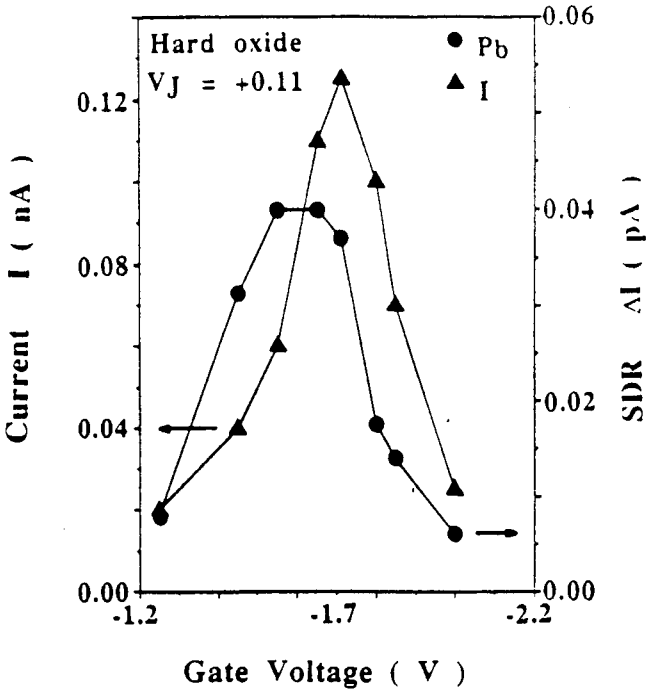

Figure 6 Recombination Current (I) and P_{bo} center SDR signal (ΔI) versus gate voltage for the "hard" device.

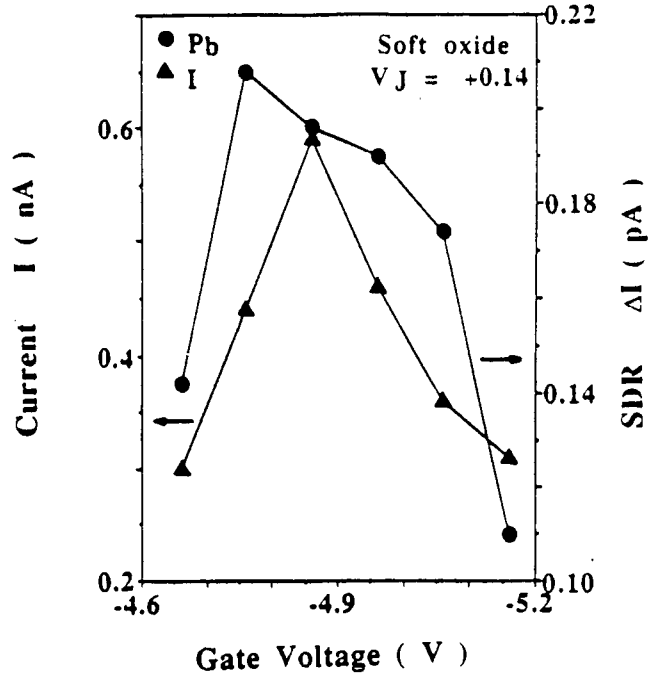

Figure 7 Recombination current (I) and P_{bo} center SDR signal (ΔI) versus gate voltage for the "soft" device.

In Figure 8 the magnetic field modulation frequency dependence of the P_{bo} center is displayed (where the ΔI's are normalized to their maximum values). Similar results were found in both the hard and soft oxides. (The junction was forward biased at 0.2 V; the frequency dependence varied little with gate bias for depletion). By using a small sinusoidal magnetic field at various frequencies, the system is driven in and out of resonance about a steady state value, the result being the determination of an electronic relaxation time associated with the rate limiting process at that paramagnetic center. With a dual-phase lock-in amplifier, both the in-phase and out-of-phase SDR signal can be monitored for various modulation frequencies. The frequency response of a system in SDR normalized to steady state is [27,30]

$$\Delta I = \omega\tau \sin(\omega\tau)/((\omega\tau)^2 + 1) + \cos(\omega\tau)/((\omega\tau)^2 + 1) \quad (4)$$

where ω is the angular modulation frequency, τ is the electronic relaxation time, $1/((\omega\tau)^2 + 1)$ is the in-phase component, and $\omega\tau/((\omega\tau)^2 + 1)$ is the out-of-phase component. From equation 4, the electronic relaxation times associated with the P_b center is found to be 0.3 msec. This τ should be the average time required for a neutral paramagnetic P_{bo} center to capture either an electron or a hole. This time is given by the inverse of the product of the number of electrons or holes times the thermal velocity (v_{th}) times the capture cross-section of a trap. The number of electrons and holes under the gate at the maximum surface recombination rate is given by equation (2), so

$$\tau = ([n_i \exp(qV_J/2kT)]\ v_{th}\ \sigma)^{-1} \quad (5)$$

For a forward bias of V_J = +0.2 V, taking $v_{th} \cong 10^7$ cm/s, and $\sigma = 4 \times 10^{-16}/cm^2$, we arrive at τ = 0.3 msec, the value obtained in Figure 8 for P_{bo} center's modulation frequency dependence.

Qualitative Discussion of E' Results

The E' signal observed by standard ESR in MOS structures was shown to be a hole trapped in an oxygen vacancy very near the Si/SiO_2 interface [8,13,14,22]. Whether the E' centers observed in SDR are associated with the deep hole trap can not be ascertained with absolute certainty at this time. What is certain, though, is that the E' center must reside close enough to the Si/SiO_2 interface to play some role in an SDR event. In Figure 9, the P_{bo} and E' resonances are displayed for the hard (9a) and soft (9b) devices. Although the P_{bo} and E' amplitudes are roughly equal in the hard oxide, the E' signals are considerably smaller in the soft oxide. Simple SDR theory indicates that only E' centers that act as recombination levels near midgap could be detected; however, it is well established [47] that paramagnetic centers that are relatively close to one another may exchange energy with one another via a spin-spin interaction. The strength of the spin-spin interaction is proportional to the inverse cube of the distance between the centers [47]. Conceivably, the E' centers near the Si/SiO_2 interface could be detected via some indirect spin-spin interaction of as yet unestablished origin.

Previous studies have investigated differences in radiation hard and soft oxides [48-50]. One recent study involving

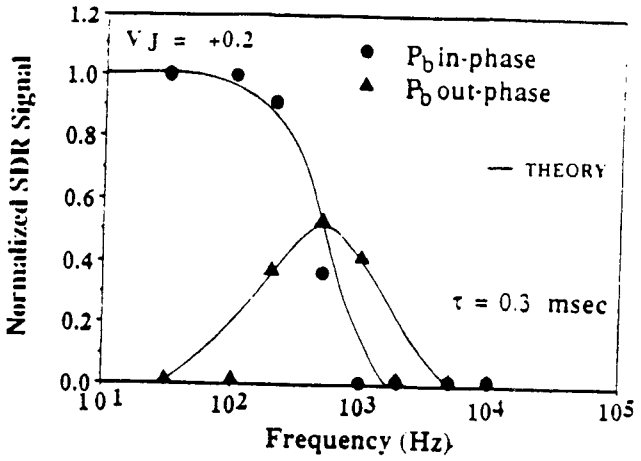

Figure 8 P_{bo} center's In-phase and Out-of-phase SDR signals versus magnetic field modulation frequency.

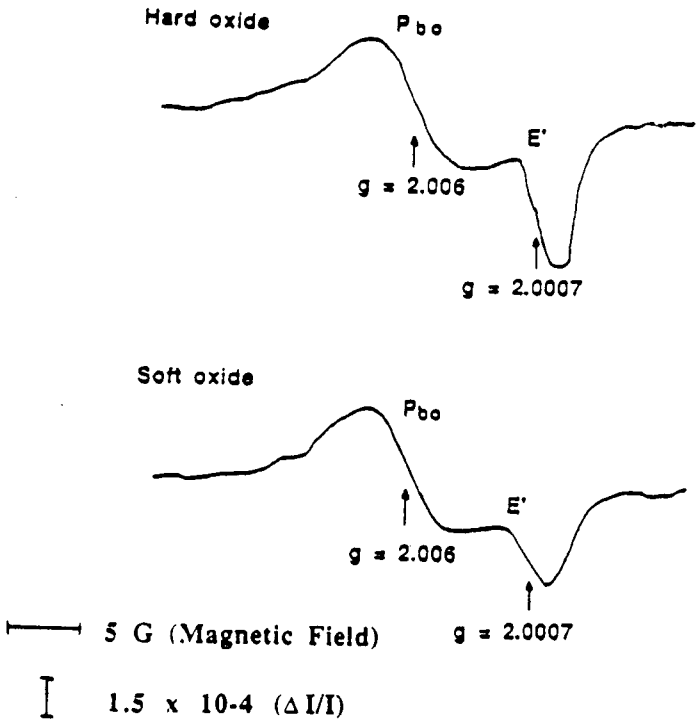

Figure 9 P_{bo} and E' spectra for both hard (9a) and soft (9b) oxides.

annihilation of holes via tunneling [48] shows that quite substantial differences exist in the distribution of trapped holes in hard and soft oxides. The trapped holes are trapped very close to the Si/SiO_2 interface in hard oxides; the trapped hole distribution extends well into the oxide in softer devices. Another study involving XPS (X-ray photoemission spectroscopy) revealed differences in the amount of strain at the Si/SiO_2 interface in hard and soft oxides [49,50]. The results indicated that in hard oxides the strained transition region was much narrower than in the soft oxides.

Our results regarding E' must be regarded as preliminary. The SDR technique is clearly sensitive to E's presence in MOSFETs; SDR shows they are not present before irradiation, but are present afterward. SDR shows that they are "close" to the Si/SiO_2 interface. The SDR results suggest that the E' centers are closer to the Si/SiO_2 boundary in hard oxides than in soft oxides.

SUMMARY AND CONCLUSIONS

In this study we used SDR to observe the radiation induced buildup of P_{bo} and E' centers in relatively hard and soft oxide devices. The SDR technique allowed rapid detection of low ($\sim 10^{11}$ P_{bo}/cm^2) densities of radiation induced defects in individual MOSFETs in integrated circuits, where conventional ESR detection is impossible. Confirming earlier studies, P_{bo} centers were found to play a dominant role in surface recombination, as one would expect for interface defects with levels near midgap. The average capture time of the midgap interface states was found to agree quite well with the SDR's modulation frequency dependence for the P_{bo} center. Finally, differences in the magnitude of the E' spectra in both the hard and soft oxides is tentatively attributed to E' centers residing, on the average, closer to the interface in a hard oxide.

ACKNOWLEDGMENTS

The authors would like to thank Greg Dunn of MIT Lincoln Laboratories for the MOSFETs used in this study. This work was sponsored by Sandia National Laboratories under Contract #03-3999 and the Defense Nuclear Agency under Contract #DNA002-86-0055.

REFERENCES

[1] H. L. Hughes and R. A. Giroux, Electronics **37**, 58 (1964).

[2] K. H. Zaininger, IEEE Trans. Nucl. Sci **NS-13**, 237 (1966).

[3] J. R. Szedon and J. E. Sandor, Appl. Phys. Lett. **6**, 181 (1965).

[4] R. J. Powell and G. F. Derbenwick, IEEE Trans. Nucl. Sci. **NS-18**, 99 (1971).

[5] P. S. Winokur and M. M. Sokoloski, Appl. Phys. Lett. **28**, 627 (1976).

[6] F. B. McLean, IEEE Trans. Nucl Sci. **NS-27**, 1651 (1980).

[7] P. M. Lenahan and P. V. Dressendorfer, Appl. Phys. Lett. **41**, 542 (1982).

[8] P. M. Lenahan and P. V. Dressendorfer, J. Appl. Phys. **55**, 3495 (1984)

[9] Y. Nishi, Jpn. J. Appl. Phys. **10**, 52 (1971).

[10] Y. Nishi, K. Tanaka, A. Ohwada, Jpn. J. Appl. Phys. **11**, 85 (1972).

[11] P. J. Caplan, E. H. Poindexter, B. E. Deal, and R. R. Razouk, J. Appl. Phys. **50**, 5847 (1979).

[12] E. H. Poindexter, P. J. Caplan, J. J. Finnegan, N. M. Johnson, D. K. Biegelsen, and M. D. Moyer in The Physics of MOS Insulators edited by G. Lucovsky, S. T. Pantelides, and F. L. Galeener, Pergamon, New York, 1980, p. 326.

[13] P. M. Lenahan and P. V. Dressendorfer, Appl. Phys. Lett **44**, 96 (1984).

[14] P. M. Lenahan, K. L. Brower, P. V. Dressendorfer, W. C. Johnson, IEEE Trans. Nucl Sci **NS-28**, 4105 (1981).

[15] P. M. Lenahan and P. V. Dressendorfer, J. Appl. Phys. **54**, 1457 (1983).

[16] Y. Y. Kim and P. M. Lenahan, J. Appl. Phys. **64**, 3551 (1988).

[17] R. A. Weeks, J. Appl. Phys. **27**, 1376 (1956).

[18] R. H. Silsbee, J. Appl. Phys. **32**, 1459 (1961).

[19] F. J. Feigl, W. B. Fowler, and K. L. Yip, Solid State Commun. **14**, 225 (1974).

[20] C. L. Marquandt and G. H. Sigel, IEEE Trans. Nucl. Sci **22**, 2234 (1975).

[21] P. M. Lenahan and P. V. Dressendorfer, IEEE Trans. Nucl. Sci **NS-29**, 1459 (1982).

[22] P. M. Lenahan and P. V. Dressendorfer, IEEE Trans. Nucl. Sci **NS-30**, 4602 (1983).

[23] H. S. Witham and P. M. Lenahan, Appl. Phys. Lett **51**, 1007 (1987).

[24] H. S. Witham and P. M. Lenahan, IEEE Trans. Nucl. Sci **NS-39**, 1147 (1987).

[25] T. Takahashi, B. B. Triplett, K. Yokogawa, and T. Sugano, Appl. Phys Lett **51**, 1334 (1987).

[26] H. Miki, M. Noguchi, K. Yokogawa, B. Kim, K. Osada, and T. Sugano, IEEE Trans. Electron Devices **35**, 2245 (1988).

[27] D. J. Lepine, Phys. Rev. **B6**, 436 (1972).

[28] I. Solomon, Solid-State Comm. **20**, 215 (1976).

[29] I. Solomon, D. Biegelsen, and J. C. Knights, Solid State Comm. **22**, 505 (1977).

[30] P. M. Lenahan and W. K. Schubert, Phys. Rev. B30, 1544 (1984).

[31] M. C. Chen and D. V. Lang, Phys Rev Lett **51**, 427 (1983).

[32] B. Henderson, Appl. Phys. Lett. **44**, 228 (1984).

[33] R. L. Vranch, B. Henderson, and M. Petter, Appl. Phys. Lett. **52**, 1161 (1988).

[34] R. M. White and J. F. Gouyet, Phys. Rev **B16**, 3596 (1977).

[35] V. S. Livov, O. V. Tretyak, and J. A. Kolomiets, Sov. Phys. Semicond. **11**, 661 (1977).

[36] D. Kaplan, I. Solomon, and N. F. Mott, J. Phys. Lett. (Paris) **39**, L51 (1978).

[37] A. S. Grove and D. J. Fitzgerald, Solid-State Electron, 9, 783 (1966).

[38] D. J. Fitzgerald and A. S. Grove, Surface Sci. 9, 347 (1968).

[39] E. H. Snow, A. S. Grove, and D. J. Fitzgerald, Proc. IEEE **55**, 1168 (1967).

[40] D. J. Fitzgerald and A. S. Grove, Proc. IEEE Lett. **54**, 849 (1966).

[41] R. F. Pierret, Solid-State Electron. **17**, 1257 (1974).

[42] W. Shockley and W. T. Read, Phys. Rev. **87**, 835 (1952).

[43] R. Castagne and A. Vapaille, Surface Sci. **28**, 157 (1971).

[44] L. M. Terman, Solid-State Electron. **5**, 285 (1962).

[45] E. H. Nicollian and J. R. Brews, MOS Physics and Technology, Wiley, New York, 1982, Chap. 6.

[46] E. H. Poindexter, P. J. Caplan, B. E. Deal, and R. R. Razouk, J. Appl. Phys. **52**, 879 (1981).

[47] A. Abrigam and B. Bleaney, Electron Paramagnetic Resonance of Transition Ions, Oxford University Press, Oxford, England,1970, Chap. 9.

[48] T. R. Oldham, A. J. Lelis, and F. B. McLean, IEEE Trans. Nucl. Sci. **NS-33**, 1203 (1986).

[49] F. J. Grunthaner, B. F. Lewis, N. Zamani, and J. Maserjian, IEEE Trans. Nucl. Sci. **NS-27**, 1640 (1980).

[50] F. J. Grunthaner, P. J. Grunthaner, and J. Maserjian, IEEE Trans. Nucl. Sci. **NS-29**, 1462 (1982).

SPIN DEPENDENT RECOMBINATION: A ^{29}Si HYPERFINE STUDY OF RADIATION-INDUCED P_b CENTERS AT THE Si/SiO_2 INTERFACE

M. A. Jupina and P. M. Lenahan
Pennsylvania State University

ABSTRACT

The spin dependent recombination (SDR) technique is used to observe the ^{29}Si hyperfine spectra of radiation-induced P_b centers at the Si/SiO_2 interface in a MOSFET. The P_b center is a paramagnetic, trivalent silicon defect that is the dominant radiation-induced interface state. The ^{29}Si hyperfine spectra give detailed atomic scale information about the P_b center. Our SDR results show that the ^{29}Si hyperfine spectra vary with surface potential. This result indicates that differences in the defect's local geometry lead to substantial differences in the defect's energy level. However, the ^{29}Si hyperfine spectra are found to be relatively independent of the ionizing radiation dosage.

INTRODUCTION

The performance of metal-oxide-semiconductor (MOS) field effect transistors (MOSFETs) may be substantially degraded by exposing the devices to ionizing radiation [1-3]. The devices experience a loss of channel conductance and transconductance as well as thresold voltage shifts. The damage involves primarily the generation of interface states at the Si/SiO_2 boundary and the trapping of holes in the oxide. Although the first significant work on radiation damage in MOSFETs took place over 25 years ago [1], a complete atomic scale picture of the radiation damage process has yet to emerge.

Several years ago, Lenahan and Dressendorfer contributed to the atomic scale understanding of the radiation damage process by identifying the point defects which are primarily responsible for the radiation-induced interface state defects and the hole trapping [4,5]. They used electron spin resonance (ESR) and electrical measurements of rather large (~1 cm^2) MOS capacitors to show that a trivalent silicon defect at the Si/SiO_2 interface, the P_b center, is the dominant radiation-induced interface state and that an oxygen deficient silicon defect in the oxide, the E' center, is the dominant hole trapping site.

Although the ESR results provide a considerable atomic scale understanding of radiation-induced defects, a clear picture of the role that a defect's configuration and the role that atomic scale strain ("bond strain") play in the radiation damage process in MOS devices is far from complete. In previous studies, the role of atomic scale strain in driving the radiation damage process at the Si/SiO_2 interface [6,7] and the role of a defect's configuration in determining the distribution of radiation-induced interface states [8,9] has been discussed. However, direct measurements of these quantities on an atomic scale have been virtually nonexistant. Hyperfine spectra of the P_b center, as observed by the spin dependent recombination (SDR) technique in MOSFETs [10,11], provides detailed atomic scale information to address these issues.

The hyperfine spectra of a paramagnetic defect results from the interaction of an unpaired electron's magnetic moment with the moment of a magnetic nucleus. The hyperfine spectra in silicon-based materials occurs since the ^{29}Si atom has a spin 1/2 nucleus which changes the local magnetic field seen by the unpaired electron in the dangling bond orbital. Because the natural abundance of the ^{29}Si atom is 4.7%, the result is two smaller satellite spectra on each side of the primary ^{28}Si

0018-9499/90/1200-1650$01.00 © 1990 IEEE

Zeeman spectra. The magnetic field separation of the hyperfine spectra gives us information about the amount of s-character and p-character a dangling bond orbital has and also how localized the unpaired electron in a dangling bond orbital is.

Previous ESR measurements [4] have shown that the P_b centers have an electronic density of states which is broadly distributed through the middle ~2/3 of the silicon band gap. The center accepts one electron (becoming paramagnetic) when the Fermi energy moves from near the valence band edge to near midgap. It accepts a second electron when the Fermi energy moves from midgap towards the conduction band edge. The P_b/MOS system thus provides a (perhaps unique) system in which the relationship between a paramagnetic defect's wave function hybridization and energy level may be experimentally observed.

We observe for the first time the surface potential dependence of the ^{29}Si hyperfine spectra of radiation-induced P_b centers by the SDR technique for devices with n-type and p-type substrates and for a device subjected to two different dosages of ionizing radiation. We find that the ^{29}Si hyperfine tensors change significantly with a change in surface potential. However, we find that the ^{29}Si hyperfine tensors are relatively unchanged for a device subjected to two different dosages of ionizing radiation.

EXPERIMENTAL PROCEDURES AND RESULTS

In our SDR hyperfine measurements, we used both n-channel and p-channel MOSFETs. The n-channel MOSFET had a 62.5 nm thick gate oxide which was grown in steam at 900 C. This device had a p-type silicon substrate with a (111) surface orientation and $2x10^{15}/cm^3$ doping density. The transistor gate material was polycrystalline silicon. The p-channel MOSFET had a 25 nm thick gate oxide which was grown in dry O_2 at 900 C and annealed for 30 minutes in N_2 at 900 C. This device had a n-type silicon substrate with a (100) surface orientation and $10^{15}/cm^3$ doping density. The transistor gate material was ~10 nm thick aluminum. Both devices had gate areas of $\sim 10^{-4}$ cm^2.

Since the P_b centers' energy levels are distributed throughout the middle two-thirds of the silicon band gap, they are effective recombination centers [12]. The SDR technique exploits the electrically-active, paramagnetic nature of the P_b center. When the electron spin resonance condition for the P_b center is satisfied, the change in the spin polarization of the trap results in the enhancement of the recombination current within a MOSFET configured as a gate-controlled diode [13]. The SDR measurements are made with the p-n junctions of the device slighty forward biased (~0.1 V). With the p-n junctions slightly forward biased and the gate bias such that the silicon surface underneath the gate is depleted of carriers, the current is dominated by the recombination processes occurring at the P_b centers at the Si/SiO_2 interface. The spin resonance of the P_b centers is then observed through changes in the recombination current.

The MOSFET of an integrated circuit was centered in a TE_{102} cavity of a model 8300 Micro-Now X-band ESR spectrometer. The loaded cavity had a Q of about 5000. A 100 mW X-band (9.5 GHz) solid state oscillator applied a continuous microwave field to the resonant cavity while a large (~3500 G) slowly varying magnetic field and a small ac (~10 G_{pp} and ~100 Hz) magnetic field were simultaneously also applied. The ac magnetic field permitted phase sensitive detection of the SDR signals. Variations in the recombination current were monitored using a current-to-voltage pre-amplifier and a lock-in amplifier (Ithaco Dynatrac Model 393). The system detected SDR currents smaller than 10 fA. The observed spectra are approximately the first derivative of an "absorption-like" curve.

In this study, the n-channel device was irradiated with ^{60}Co gamma rays to a total dosage of 3 Mrads(Si), while a bias of +6.25 V was applied to the poly-Si gate. The p-channel device was irradiated with VUV light (10.2 eV) to two different total dosages (4 hours and 12 hours, respectively),

while a bias of +5 V was applied to its semi-transparent aluminum gate. After irradiation, the interface state density (D_{it}) versus the silicon band gap energy (0 eV represents midgap) is as shown in Figure 1 for both devices and for the two dosages of VUV irradiation for the semi-transparent gate device. These results were obtained from a Terman analysis [14] of a high frequency (1MHz) capacitance versus gate voltage (CV) curve of the MOSFET.

In Figure 2 and 3, we illustrate four SDR traces from the n-channel device with the (111) silicon substrate. The traces were taken at two orientations of the Si/SiO_2 interface with respect to the magnetic field: 0^o corresponds to the magnetic field parallel to the <111> direction as shown in Figure 2 and 90^o corresponds to the magnetic field perpendicular to the <111> direction as shown in Figure 3. At both orientations the measurement was made at two values of the surface potential which corresponds to a difference of approximately 0.3 eV. Each of the four spectra consist of a very large central line and two smaller satellite spectra. The central line has a g-value of g = 2.0014 when the magnetic field is parallel to the <111> direction and a g-value of g = 2.008 when the field is perpendicular to the <111> direction. The central line's g-tensor is independent of gate bias. However, the hyperfine tensor is not.

When the magnetic field orientation is parallel to the <111> direction and the gate bias places E_{Fp} near midgap, the hyperfine splitting is 134 G; however, for a gate bias placing E_{Fp} near flat band, the hyperfine splitting changes to 152 G. When the magnetic field orientation is perpendicular to the <111> direction and with E_{Fp} near midgap, the hyperfine splitting is 98 G; again, with E_{Fp} near flat band, the hyperfine splitting changes to 92 G. The positions of E_{Fp} at the silicon surface for both gate biases are denoted in Figure 1 by solid triangles labelled A (flat band) and B (midgap).

In our SDR study, as in a previous ESR study of radiation-induced interface states [15], only the P_{b0} center is observed on oxidized (100) silicon

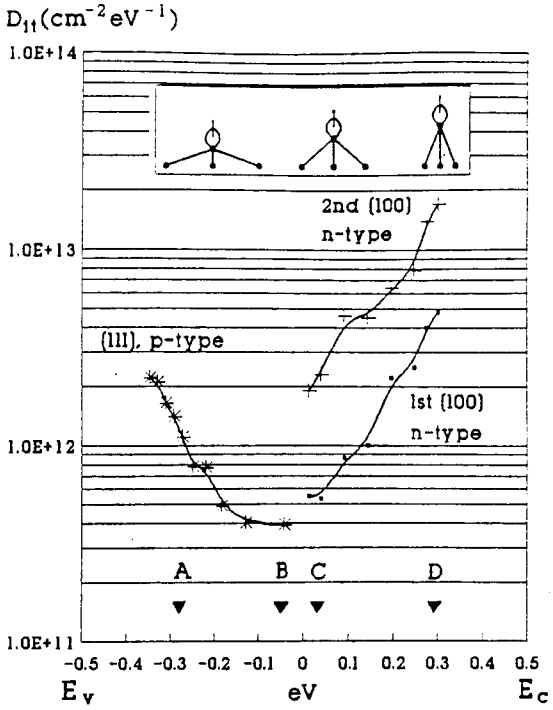

Figure 1. A plot of the interface state density (D_{it}) versus the silicon band gap energy (0 eV represents midgap). E_c and E_v are the conduction and valence energies, respectively. The solid triangles denoted by A and B represent the position of E_{Fp} at the silicon surface for each set of hyperfine traces in Figures 2 and 3, while the solid triangles denoted by C and D represent the position of E_{Fn} at the silicon surface for each set of hyperfine traces in Figures 4 and 5. The ball and stick models qualitatively illustrate the relaxation of the P_b center's structure as a function of energy.

surfaces after irradiation. Previous ESR measurements [15,16] of g-tensor mappings indicate that the P_{b0} center at the $SiO_2/Si(100)$ interface is essentially identical to the P_b center at the $SiO_2/Si(111)$ interface. The P_{b0} center has four possible orientations, each lying 54.7^o with respect to the <100> direction. Due to the symmetry of the g-tensor of the P_{b0} center, the hyperfine spectra of the P_{b0} center are best resolved at the orientations of 0^o and 55^o with respect to the <100> direction or equivalently, at the orientations of 55^o and 0^o with respect to the <111> direction.

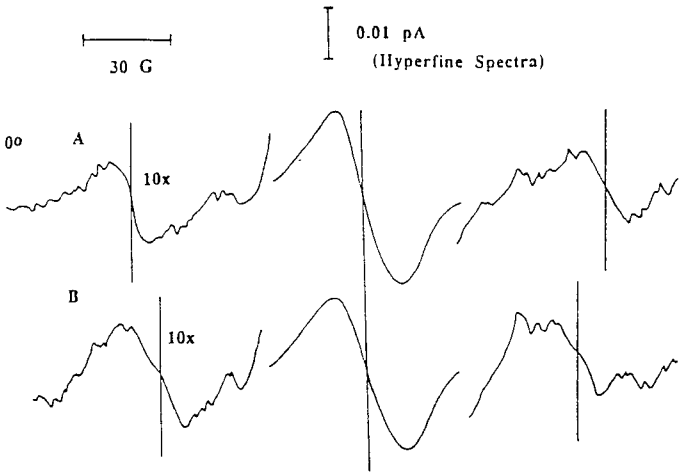

Figure 2. SDR hyperfine spectra for two different positions of E_{Fp} at the silicon surface. The positions of E_{Fp} for A and B are shown in Figure 1. The orientation of 0^o is defined by the angle θ in Figure 6.

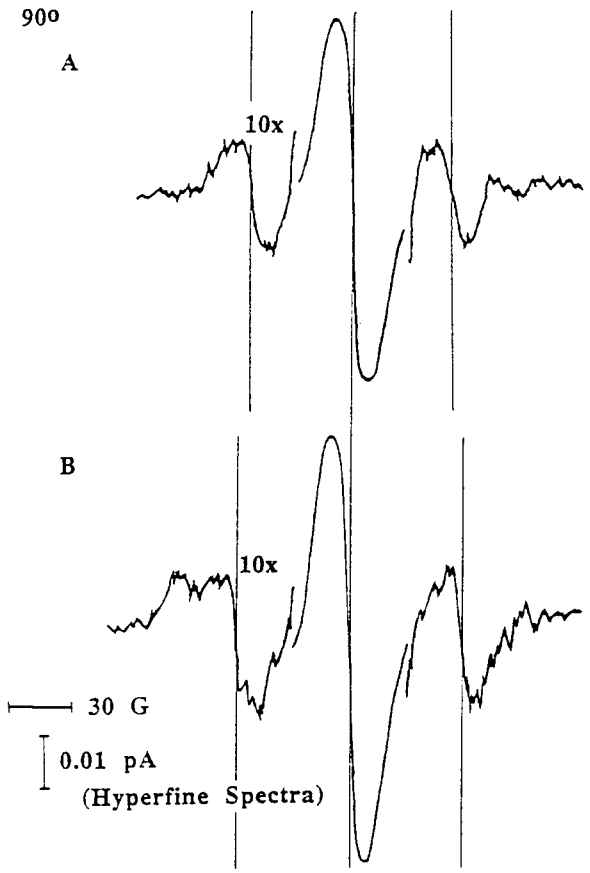

Figure 3. SDR hyperfine spectra for two different positions of E_{Fp} at the silicon surface. The positions of E_{Fp} for A and B are shown in Figure 1. The orientation of 90^o is defined by the angle θ in Figure 6.

In Figures 4 and 5, we illustrate four SDR traces from the p-channel device with the (100) silicon substrate after an initial 4 hour dose of VUV irradiation. The traces were taken at two orientations of the $SiO_2/Si(100)$ interface with respect to the magnetic field: 0^o (Figure 4) and 55^o (Figure 5) with respect to the <111> direction. At both orientations the measurement was made again at two values of the surface potential which corresponds to a difference of approximately 0.3 eV.

When the magnetic field orientation lies 55^o with respect to the <111> direction (Figure 5) and the gate bias places E_{Fn} near midgap, the hyperfine splitting is 106 G; however, for a gate bias placing E_{Fn} near flat band, the hyperfine splitting changes to 92 G. When the magnetic field orientation is parallel to the (111) direction (Figure 4), two possible hyperfine splittings are observed for g = 2.0014 and g = 2.0073. With E_{Fn} near midgap, the hyperfine splittings are 133 G (g = 2.0014) and 95 G (g = 2.0073); again, with E_{Fn} near flat band, the hyperfine splittings change to 110 G and 85 G, respectively. The positions of E_{Fn} at the silicon surface for both gate biases are denoted in Figure 1 by solid triangles labelled C (midgap) and D (flat band).

After the p-channel device with the (100) silicon substrate was subjected to a second dose of VUV irradiation for a total of 12 hours, the hyperfine splittings for both orientations and gate biases were found to be relatively unchanged. These results along with the previous results are summarized in Table 1.

DISCUSSION OF RESULTS

Our hyperfine results of Figures 2 through 5 correspond to P_b centers with energy levels that span ~2/3 of the silicon band gap. These figures demonstrate that these P_b centers have significantly different hyperfine tensors. Therefore, these hyperfine results can be analyzed to yield information about differences in the hybridization

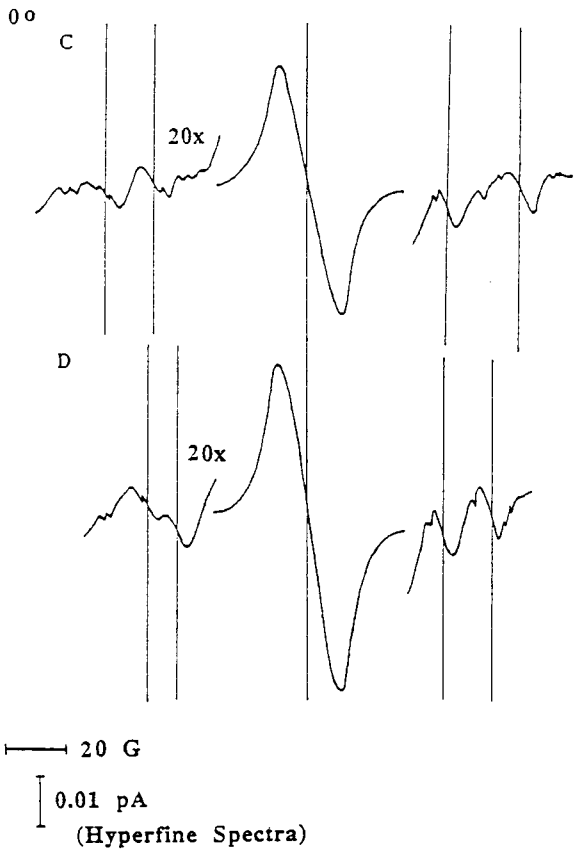

Figure 4. After 4 hours of VUV, SDR hyperfine spectra for two different positions of E_{Fn} at the silicon surface. The positions of E_{Fn} for C and D are shown in Figure 1. The orientation of 0^{o} is defined by the angle θ in Figure 6.

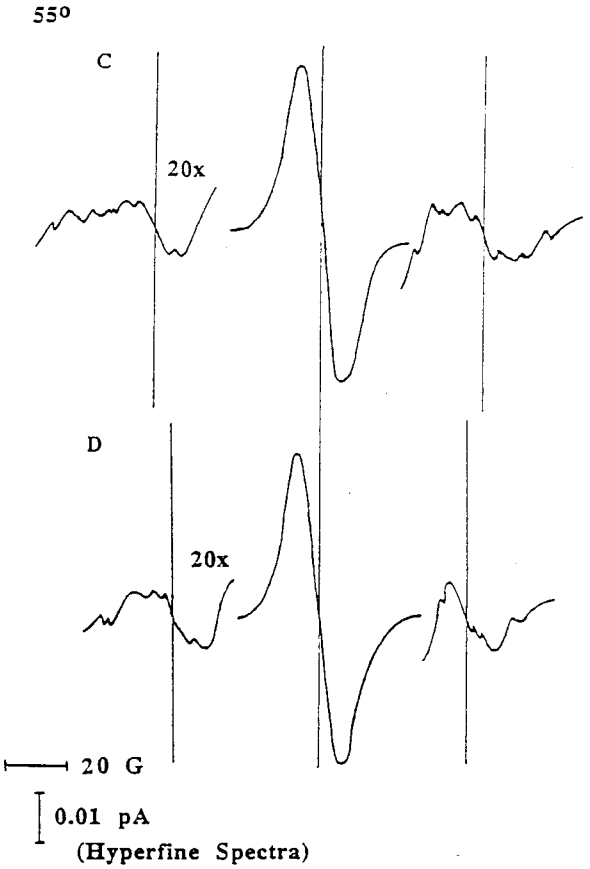

Figure 5. After 4 hours of VUV, SDR hyperfine spectra for two different positions of E_{Fn} at the silicon surface. The positions of E_{Fn} for C and D are shown in Figure 1. The orientation of 55^{o} is defined by the angle θ in Figure 6.

and bond angles which correspond to the differences in energy level.

Using the standard linear combination of atomic orbitals (LCAO) approach [17], the effective hyperfine splitting of a dangling bond due to the central silicon atom is given by a second rank tensor with axial symmetry; this yields an orientation dependent hyperfine coupling of the form

$$A(\theta) = A_s + A_p(3\cos^2\theta - 1) \qquad (1)$$

where θ is the orientation of the magnetic field with respect to the P_b center's C_{3v} symmetry axis (<111> axis) as shown in Figure 6, A_s is the measured isotropic interaction, and A_p is the measured anisotropic interaction. The isotropic (Fermi contact) interaction, A_{iso}, with the central silicon atom of the defect is given by

$$A_{iso} = (8\pi/3)g_e\mu_e g_N\mu_N |\Psi_{3s}(0)|^2 \qquad (2)$$

and the anisotropic dipole-dipole interaction A_{aniso} is approximately given by

$$A_{aniso} = (2/5)g_e\mu_e g_N\mu_N\langle r_{3p}^{-3}\rangle \qquad (3)$$

where g_e and g_N denote the electronic and nuclear g-values, respectively, and μ_e and μ_N denote the electronic and nuclear magnetons, respectively. Here $|\Psi_{3s}(0)|^2$ represents the value of the 3s wavefunction at the central silicon nucleus and $\langle r_{3p}^{-3}\rangle$ represents the expectation value of r^{-3} evaluated over the central silicon atom's 3p wave function.

A molecular cluster with a dangling bond on a silicon atom is shown in Figure 6. At the center silicon site, we approximate Ψ as a hybrid 3s3p orbital given by

$$\Psi = \alpha\eta(\Psi_{3s}) + \beta\eta(\Psi_{3p}) \qquad (4)$$

Table 1. Summary of the Hyperfine data for the P_b center.

(111), p-type

	A_{iso}(G)	A_{aniso}(G)	η^2	α^2	β^2	ρ (deg)	Φ (deg)
A	112	20	0.74	0.13	0.87	104.3	114.1
B	110	12	0.48	0.19	0.81	107.1	111.7

(100), n-type

		A_{iso}(G)	A_{aniso}(G)	η^2	α^2	β^2	ρ (deg)	Φ (deg)
C	1st	105	14	0.54	0.16	0.84	105.8	112.9
	2nd	103	13	0.50	0.17	0.83	106.3	112.5
D	1st	92	9	0.37	0.21	0.79	108.0	110.9
	2nd	95	10	0.40	0.20	0.80	107.5	111.3

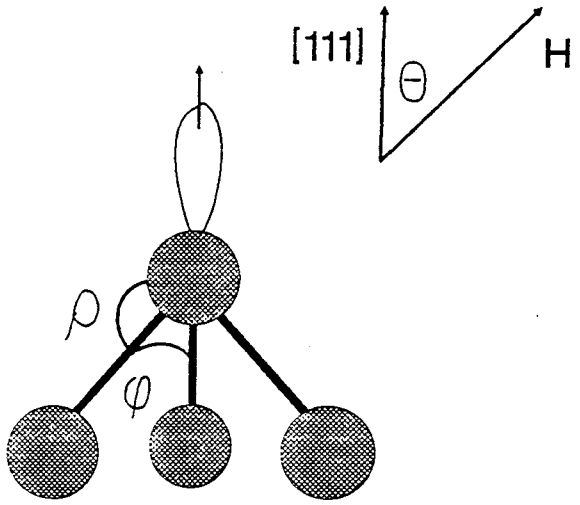

Figure 6. A molecular cluster displaying a silicon dangling bond. The angles ρ, Φ, and θ are defined in the text. The symmetry axis is denoted by the [111] axis and H is the magnetic field direction with respect to this axis.

The localization parameter, η^2, represents the fraction of the total wavefunction localized on the central silicon site. For the unpaired electron on this site, the percentage of s-character is given by α^2 and the percentage of p-character is given by β^2. For an "ideal" sp^3 dangling bond orbital, the parameters would be $\eta^2 = 1$, $\alpha^2 = 1/4$, and $\beta^2 = 3/4$.

At this point, $|\Psi_{3s}(0)|^2$ is approximated by an atomic silicon Hartree-Fock 3s wave function and $\langle r_{3p}^{-3} \rangle$ is approximated by the expectation value of r^{-3} evaluated over an atomic silicon Hartree-Fock 3p wave function. For $|\Psi_{3s}(0)|^2 = 3.807\ a_o^{-3}$ and $\langle r_{3p}^{-3} \rangle = 2.041\ a_o^{-3}$ (where a_o is the Bohr radius), the atomic values for A_{iso} and A_{aniso} are 1206 G and 31 G, respectively [18]. By comparing the theoretical values of A_{iso} and A_{aniso} with the measured values of A_s and A_p and assuming the normalization condition of $\alpha^2 + \beta^2 = 1$, we obtain the hybridization parameters for the four values of surface potential.

Brower was the first to observe the ^{29}Si hyperfine spectra of the P_b center [19]. He used standard ESR detection at 20 K. His measurements were on oxidized p-type (111) wafers. The relatively high density of P_b centers ($\sim 4 \times 10^{12}/cm^2$) in his large area ($\sim 30\ cm^2$) sample was induced through high temperature processing. Brower's analysis of the hyperfine spectrum indicated that approximately 80% of the total wavefunction is localized on the central silicon atom and that the hybrid orbital on this silicon atom is 12% s-like and 88% p-like.

In addition to the hyperfine and LCAO parameters we also list bond angles ρ and Φ in Table 1 (angles defined in Figure 6). Coulson has argued that bond angles may be calculated from the sp hybridization ratio [20]. For a point defect with C_{3v} symmetry and orthogonal sp hybrids, the angle between the dangling bond and the back bonds should be given by

$$\tan \rho = -(2(1 + \lambda^2))^{1/2} \qquad (5)$$

and the angle Φ between any two of the back bonds should be given by

$$\cos \Phi = (1.5 / (2\lambda^2 + 3) - 1/2) \qquad (6)$$

where, in both cases, $\lambda = \beta/\alpha$.

A number of authors have argued that hyperfine parameters may be used to calculate defect bond angles, generally using an analysis similiar to our own [21-23]. Although our arguments regarding bond angles are physically reasonable, the values for ρ and Φ in Table 1 should not be viewed as extremely precise. They are subject to several

sources of error. For example, there is a worst-case error of +/- 2.5 G in the hyperfine splittings. As another example, the LCAO model may not be an extremely precise description for unpaired spins on silicon atoms at the Si/SiO_2 interface [24]. Nevertheless, our results show that a difference of several degrees (~3 degrees) in the angle correspond to several tenths of an electron volt change (~0.5 eV) in P_b center's energy level.

Calculations for the neutral one-electron level of the P_b-like centers indicate that the energy is minimized when the s-character is within the range of $0.08 < \alpha^2 < 0.25$ [25]. Similiar calculations [26] also indicate that the back bonds are relaxed to a more planar configuation than would be anticipated for an "ideal" sp^3 hybrid. For all values of the amount of s-character at each surface potential evaluated in our measurements (Table 1), this appears to be the case.

The general trend observed in Table 1 is that the P_b centers' hybridization is less s-like and its structure is slightly more relaxed-back in the lower half of the silicon band gap than in the upper half of the silicon band gap. Consequently, this trend is consistent with the tight-binding approximation of diamond-structured materials, where the valence band is strongly p-like, whereas the conduction band is strongly s-like [27]. These conclusions are qualitatively illustrated in Figure 1 with ball and stick models.

For the device subjected to two different dosages of ionizing radiation, we find the hyperfine splittings to be relatively unchanged at each of the surface potentials investigated (Table 1) and the interface state density distributions to be qualitatively the same in the upper half of the silicon band gap (Figure 1). This observation is consistent with the notion that the creation of an interface state involves the release of very localized strain at the Si/SiO_2 interface, whereas the macroscopic strain at the interface is relatively unchanged. If the overall strain at the Si/SiO_2 interface did change with the level of ionizing radiation, the P_b center's geometry and thus ^{29}Si hyperfine parameters would change significantly at a given energy level [26].

CONCLUSIONS

Through the use of the SDR technique, our results establish that the local geometry of a P_b center can directly determine its energy level within the silicon band gap. The hybridization parameters of the P_b centers in the upper half of the silicon band gap are found to be more s-like and more delocalized than the hybridization parameters in the lower half of the silicon band gap. Finally, no significant differences in the hyperfine parameters of the P_b center are observed for two different levels of irradiation of a device.

ACKNOWLEDMENTS

The authors would like to thank Nelson Saks of the Naval Research Laboratory for supplying the MOSFETs used in this study. This work was sponsored by the Defense Nuclear Agency under contract #DNA002-86-0055 and Sandia National Laboratories under contract #03-3999.

REFERENCES

1. H. L. Hughes and R. A. Giroux, "Space Radiation Affects MOSFETs," Electronics 37, 58 (1964).
2. R. J. Powell and G. F. Derbenwick, "Vacuum Ultraviolet Radiation Effects in SiO_2," IEEE Trans. Nucl. Sci. NS-18, 99 (1971).
3. F. B. McLean, "A Framework for Understanding Radiation-Induced Interface States in SiO_2 MOS Structures," IEEE Trans. Nucl. Sci. NS-27, 1651 (1980).
4. P. M. Lenahan and P. V. Dressendorfer, "Effect of Bias on Radiation Induced Paramagnetic Defects at the Silicon-Silicon Dioxide Interface," Appl. Phys. Lett. 41, 542 (1982).
5. P. M. Lenahan and P. V. Dressendorfer, "Hole Traps and Trivalent Silicon Centers in Metal/Oxide/Semiconductor Devices," J. Appl. Phys. 55, 3495 (1984).

6. F. J. Grunthaner, B. F. Lewis, N. Zamini, J. Maserjian, and A. Madhukar, "XPS Studies of Structure-Induced Radiation Effects at the Si/SiO_2 Interface," IEEE Trans. Nucl. Sci. NS-27, 1640 (1980).
7. F. J. Grunthaner, P. J. Grunthaner, and J. Maserjian, "Radiation-Induced Defects in SiO_2 as Determined with XPS," IEEE Trans. Nucl. Sci. NS-29, 1462 (1982).
8. Y. Wang, T.P. Ma, and R. C. Barker,"Orientation Dependence of Interface-Trap Transformation," IEEE Trans. Nucl. Sci. NS-36, 1784 (1989).
9. V. Zekeriya and T. P. Ma, "Dependence of X-ray Generation of Interface Traps on Gate Metal Induced Interfacial Stress in MOS Structures," IEEE Trans. Nucl. Sci. NS-31, 1261 (1984).
10. R.L. Vranch, B. Henderson, and M. Pepper, "Spin Dependent Recombination in Irradiated Si/SiO_2 Device Structures," Appl. Phys. Lett. 52, 1161 (1988).
11. M. A. Jupina and P. M. Lenahan, "A Spin Dependent Recombination Study of Radiation Induced Defects At and Near the Si/SiO_2 Interface," IEEE Trans. Nucl. Sci. NS-36, 1800 (1989).
12. W. Shockley and W. T. Read, "Statistics of the Recombination of Holes and Electrons," Phys. Rev. 87, 835 (1952).
13. A. S. Grove and D. J. Fitzgerald, "Surface Effects on P-N Junctions: Characteristics of Surface Space-Charge Regions Under Non-Equilibrium Conditions," Solid State Electron 9, 783 (1966).
14. L. M. Terman, "An Investigation of Surface States at a Silicon/Silicon Oxide Interface Employing Metal-Oxide-Silicon Diodes," Solid State Electron. 5, 285 (1962).
15. Y. Y. Kim and P. M. Lenahan, "Electron Spin Resonance Study of Radiation - Induced Paramagnetic Defects in Oxides Grown on (100) Silicon Substrates," J. Appl. Phys. 64, 3551 (1988).
16. E. H. Poindexter, P. J. Caplan, B. E. Deal, and R. R. Razouk, "Interface States and Electron Spin Resonance Centers in Thermally Oxidized (111) and (100) Silicon Wafers," J. Appl. Phys. 52, 879 (1981).
17. G. D. Watkins and J. W. Corbett, "Defects in Irradiated Silicon: Electron Paramagnetic Resonance and Electron-Nuclear Double Resonance of the Si-E Center," Phys. Rev. 134, A1359 (1964).
18. J. R. Morton, "Electron Spin Resonance Spectra of Oriented Radicals," Chem. Rev. 64, 453 (1964).
19. K. L. Brower, "^{29}Si Hyperfine Structure of Unpaired Spins at the Si/SiO_2 Interface," Appl. Phys. Lett. 43, 1111 (1983).
20. C. A. Coulson, Valence, Oxford University, London, 1961, p. 203.
21. D. L. Griscom, E. J. Friebele, and G. H. Sigel, "Observation and Analysis of the Primary ^{29}Si Hyperfine Structure of the E' Center in Non-Crystalline SiO_2," Solid-State Comm. 15, 479 (1974).
22. P. W. Atkins and M. C. R. Symons, The Structure of Inorganic Radicals, Elsevier, Amsterdam, 1967, pp. 17-23.
23. R. A. B. Devine and J. Arndt, "Si-O Bond-Length Modification in Pressure-Densified Amorphous SiO_2," Phys. Rev. B37, 6579 (1987).
24. M. Cook and C. T. White, "Molecular Electronic Structure Theory in the Study of Localized Defects," Semicond. Sci. Technol. 4, 1012 (1989).
25. W. A. Harrison, Electronic Structure and the Properties of Solids, Freeman, San Francisco, 1980, p. 187.
26. A. H. Edwards, "Theory of the P_b Center at the <111> Si/SiO_2 Interface," Phys. Rev. B36, 9638 (1987).
27. S. Wang, Fundamentals of Semiconductor Theory and Device Physics, Prentice-Hall, Englewood Cliffs, 1989, pp. 170-176.

Direct observation of interfacial point defects generated by channel hot hole injection in *n*-channel metal oxide silicon field effect transistors

J. T. Krick[a] and P. M. Lenahan
The Pennsylvania State University, University Park, Pennsylvania 16802

G. J. Dunn
Lincoln Laboratory, Massachusetts Institute of Technology, Lexington, Massachusetts 02173

(Received 14 August 1991; accepted for publication 22 October 1991)

Using a modified electron spin resonance technique known as spin-dependent recombination, we have found that channel hot hole injection in *n* channel metal oxide silicon (MOS) transistors creates the trivalent silicon dangling bond defect known as the P_{b_0} center. This letter reports the first direct identification of the atomic structure of interfacial point defects created by channel hot carrier stressing in MOS transistors.

With recent advances in the fabrication technology of integrated circuits, the size of metal oxide silicon (MOS) devices has ventured deep into the submicrometer realm. Unfortunately, inherent in the reduction of device geometries are several physical mechanisms which pose a serious threat to the reliability of large scale integrated circuits. One of the most serious of such factors, the channel hot-carrier effect, is due to the large electric fields present in the devices.[1] With the advent of a reliable charge pumping technique,[2] a great deal has been learned about the consequences of hot-carrier stressing in MOS transistors. In conventional Si/SiO_2 systems, the degradation of *n*MOS transistors is far greater than that which occurs in *p*MOS devices and has been shown to be dominated by the generation of interface states in a localized region adjacent to the drain.[3] While the actual mechanisms of this interface state generation are still unclear, hole injection is thought to play a key role in the process.[4]

Nevertheless, a fundamental understanding of the physical defects generated during hot carrier stressing is not yet available. In the past, the technique of electron spin resonance (ESR) has been used to identify various point defects created by ionizing radiation,[5] high field stress,[6] and low electron injection.[7] Unfortunately, because conventional ESR techniques require very large sample areas—typically ~ 1 cm^2, it is impossible to apply conventional ESR to investigations of hot-carrier-induced defects in short channel transistors. A modified electron spin resonance technique called spin-dependent recombination (SDR) has allowed improved sensitivity over conventional ESR techniques and has been successfully used to examine interfacial point defects in large area MOS systems.[8,9] Recent refinements of the spin-dependent recombination technique, however, have dramatically reduced the sample area and defect densities required for the accurate ESR detection of interfacial point defects.[10] We exploit these refinements in this study of hot carrier damage. To the best of our knowledge, the measurements reported here are the most sensitive ESR measurements ever made in solids.

The existence of spin-dependent recombination of carriers in silicon was first demonstrated by Lépine in 1970.[11] Although Lépine's original explanation of the phenomena is clearly an oversimplification,[12,13] it does provide a qualitative understanding. In his explanation of the phenomenon,[11] Lépine assumed that conduction electrons and holes recombine through a deep level recombination center which possesses an unpaired electron. When a magnetic field is applied to the sample, the spins of the unpaired electron in the recombination center and of the conduction electrons and holes will be polarized; that is, their spins will tend to line up with the magnetic field. Since only those conduction electrons whose spins are antiparallel to the spin of the unpaired trapped electron can "fall" into the deep level trap, the applied magnetic field has the effect of reducing the deep level's capture cross section. If microwave radiation of the appropriate frequency is applied to flip the spin of the recombination center's unpaired electron, the previously forbidden electron transitions will now be allowed and the recombination process will be encouraged. As in standard electron spin resonance detection, this applied critical microwave frequency is given by $h\nu = g\beta H$ where ν is the microwave frequency, H is the magnitude of the applied magnetic field, and β is the Bohr magneton. The constant g is actually dependent on the orientation of the applied magnetic field; its value can, in a well characterized material system, be viewed as a fingerprint identifying the structure of the defect. Spin-dependent recombination, therefore, can provide a direct method for identifying the atomic structure of defects which participate in the recombination process.[9–13] In this study, we have used SDR to provide the first account of the structure of the interfacial point defects created in short-channel *n*MOS transistors as a result of channel hot hole stressing.

The conventional source/drain devices examined in this experiment were 2700 μm wide with an effective length $L_{\text{eff}} = 0.9$ μm and a 300 Å gate oxide grown on a (100) oriented *p*-type silicon substrate. Variable frequency charge pumping measurements[2] were used to characterize the average interface state density ($\bar{D}_{it}$) in each device before and after constant voltage stressing. Prestress interface state densities were typically $\bar{D}_{it} \approx 4 \times 10^{10}$/eV cm^2. Threshold voltages were determined using a constant current method

[a]Present address: Department of Electrical Engineering and Computer Science, University of California at Berkeley, Berkeley, California 94720.

 0003-6951/91/513437-03$02.00

(i.e., the gate voltage V_g at which the drain current $I_d = 0.1\ \mu A/\mu m$ width at drain voltage $V_d = 100$ mV) and were ≈ 0.82 V in unstressed devices. The channel hot-carrier stress voltages of $V_f = 8$ V and $V_g = 1$ V (i.e., V_g slightly above threshold) were specifically chosen to focus on hole injection.[3] The SDR spectrometer used in this study was based on a Micro-Now model 8330A microwave bridge coupled with a transverse electric $(TE)_{102}$ microwave cavity. This cavity was then centered between the poles of a 4 in. electromagnet biased by a Hewlett Packard 6268B power supply. A Micro-Now model 8320A field controller allowed accurate control of the magnitude and ramp rate of the applied magnetic field. Sinusoidal magnetic field modulation (typically $3G_{pp}$ at 25 Hz) was provided by Helmholtz coils and the corresponding variations in the recombination current were detected using a Stanford Instruments model 510 lock-in amplifier. The transistors were mounted on rectangular quartz rods and centered in the cavity with the (100) Si/SiO_2 interface perpendicular to the applied magnetic field, unless indicated otherwise. Constant voltage channel hot hole stressing was performed *in situ* in the absence of any applied magnetic field or microwave energy; hence, it was not necessary to move the device at any point during the experiment. The magnetic field settings of the spectrometer and the g factor of the SDR signal were calibrated by performing separate ESR measurements on a weak pitch standard ($g = 2.0028$).

In the SDR technique, the MOS transistor is configured as a gate-controlled diode by slightly forward biasing the source-to-substrate and drain-to-substrate n–p junctions. Under these bias conditions, the current flowing through the junctions is dominated by the effects of recombination. When an appropriate gate bias is chosen to deplete the channel of charge carriers, the states at the Si/SiO_2 interface will act as additional recombination centers and can dominate the recombination process. Thus, a peak in the recombination current occurs at a gate voltage corresponding to the point at which the electron and hole quasi-Fermi levels are split about midgap. Figure 1 shows typical recombination current trace, at a constant junction forward bias of -0.25 V, of a device before and after channel hot hole injection. Initially, there is only one fairly narrow peak corresponding to the depletion of the undamaged channel oxide ($\bar{D}_{it} = 4\times 10^{10}/\ cm^2\ eV$). After 1000 s of stress at $V_d = 8$ V and $V_d = 1$ V, however, a second peak appears at a more negative gate voltage. The presence of this peak can easily be explained by the effects of varying amounts of positive charge trapping and interface state generation brought on by the channel hot hole stress. During this stress, holes injected into the oxide region adjacent to the drain can either be trapped as positive oxide charge or, by an as yet unknown mechanism, create a substantial amount of interface states. Thus, a more negative gate voltage would be required to compensate for trapped positive oxide charge in order to deplete the area under the damaged portion of the oxide and allow the generated interface states to participate in the recombination process. We can, therefore, consider the post-stress recombination current

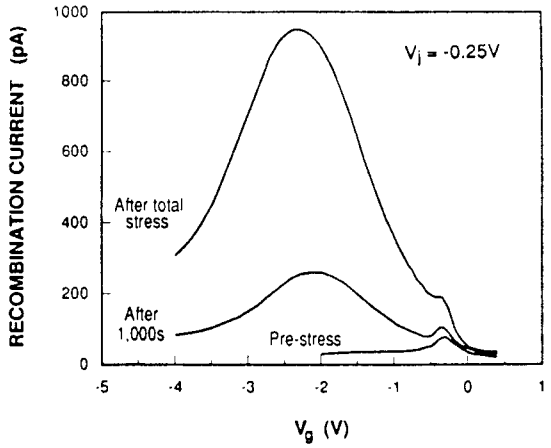

FIG. 1. Dependence of the forward biased ($V_j = -0.25$ V) gated-diode recombination current on the applied gate voltage for an nMOS transistor subjected to constant voltage stressing. The stress conditions for the "after 1000's" trace were $V_d = 8$ V and $V_g = 1$ V for 1000 s. The "total stress" consisted of 10 000 s at $V_d = 8$ V and $V_g = 1$ V and 10 000 s at $V_s = 8$ V and $V_g = 1$ V.

trace to be the sum of two separate current peaks: one corresponding to the undamaged oxide area and one at a more negative gate voltage corresponding to the damaged portion of the oxide. The SDR measurements in this study were performed while biasing the MOS structure at a gate voltage corresponding to the maximum in the recombination current.

The effect of this channel hot hole stress on the corresponding SDR spectrum of the transistor is shown in Fig. 2. Consistent with previous work,[3] the first 1000 s stress introduced a negligible threshold voltage shift ($\Delta V_t = -10$ mV) while generating a significant number of interface states ($\bar{D}_{it} = 1.0\times 10^{11}/\text{eV cm}^2$). An SDR signal is clearly visible as a direct result of this hot-carrier stress. To further degrade the device, the transistor was subjected to an additional 9000 s of stress in the forward

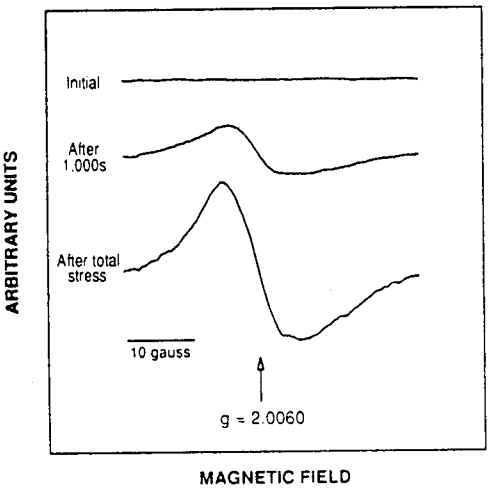

FIG. 2. SDR spectra for a transistor which has been subjected to channel hole hot stressing. The applied magnetic field is oriented perpendicular to the (100) Si/SiO_2 plane. The SDR measurements were performed while biasing the transistor at gate voltages corresponding to the peaks in the recombination current shown in Fig. 1.

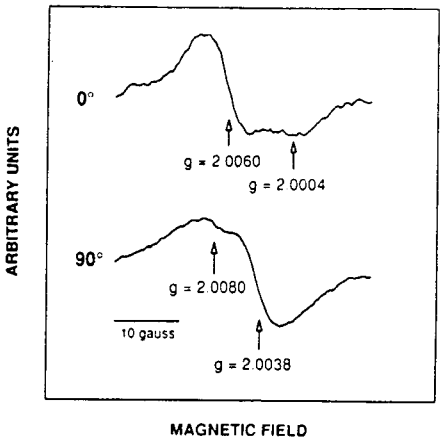

FIG. 3. Dependence of the observed SDR signal on the orientation of the applied magnetic field. The angles given indicate the direction of the applied external magnetic field with respect to the normal of the Si/SiO_2 interface. The orientation dependence is consistent with that of the P_{bo} center. The sample was rotated 90° about a (110) axis in the (100) interface plane. The position of $g = 2.0004$ is included to illustrate the possible presence of an E' signal.

direction and 10 000 s of stress in the reverse direction (i.e., $V_s = 8$ V and $V_g = 1$ V). This additional stressing nearly quadrupled the average interface state density ($\bar{D}_{it} = 3.6 \times 10^{11}$/eV cm^2) and resulted in a corresponding fourfold increase in the SDR signal. Although the SDR technique does not measure absolute spin concentrations it clearly does indicate relative changes in spin concentration. In all of our stressed devices, it was found that the amplitude of the observed SDR signal roughly scaled with the average interface state density determined by charge pumping. It was also found that the amplitude of the observed SDR signal depended on the applied gate bias; no appreciable signal was apparent when the MOS structure was biased in accumulation or inversion. Since under these bias conditions interface states cannot participate in the recombination process, we conclude that the observed SDR signal must correspond to an electrically active defect at the Si/SiO_2 interface.

Two interfacial point defects have been observed by ESR in the (100) Si/SiO_2 system: the P_{bo} and P_{bl} centers.[14] The P_{bo} center is known to be a dangling bond on a silicon atom which is bonded to three other silicon atoms at the Si/SiO_2 interface. The structure of the P_{bo} center has a characteristic ESR g value of 2.0060 for the magnetic field orientation perpendicular to the (100) interface plane.[14] The g values calculated for the SDR spectra observed in all of our stressed transistors agree with this previously reported value within the experimental error of ± 0.0003. By rotating the sample 90° about the (110) axis, we would expect that if the observed SDR signal were in fact the P_{bo} center, it would split into two lines: one at $g \approx 2.0080$ and the other at $g \approx 2.0038$.[14] Such a magnetic field orientation dependence was observed and is shown in Fig. 3. Thus, we conclude that P_{bo} centers are generated by channel hot hole injection in n-channel transistors.

In our stressed transistors we have observed somewhat varying degrees of asymmetry in the signal line shape with a consistent broadening occurring at lower g values. This effect could be due to the presence of much weaker signals corresponding to other point defects (most notably the P_{bl} and E' centers). Though most of the E' centers in MOS structures are hole traps in the oxide,[15] the SDR technique has been shown to be sensitive to such defects.[10] Therefore it is conceivable that some E' centers could be present "close enough" to the Si/SiO_2 interface to participate in the recombination process. We have included the position of $g = 2.0004$ corresponding to the E' center in Fig. 3 in order to illustrate that this center could account for the observed signal asymmetry. However, it is impossible to provide incontrovertible proof of such a defect's existence in our stressed transistors. Thus, since we fail to observe any other appreciable SDR signals and since the magnitude of the P_{bo} SDR signal roughly scales with average interface state generation, our results strongly indicate that P_{bo} centers are the dominant point defects created as a result of channel hot hole injection in nMOS transistors.

Poindexter *et al.*[14] have identified two P_b centers in as processes oxides on (100) silicon surfaces P_{bo} and P_{bl}. Our results clearly indicates that the P_{bo} defect dominates in the hot hole injection damage. Earlier studies of radiation induced interface state generation indicated that P_{bo} centers also dominate in that process.[10,16] Our results coupled with earlier radiation damage results indicate that the P_{bo} center is the dominant *generated* trivalent silicon center in (100) silicon interface device structures.

This work has been sponsored by the Defense Nuclear Agency under Contract No. DNA 002-80-0055 and by the Office of Naval Research. We thank Brian Doyle for the samples used in this study.

[1] T. H. Ning, P. W. Cook, R. H. Dennard, C. M. Osburn, S. E. Schuster, and H. N. Yu, IEEE Trans. ED **26**, 346 (1979).
[2] G. Groeseneken, H. E. Maes, N. Beltran, and R. F. DeKeersmaecker, IEEE Trans. ED **31**, 42 (1984).
[3] P. Heremans, R. Bellens, G. Groeseneken, and H. E. Maes, IEEE Trans. ED **35**, 2194 (1988).
[4] P. Heremans, H. E. Maes, and N. Saks, IEEE EDL 7, 428 (1986).
[5] P. M. Lenahan and P. V. Dressendorfer, J. Appl. Phys. **54**, 1457 (1983).
[6] W. L. Warren and P. M. Lenahan, Appl. Phys. Lett. **49**, 1296 (1986).
[7] R. E. Mikawa and P. M. Lenahan, Appl. Phys. Lett. **46**, 550 (1985).
[8] B. Henderson, Appl. Phys. Lett. **44**, 228 (1984).
[9] R. L. Vranch, B. Henderson, and M. Pepper, Appl. Phys. Lett. **52**, 1161 (1988).
[10] M. A. Jupina and P. M. Lenahan, IEEE Trans. NS **36**, 1800 (1989).
[11] D. J. Lepine, Phys. Rev. B **6**, 436 (1972).
[12] V. S. L'vov, O. V. Tretyak, and I. A. Kolomiets, Sov. Phys. Semicond. **11**, 661 (1977).
[13] D. Kaplan, I. Soloman, and N. F. Mott, Le J. Phys. Lett. **39**, 51 (1978).
[14] E. H. Poindexter, P. J. Caplan, B. E. Deal, and R. R. Razouk, J. Appl. Phys. **52**, 879 (1981).
[15] P. M. Lenahan and P. V. Dressendorfer, J. Appl. Phys. **55**, 3495 (1984).
[16] Y. Y. Kim and P. M. Lenahan, J. Appl. Phys. **64**, 3551 (1988).

Publications Involving the Role of Hydrogen in Radiation Damage
June 1, 1989 - May 31, 1992

J.T. Krick, J.W. Gabrys, D.I. Semon, and P.M. Lenahan, "A Search for Protons in Irradiated MOS Oxides," Paper presented at INFOS ' 91, Liverpool, England, April 1991, Proceedings of INFOS '91 Conference, W. Eccleston editor, William Hilger, Bristol (1991) p. 299.

J.F. Conley and P.M. Lenahan, "Room Temperature Reactions Involving Silicon Dangling Bond Centers and Molecular Hydrogen in Amorphous SiO_2 Thin Films on Silicon," submitted to Applied Physics Letters (1992)

Paper presented at INFOS '91, Liverpool, April 1991
Contributed Papers, Section 7

A search for protons in irradiated MOS oxides

J.T. Krick, J.W. Gabrys, D.I. Semon, and P.M. Lenahan

The Pennsylvania State University, University Park, PA 16802 USA

ABSTRACT: The technique of electron spin resonance (ESR) has been used in an attempt to detect protons in irradiated Si/SiO_2 structures. We searched for ESR signals of hydrogen in oxides which had been heavily irradiated at low temperature (T≈210K) and then subjected to electron photoinjection at 77K.

1. INTRODUCTION

In the past twenty years, a great deal of progress has been made in characterizing radiation-induced damage in the metal-oxide-semiconductor (MOS) transistor. More recently, several studies regarding the time, temperature and field dependence of interface state generation following electron beam irradiation[1-4] have been used to explore the kinetics of the radiation damage process. The results of these LINAC studies have been rather convincingly interpreted in terms of a two-step process proposed by McLean[5].

In the McLean model, holes created during irradiation are thought to release positive ions -- almost certainly protons -- which then drift to the interface under the influence of an applied electric field. Upon reaching the interface, the protons are thought to react with hydrogen groups (ie. by breaking Si-H or Si-O-H bonds to form H_2 or H_2O) and leave behind a silicon dangling bond. These interfacial dangling bonds, known as P_b centers, have been shown using the technique of electron spin resonance (ESR) to be the dominant radiation-induced interface state in MOS devices[6]. In this study, we have used ESR in an attempt to verify an important aspect of the model proposed by McLean, the creation of protons in the oxide.

The idea behind our experiment is relatively straightforward. The radiation-induced interface state buildup is known to last many hours at a relatively low temperature[7]. Thus, if proton drift to the interface is the rate limiting step in this process, it should be possible to 'freeze' the protons in place by maintaining the MOS sample at such a temperature both during and after irradiation. Unfortunately, protons, without an unpaired electron, are undetectable by ESR techniques. However, they could be rendered paramagnetic by capturing an electron to form atomic hydrogen; a species which has a distinctive and easily identifiable ESR lineshape consisting of two very narrow ($\Delta H_{pp} \approx 2G$) lines separated by 503 gauss[8].

2. EXPERIMENTAL DETAILS

The samples used in this study were 0.2mm thick 400 Ωcm <111> oriented p-type silicon wafers polished on both sides. The 1200Å wet oxides examined were grown on both sides of the wafers at 1100°C and subjected to a 1150°C Argon anneal for 90 minutes. A 20 minute anneal in forming gas at 450°C completed the processing sequence. ESR samples of dimensions $0.35x2cm^2$ were then cut from the processed wafers. These radiation "soft" oxidizing and annealing conditions were specifically chosen in order to maximize the anticipated hydrogen ESR signal. Furthermore, the use of thin, high resistivity silicon

wafers allowed us to 'stack' three slices in the spectrometer in an effort to maximize the sample oxide volume.

The Si/SiO_2 samples were irradiated to doses of 15 to 50 Mrad using sequences of 125 Krad LINAC pulses. The temperature of the samples during irradiation (T=210K) was such that any atomic hydrogen created during irradiation would quickly disappear[8]; at this temperature, however, the interface state buildup is known to last many hours. After irradiation, the samples were then cooled to 100K and exposed to ultraviolet illumination. The UV illumination was used to photoinject electrons into the oxide from the silicon substrate; The electrons would then presumably be captured by protons to form atomic hydrogen. Finally, electron spin measurements were performed on the samples and the resulting ESR traces were averaged for a period of several hours.

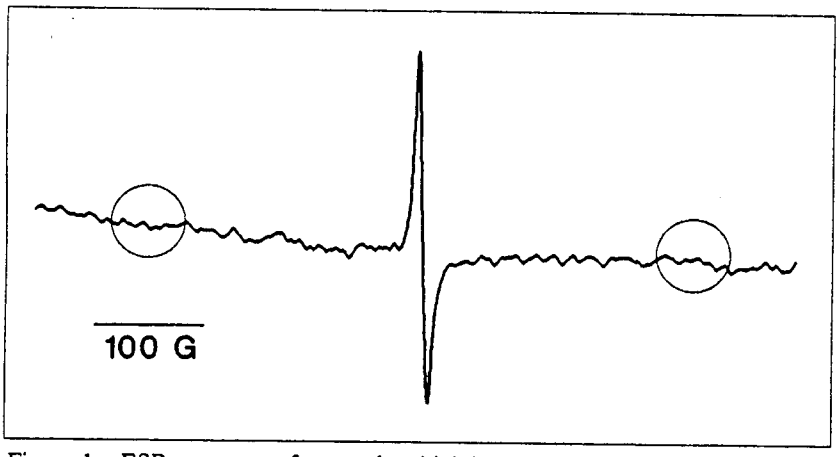

Figure 1: ESR spectrum of a sample which has been LINAC irradiated and exposed to UV illumination at low temperature. The scan width is 700G and is centered on g=2.000. The trace shown is the average of 25 3.2 minute sweeps performed at T=100K. Signals corresponding to atomic hydrogen would appear within the circles shown. However, no atomic hydrogen signal is detected.

The ESR trace shown in figure 1 is typical of the ten measurements performed on Si/SiO_2 samples which have undergone pulsed LINAC irradiation and subsequent UV illumination. The trace was performed on three samples irradiated to a total dose of 15 Mrad at a temperature of 213K. The samples were then exposed to intense UV illumination while immersed in liquid nitrogen for a total of 20 minutes (10 minutes on each side). The UV source was a focused 100W mercury-xenon lamp which emitted photons of energy $\leq$5eV. After transferring the samples to the "cold finger" of an ESR cavity in a test tube filled with liquid nitrogen, electron spin resonance measurements were performed at 100K. The magnetic field sweep width used was 700G and the signal shown is the average of 25 separate 3.2 minute sweeps. Signals corresponding to the presence of atomic hydrogen would appear in the circles shown. However, no atomic hydrogen signal is observed. Comparing this irradiated sample trace to that which we obtained with a calibrated spin standard, we estimate that the total concentration of atomic hydrogen is less than $1x10^{11}/cm^2$; we believe that this limit is, in turn, accurate to a factor of two. As a result, we conclude with a high degree of certainty that the density of atomic hydrogen is less than $2x10^{11}/cm^2$ in these irradiated samples.

3. DISCUSSION

On the basis of the model proposed by McLean, we had -- perhaps naively -- anticipated a *huge* hydrogen ESR signal. Our oxides were intentionally processed to be radiation "soft."

Since they were subjected to such high radiation doses, we would expect average interface state densities of $\geq 10^{12}/cm^2eV$. Assuming that one proton is required to create an interface state defect, we would, therefore, expect *at least* the same proton concentration -- though one several times greater seemed quite likely -- in the oxide following irradiation (if protons drift to the interface and interact with an existing imperfection (ie. H-Si=Si_3) to create an interface state, one might guess that the efficiency would be far lower than one defect per proton). Thus, with a spectrometer sensitivity of $\approx 1x10^{11}/cm^2$, we had expected to observe an atomic hydrogen signal.

The success of our experiment, in terms of evaluating the validity of the proton model proposed by McLean, relies on two factors: (1) protons must be present in the oxide following irradiation and (2) photoinjected electrons must be captured by protons which, presumably, have a large coulombic capture cross section. It is also conceivable that errors in temperature control could affect our ability to see atomic hydrogen. However, in two runs we exposed the irradiated oxides to UV illumination only after placing the samples into the chilled cold finger inside the ESR cavity. The outcome was identical in each case -- *no detectable hydrogen signal.*

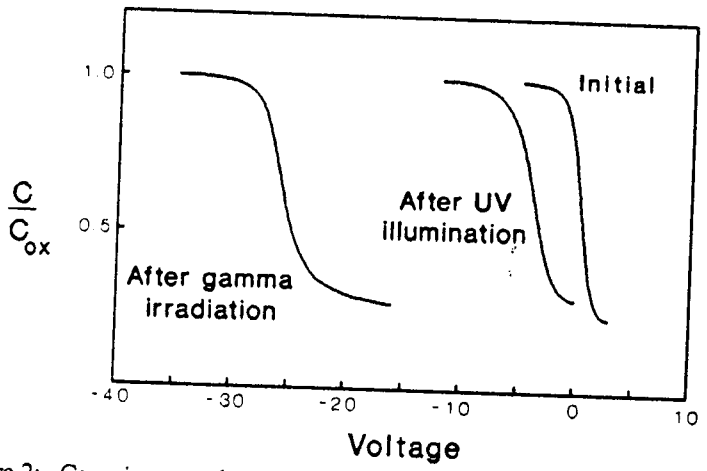

Figure 2: Capacitance-voltage measurements of a gamma irradiated 1000Å oxide which has been exposed to UV illumination while immersed in liquid nitrogen. The illumination scheme is identical to that of the LINAC irradiated samples. Photoinjection of electrons annihilates the majority of the positive oxide charge.

To test the effectiveness of our photoinjection technique, capacitance-voltage (CV) measurements were performed on a 1000Å oxide which had been first gamma irradiated and then exposed to UV illumination while immersed in liquid nitrogen (figure 2). The illumination process used here was identical to that of the LINAC samples shown in figure 1. Exposure to UV illumination clearly annihilates most of the positive charge; electrons are photoinjected into the oxide and are captured by the large capture cross section hole centers. Presumably, protons present in the oxides of samples subjected to LINAC irradiation would have a similarly large capture cross section and would thus be equally effective in trapping injected electrons. Therefore, we provisionally assume that the number of protons present in the oxides of our samples following irradiation is quite small ($\leq 10^{11}cm^2$).

If the proton model is correct, the flaw in our experiment would have to be the lack of an

applied electric field during irradiation. It is well known that the amount of radiation-induced interface state buildup is dependent on the magnitude and direction of the applied electric field[2]. If an electric field in the oxide were required for substantial proton release, we would be unable to see atomic hydrogen in our experiment. Secondly, the presence of an electric field would affect the probability of electron capture by positively charged species (holes or protons). At the temperatures used in our irradiation experiments, atomic hydrogen formed by electron trapping on a proton would quickly dissipate from the oxide and thus would not be detected in our ESR measurements.

4. CONCLUSION

We have used the technique of electron spin resonance in an attempt to examine the role of protons in the degradation of irradiated MOS structures. Based on our interpretation of the proton model proposed by McLean, we expected to generate a large atomic hydrogen signal by irradiating MOS oxides and subsequently photoinjecting electrons at low temperatures. We did not. From our results, we conclude that after irradiation in the absence of an applied electric field, the concentration of protons in the oxide must be less than $\approx 1 \times 10^{11} cm^2$. Our findings do not invalidate the proton drift models. However, our results do show that protons are not generated in large numbers in unbiased soft oxides subjected to high levels of irradiation. Nevertheless, further ESR experiments in which an electric field is applied during irradiation would provide a more conclusive test to determine the role of protons in radiation-induced degradation in MOS structures.

REFERENCES

1. P.S. Winokur, H.E. Boesch, J.M. McGarrity and F.B. McLean, *J. Appl. Phys.* **50**, 3492 (1979).
2. Earlier work in this area is summarized by P.S. Winokur in "Radiation Induced Interface Traps" of Ionizing Radiation in MOS Devices, T.P. Ma and P.V. Dressendorfer editors, Wiley Interscience, New York (1989).
3. N.S. Saks and D.B. Brown, *IEEE Trans. Nuc. Sci.* **NS-36**, 1848 (1989).
4. N.S. Saks and D.B. Brown, *IEEE Trans. Nuc. Sci.* **NS-37**, 1624 (1990).
5. F.B. McLean, *IEEE Trans. Nuc. Sci.* **NS-27**, 1651 (1980).
6. P.M. Lenahan and P.V. Dressendorfer, *J. Appl. Phys.* **54**, 1457 (1983) and references contained therein.
7. P.S. Winokur, H.E. Boesch, J.M. McGarrity and F.B. McLean, *IEEE Trans. Nuc. Sci.* **NS-24**, 2113 (1977).
8. T.E. Tsai, D.L. Griscom and E.J. Friebele, *Phys. Rev. B* vol. **40** no. 9, 6374 (1989)

ROOM TEMPERATURE REACTIONS INVOLVING SILICON DANGLING BOND CENTERS AND MOLECULAR HYDROGEN IN AMORPHOUS SiO_2 THIN FILMS ON SILICON

J. F. Conley and P. M. Lenahan
The Pennsylvania State University
University Park, Pennsylvania 16802

Abstract

Exposing thin films of amorphous SiO_2 to molecular hydrogen at room temperature converts some silicon dangling bond defects, E' centers, into two hydrogen coupled complexes. We argue that these reactions may play important roles in radiation and hot carrier instabilities in metal/oxide/silicon devices.

When metal/oxide/silicon MOS devices are subjected to ionizing radiation, hot carrier damage, or any process in which charge carriers are present in the oxide, interface states are created at the Si/SiO_2 interface.[1-9] The presence of holes in the oxide is most effective in triggering the interface state generation process.[8,9] Studies of the transient response of irradiated devices shows that most of the damage occurs in seconds to minutes after irradiation at room temperature.[4-6]

For many years, it has been widely suspected that hydrogen also plays an important role in determining the radiation response of MOS field effect transistors (MOSFETs). The suspicion seems well justified. Early studies of MOS radiation damage showed that the radiation tolerance, or radiation hardness, of the devices was strongly affected by hydrogen in high temperature processing steps.[1-3] A number of studies of the time, temperature, and field dependence of the interface state creation process[4-6] have been interpreted by McLean[10] in terms of a two stage model. In McLean's model,[10] holes interact in some way with the oxide to liberate a hydrogen species which then drifts to the Si/SiO_2 interface. At the interface, the hydrogen reacts to form silicon dangling bond interface state defects. The McLean model is consistent with many early kinetic studies[4-6]; recent studies of damage kinetics[11,12] also appear to strongly support his model.

Recently, considerable evidence has suggested that molecular hydrogen may play a significant role in the radiation damage process. For example, the density of radiation induced interface states can be significantly enhanced by placing irradiated MOS devices in an ambient rich in molecular hydrogen.[13,14,15]

Although experimental evidence regarding hydrogen's role in the radiation damage process is fairly compelling, it consists almost entirely of electronic measurements. There is little direct experimental evidence regarding the atomic scale structures involved in reactions of hydrogen and radiation damage centers in silicon dioxide films on silicon. Reactions of particular interest would obviously involve SiO_2 hole trap sites and hydrogen and would proceed in a period of seconds to minutes at room temperature.

In this letter we report evidence for several reactions involving E' centers and hydrogen which take place when SiO_2 films are exposed to hydrogen at room temperature. (The E' center is an unpaired electron residing in an sp hybridized orbital of a silicon bonded to three oxygens;[16] in thermal oxides the E' is a hole trapped in an oxygen vacancy.[17]) These reactions take place within minutes after our very thick

(≃4800 Å) oxide films are exposed to hydrogen. We think that these reactions may play a part in the MOS-interface state radiation damage process for several reasons. (1) The E' center is the dominant deep hole trap in MOS oxides.[17] (2) The reactions take place in a time scale which is of the correct order of magnitude expected in the damage process. (3) It is known that, or at least strongly suspected that, molecular hydrogen is present in irradiated MOS oxides.[18] (4) Recent studies suggest that the radiation damage at the Si/SiO_2 interface may be triggered by a reaction involving hydrogen at the hole capture site.[19]

Our study involves electron spin resonance (ESR) measurements of SIMOX (separation by implantation of oxygen) buried oxides. The ESR measurements were conducted at room temperature on an X-band commercial spectrometer using a TE_{104} cavity and a calibrated weak pitch standard. The system allows an absolute accuracy in spin density of better than a factor of two and a relative accuracy in spin density of approximately ± 10%. The 4800Å thick SIMOX buried oxides utilized in this study were prepared by implanting 1.8×10^{18} oxygens/cm^2 at an energy of 200 keV. The ion current density during deposition was 34 mA/cm^2. The temperature of the substrate during implantation was 640°C. The implant step was followed by a 5 hour anneal at 1315°C in an ambient of 99.5% Ar and 0.5% O_2. The silicon surface orientation was (100); the silicon is n-type with a resistivity of about 30Ω cm. A residual oxide layer formed by the high temperature anneal, as well as the top silicon layer, were removed by etches in HF (oxide) and KOH (silicon) prior to the study. The etches were carried out at room temperature. After etching, the samples were cut into 3.5 mm x 20 mm rectangles and, with the oxides protected, were subjected to a buffered HF etch at room temperature. This last etch removes mechanical damage from the edges of the samples.

Earlier, we demonstrated that SIMOX buried oxides exhibit an extremely high (~10^{18}/cm^3) density of E' precursors.[20,21] The density of E' precursors is about one order of magnitude higher than that observed in thermal thin films. Therefore, these oxides make an ideal system in which to study hydrogen/E' interactions in thin films. This increased E' density makes it possible to observe several otherwise difficult to observe hydrogen E' complexes.

SIMOX buried oxides likely exhibit a high level of short range disorder; since the oxides were annealed at 1315°C they should also be under a high level of compressive stress. Although these oxides are not identical to the thermal SiO_2 films of MOS gate oxides, we would argue that the reactions observed here are also likely to take place at

some sites in thermal oxides. (One might anticipate that the vicinity of the thermal SiO_2/Si boundary would be highly disordered. Most of the radiation induced E' centers in MOS devices irradiated under positive bias [the worst radiation damage case] are near the Si/SiO_2 interface.[17])

We subjected the Si/SiO_2 samples to ~40 hours of vacuum ultraviolet ($hc/\lambda \leq 10.2eV$) irradiation from a deuterium lamp. (A second set of samples were exposed to 210 Mrad of gamma irradiation from a Co^{60} source. These gamma irradiated samples were not subjected to the KOH etch; they retained the ~1μm silicon overlayer. The gamma irradiated samples and the VUV irradiated samples exhibit nearly identical ESR spectra.) A post VUV irradiation trace is illustrated in figure 1a. A very strong signal appears at a zero crossing g = 2.0005 and a weak doublet signal appears with a separation of 74G. (The g is defined as $g=h\nu/\beta H$, where his Planck's constant, ν is microwave frequency, b is the Bohr magneton and H is the field at resonance.) The strong center line is due to ordinary E' centers illustrated in Figure 2a; the weak doublet spectra is due to an E' center in which the paramagnetic silicon is bonded to two oxygens and a hydrogen atom; its structure is illustrated in Figure 2b.[22,23] The weak doublet spectra comprises 3-5% of the total E' spins.

In Figure 1b and 1c we illustrate ESR traces taken on the same samples of Figure 1a, but after ten minutes (1b) and one hour (1c) exposure to ($10\%H_2/90\%N_2$) forming gas at room temperature and atmospheric pressure. Note the large increase in the doublet spectra at 74G separation and the appearance of two "bumps" on the center line with a separation of about 10.4G. The 10.4G doublet spectra is due to the hydrogen complex defect illustrated in Figure 2c[23]. Although this is not clear from the figure, the original E' line amplitude decreases by 25 to 30% during the one hour H_2 exposure; most of the change occurs in the first ten minutes. While most of the 10.4G change also takes place within 10 minutes, only about 30% of the 74G change takes place within that time. The number of defects associated with the sum of the newly created 10.4G and 74G doublet signals are approximately equal to 25% of the initial E' amplitude. (The total number of spins is preserved.) We thus tentatively conclude that we are observing a transformation of standard E' centers (2a) into two hydrogen complexed E' centers (2b and 2c). It may be worth noting that the process occurs in a time period which is roughly equal to the time required for the molecular hydrogen to diffuse across the oxide.[18]

In Figure 3 we illustrate a narrow ESR trace with spectrometer settings optimized to accurately illustrate the 10.4G doublet line shapes. The fully resolved line shapes are

what one would expect from the structure of Figure 1c;[23] however, the doublet splitting appears to be slightly greater than 10.4G.

Triplett, Takahashi, and coworkers[24,25] were first to observe E'/hydrogen complexes in thin SiO_2 films on silicon. They subjected thermally grown oxides to very heavy irradiation (~2 x 10^{10} rads) and then briefly exposed the oxides to 10%H_2/90%N_2 forming gas at 110°C. They noted a substantial decrease in the central E' line and the appearance of the 74G doublet signal corresponding to a density which closely matched the decrease in the central E' intensity. In the pioneering Triplett/Takahashi study, it was noted that a one minute exposure to UV illumination from a 250 watt mercury lamp annihilated the 74G doublet signal and slightly increased the central E' signal; the UV illumination resulted in a loss of oxide space charge which closely corresponded to the net change in the sum of E' and 74G doublet detects. (The original positive charge density in the oxides closely matched the initial E' density.)

Following the example of Triplett, Takahashi and coworkers, we subjected the VUV irradiated/hydrogen soaked oxides to a brief (~4 minute) exposure of UV illumination ($hc / \lambda \lesssim 5eV$) from a mercury-xenon lamp. We found, as did Triplett and Takahashi, that the brief exposure annihilated the 74G doublet signal and resulted in a modest increase in the ordinary E' signal. In addition, we found that this illumination reduced the 10.4G signal amplitude by about 25%.

In an attempt to further assess the electronic properties of the three E' defects present in our VUV irradiated-hydrogen soaked oxides, we exposed the oxides to both UV and notch filtered vacuum ultraviolet VUV illumination ($hc / \lambda \simeq 10.2eV$) with bias applied across the oxides during the illumination. The bias was applied with either positive or negative corona discharge ions; the corona ion potential was measured with a Kelvin probe electrostatic voltmeter.

We UV irradiated ($hc / \lambda \lesssim 5eV$) the oxides under positive oxide bias (oxide field ~1 to 3MV/cm) to photoinject electrons for the silicon into the oxide. The photoinjection of approximately 5 x 10^{13} electrons/cm^2 resulted in a near complete annihilation of the 74G signal (this also occurred with the unbiased UV illumination) but the ordinary E' signal increased by an amount (+35% vs. +20%) significantly larger than was observed in the unbiased UV illumination. The 10.4G doublet signal was reduced by $\simeq$50% during the process.

We also subjected oxides to UV illumination under negative oxide bias. The negative bias (oxide held ~1 to 3 MV/cm) should substantially impede electron photoinjection. We found that this negative bias illumination also completely eliminated the 74G signal, substantially reduced ($\simeq$50%) the 10.4G signal, but did not change the central E' amplitude.

The results of our positive, negative, and zero bias UV illuminations suggest that the central E' signal increases are result of electron photoinjection into the oxide. In addition, these results strongly suggest that both the 10.4G and 74G signals are responding directly to the UV photons.

In order to evaluate these conclusions we had to inject electrons and holes into the oxides without exposing the oxide bulk to ultraviolet photons. We did this by again charging the oxide surfaces with corona ions, but then exposing the oxides to vacuum ultraviolet ($hc/\lambda \simeq 10.2eV$) light from a notch filtered deuterium lamp. The oxide's optical absorption coefficient is extremely large for photons of this energy ~10^6/cm; thus virtually all the photons are absorbed in the top 100Å of the 4800Å oxide. Under positive corona bias the bulk of the oxide is flooded with holes; under negative corona bias the bulk of the oxide is flooded with electrons. In both cases the fluence of injected charge carriers was about 5 x $10^{13}/cm^2$ and the average oxide field during the process was ~1 to 3MV/cm. We found that when electrons were injected into the oxide the simple E' amplitude was substantially increased (≈+35%), but we observed little change in the 10.4G or 74G doublet signals. Injecting holes into the oxide also resulted in a substantial (≈+35%) increase in the simple E' and also did not significantly change either the 74G or 10.4G doublet amplitude.

The results of the VUV illumination measurements strongly suggest that the changes observed in the 10.4G and 74G signals with UV illumination are due to photons interacting with the defects. The results also suggest strongly that the E' signal can be increased by electron capture at previously diamagnetic sites. This does not appear to happen in SIMOX oxides which have not been exposed to hydrogen. As we had reported earlier, [20,21] prior to hydrogen exposure, the injection of holes into the oxide consistently results in a substantial increase in E' density. Prior to hydrogen exposures the injection of electrons into the oxide consistently decreases E' density. These new results strongly suggest that the E'/hydrogen reactions involve substantial structural changes at the E' site. Our results also suggest that the hydrogen exposure can result in the creation of silicon

single dangling bond sites from sites which had initially been holes trapped at oxygen vacancies.

These results demonstrate several things: (1) Room temperature reactions involving molecular hydrogen and the dominant deep hole trapping center in MOS oxides can be both thermodynamically and kinetically favorable. The reaction takes place in minutes - the process is apparently complete in an hour or less in these very thick oxides (4800Å); most of the 10.4G signal appears within 10 minutes and most of the E' density drop also occurs within the first 10 minutes. Hydrogen reactions at E' sites can clearly involve bond breaking events beyond the central silicon; the 10.4G signal is associated with a hydrogen atom bonded to an oxygen which is in turn bonded to the E' silicon. In addition, it appears that the hydrogen creates E' sites which capture electrons with large capture cross section when they are diamagnetic; they become paramagnetic upon electron capture. These results may be relevant to the basic mechanisms of radiation damage.

Our results provide chemical and structural experimental evidence which is consistent with and tends to support ideas recently expressed in a number of studies of the electronic response of MOS devices to ionizing radiation. As mentioned previously, quite strong experimental evidence implicates hydrogen/hole interactions and hydrogen drift in the buildup of interface states at the Si/SiO_2 boundary.[4-6,10-12] A recent study of the kinetics of radiation damage has suggested that hole trapping in the oxide is required to initiate the radiation damage process.[19] Several recent studies[13-15] show that an ambient rich in molecular hydrogen considerably enhances the creation of Si/SiO_2 interface states. These studies have generally proposed that some sort of hydrogen "cracking" process takes place at some of the hole trap sites. Since the hole trap sites are primarily E' centers, our results are consistent with and support these ideas.

Acknowledgments

This work has been supported in part by DNA and the Office of Naval Research. We thank Dr. Peter Roitman of NIST for supplying us with samples and for very useful discussions.

References

1. K.G. Aubuchon, E. Harari, D.H. Leong, and C.P. Chang, IEEE Trans. NS-21, 167 (1974).
2. K.G. Aubuchon, and E. Harari, IEEE Trans.Nucl.Sci. NS-22, 2181 (1975).
3. G.F. Derbenwick, and B.L. Gregory, IEEE Trans.Nucl.Sci., 22, 2151 (1975).
4. P.S. Winokur, J.M. McGarrity, and H.E. Boesch, IEEE Trans.Nucl.Sci., NS-23, 1580 (1976).
5. P.S. Winokur, H.E. Boesch, J.M. McGarrity, and F.B. McLean, IEEE Trans.Nucl.Sci., 24, 2113 (1977).
6. P.S. Winokur, and H.E. Boesch, Jr., IEEE Trans.Nucl.Sci., 27, 1647 (1980).
7. T.H. Ning, P.W. Cook, R.H. Dennard, C.M. Osburn, S.E. Schuster, and H.N. Yu, IEEE Trans.ED, 26, 346 (1979).
8. P. Heremans, H.E. Maes, and N. Saks, IEEE EDC, 7, 428 (1986).
9. P.S. Winokur and M.M. Sokoloski, Appl.Phys.Lett., 28, 627 (1976).
10. F.B. McLean, IEEE Trans.Nucl.Sci., NS-27, 1651 (1980).
11. N.S. Saks, and D.B. Brown, IEEE Trans.Nucl.Sci., 37, 1624 (1990).
12. N.S. Saks, C.M. Dozier, and D.B. Brown, IEEE Trans.Nucl.Sci., 35, 1168 (1988).
13. R.A. Kohler, R.A. Kushner, and K.H. Lee, IEEE Trans.Nucl.Sci., 35, 1492 (1988).
14. R.E. Stahlbush, B.J. Mrstik, and R.K. Lawrence, IEEE Trans.Nucl.Sci., 37, 1641 (1990).
15. B.J. Mrstik and R.W. Rendell, IEEE Trans.Nucl.Sci., 38, 1101 (1991).
16. R.H. Silsbee, J.Appl.Phys., 32, 1459 (1961).
17. P.M. Lenahan and P.K. Dressendorfer, J.Appl.Phys., 55, 3495 (1984).
18. D.L. Griscom, J.Appl.Phys., 58, 2524 (1985).
19. M.R. Shaneyfelt, J.R. Schwank D.M. Fleetwood, P.S. Winokur, K.L. Hughes, and F.W. Sexton, IEEE Trans.Nucl.Sci., 37, 1632 (1990).

20. J.F. Conley, P.M. Lenahan, and P. Roitman, Proceedings of the 1991 Insulating Films on Semiconductors Conference, W. Eccleston, editor, Institute of Physics, Adam Hilger, Bristol England, (1991) p. 259.

21. J.F. Conley, P.M. Lenahan, and P. Roitman, IEEE Trans.Nucl.Sci., 38, 1247 (1991).

22. John Vitko, J. Appl.Phys., 49, 5530 (1978).

23. T.E. Tsai and D.L. Griscom, J.Non.Cryst.Sol. 91, 170 (1987).

24. B.B. Triplett, T. Takahashi, and T. Sugano, Appl.Phys.Lett. 50, 1663 (1987).

25. T. Takahashi, B.B. Triplett, K. Yokogawa, and T. Sugano, Appl.Phys.Lett., 51, 1344 (1987).

Figure Captions

Figure 1. Trace (a) illustrates ESR data from a SIMOX oxide sample after exposure to VUV illumination. The large central line corresponds to the ordinary E' defect. Trace; (b) illustrates a trace after the sample was exposed to 10 minutes of exposure to a 10% H_2 ambient; Trace (c) illustrates the trace after one hour exposure to H_2. An additional hour of exposure did not significantly alter the spectra.

Figure 2. This figure schematically illustrates the structure of (a) ordinary E' centers, (b) 74G doublet centers, and (c) 10.4G doublet centers.

Figure 3. This narrow scans figure illustrates the 10.4G spectrum with the spectrometer settings optimized to yield a relatively accurate line shape for the 10.4G doublet lines. The doublet patterns closely match that of the central E' line.

Hydrogen Interactions With E' at Room Temperature

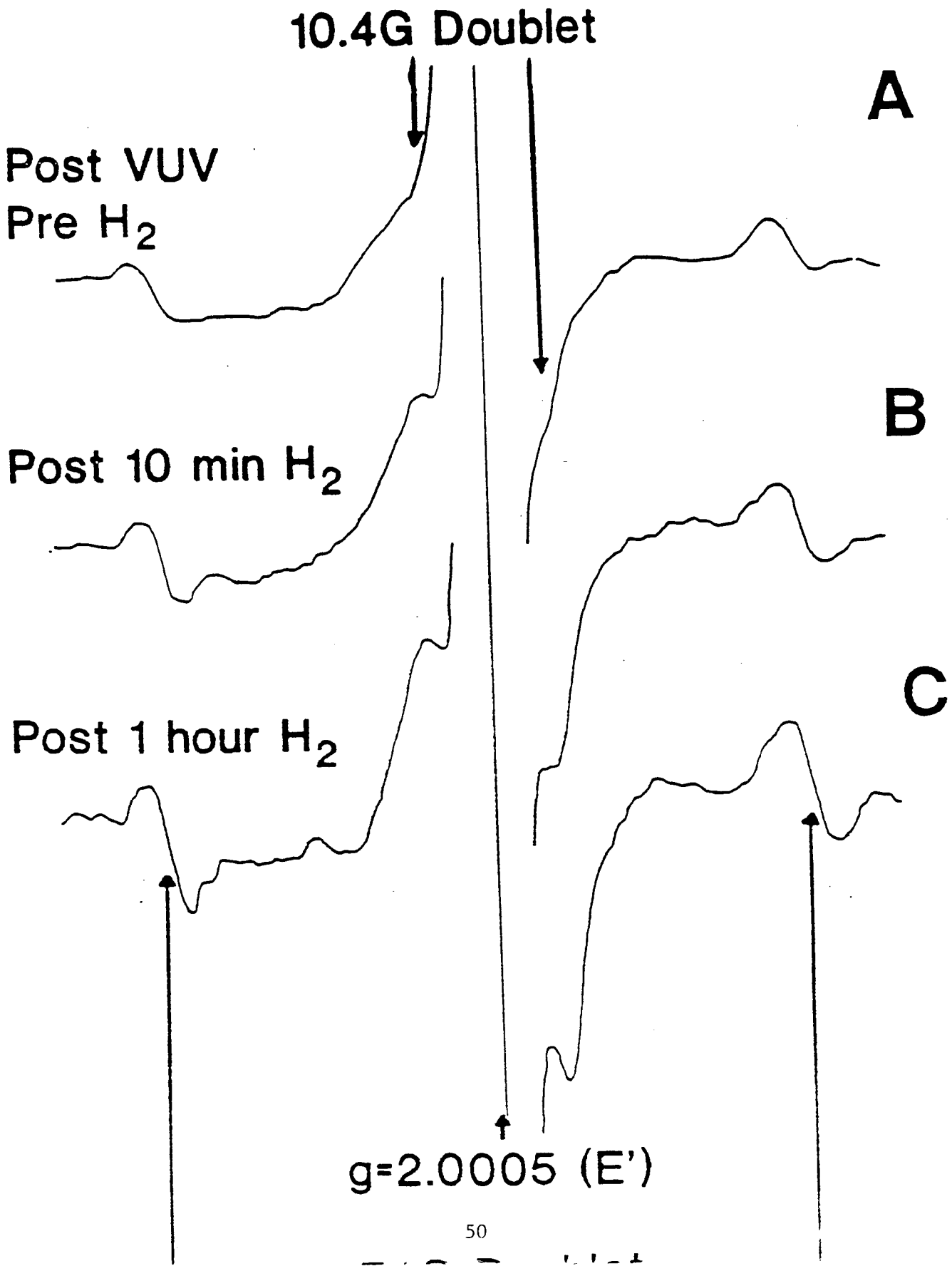

Defect Models

A

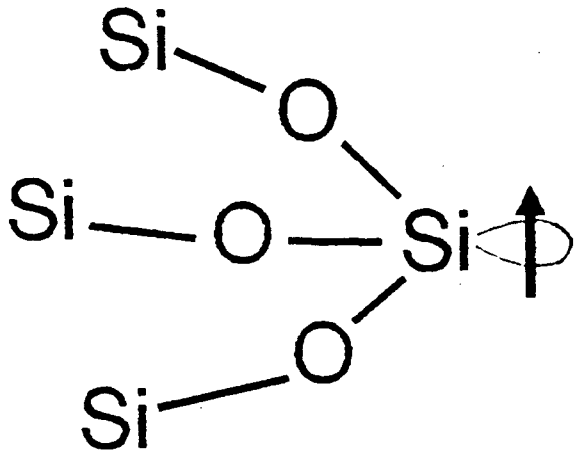

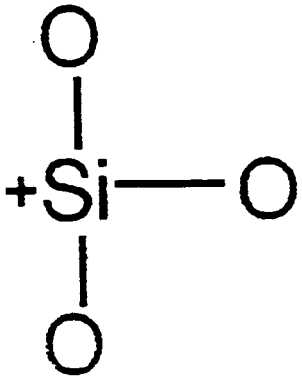

E'

B

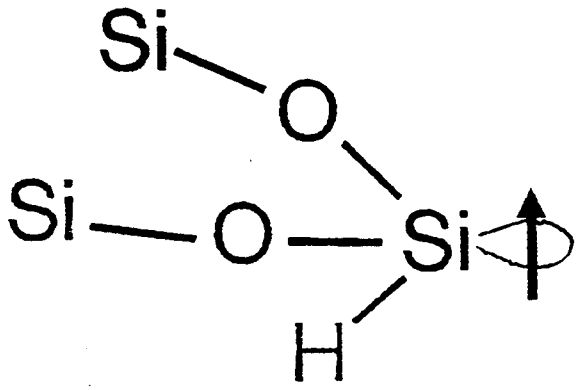

74G doublet

?

C

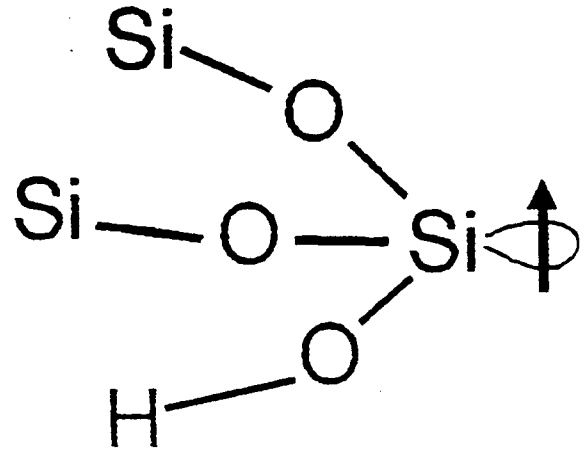

10.4G doublet

?

"Hi-Res" ESR Trace of 10.4G Doublet

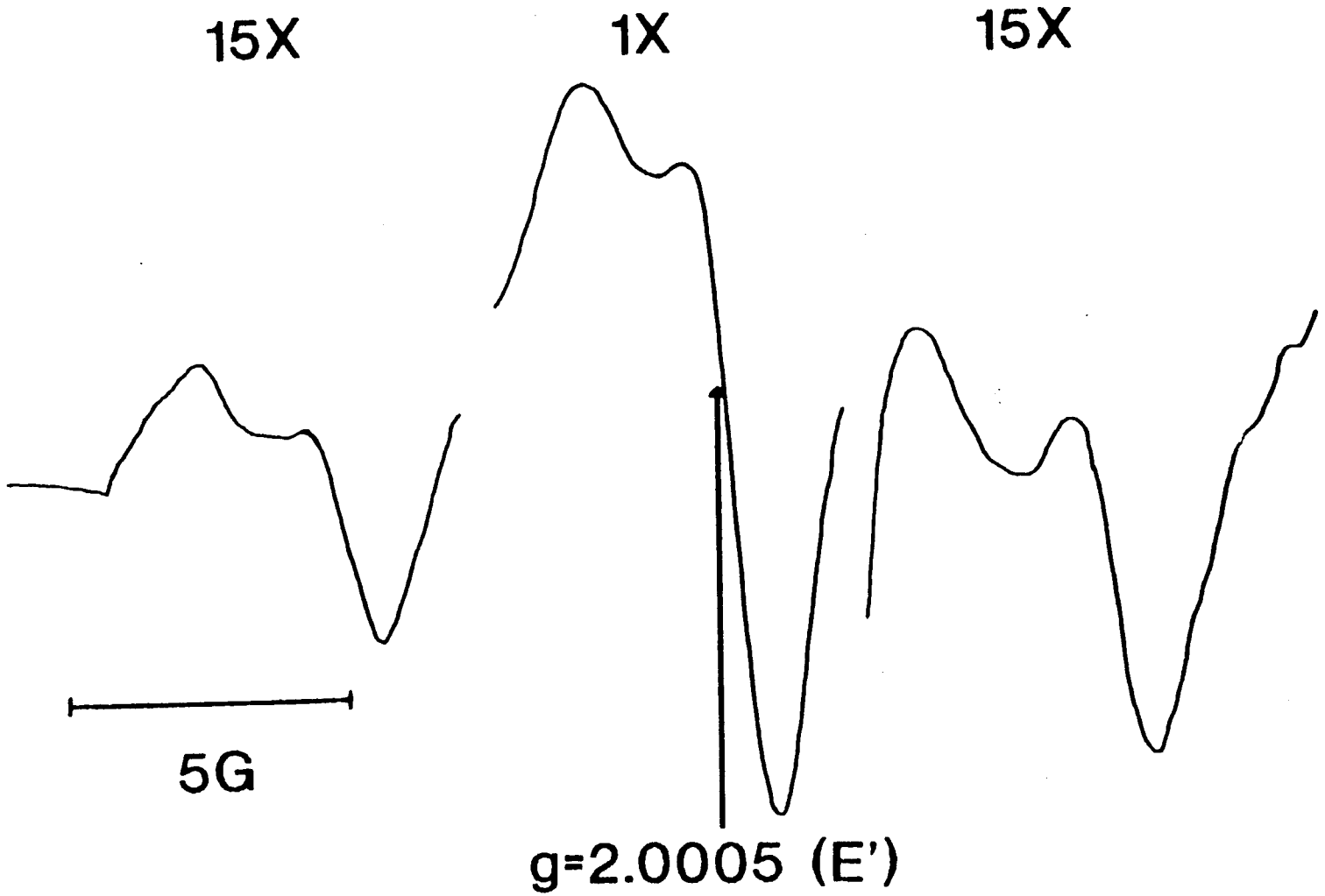

Publications Involving "Bond Strain"
and Possible Structural Changes at the Hole Capture Site
June 1, 1989 - May 31, 1992

W.L. Warren, P.M. Lenahan, C.J. Brinker, "Relationship Between Strained Silicon - Oxygen Bonds and Radiation Induced Paramagnetic Point Defects in Silicon Dioxide" Solid State Communications, 79, 137 (1991)

W.L. Warren, P.M. Lenahan, C.J. Brinker, "Experimental Evidence for Two Fundamentally Different E' Precursors in Amorphous Silicon Dioxide," J. Non-Crystalline Solids, 136, 151 (1991)

Solid State Communications, Vol. 79, No. 2, pp. 137-141, 1991.
Printed in Great Britain.

0038-1098/91$3.00+.00
Pergamon Press plc

RELATIONSHIP BETWEEN STRAINED SILICON-OXYGEN BONDS AND RADIATION INDUCED PARAMAGNETIC POINT DEFECTS IN SILICON DIOXIDE

W. L. Warren
Electronic Properties of Materials Division
Sandia National Laboratories
Albuquerque, NM 87185

P. M. Lenahan
The Pennsylvania State University
University Park, PA 16802

C. J. Brinker
Inorganic Materials Chemistry Division
Sandia National Laboratories
Albuquerque, NM 87185

(Received March 20, 1991 by A. Pinczuk)

We have investigated the radiation induced generation of paramagnetic point defects in high surface area sol-gel silicates containing various concentrations of the Raman active 608 cm^{-1} D_2 band attributed to strained cyclic trisiloxanes (3-membered rings). Our results suggest a correlation between the concentration of the 3-membered rings with the concentration of radiation induced paramagnetic E' (trivalent silicon center) and oxygen centers, thus, providing the first substantive evidence of the relationship between a specific strained siloxane structure and radiation damage in amorphous silicon dioxide.

It has long been recognized that amorphous silicon dioxide (a-SiO_2) can be damaged by ionizing radiation [1-3], for example, it damages the insulating layers of metal oxide semiconductor field effect transistors [1]. Thus, a detailed understanding of the mechanisms and structural origins of the radiation damage process in a-SiO_2 is of considerable interest.

Extensive ESR studies have been performed on crystalline quartz and bulk a-SiO_2 subjected to various forms of irradiation [2-6]. These investigations have identified several intrinsic point defects: E' centers, peroxy radicals and non-bridging oxygen hole centers (NBOHC's). The E' center is an unpaired electron on a silicon bonded to three oxygens [4,5]. One theoretical model [7-9], also established experimentally [10], identifies the precursor of the E' center as an oxygen vacancy ($O_3Si-SiO_3$). The peroxy radical ($\cdot O-O-SiO_3$) and NBOHC ($\cdot O-SiO_3$) have been identified as two intrinsic paramagnetic oxygen centers that predominate in irradiated "dry" (< 1 ppm OH) and "wet" silicas respectively [2,3,6]. The precursors for the peroxy radical and NBOHC are believed to be an oxygen surplus site ($O_3Si-O-O-SiO_3$) [6] and a hydroxyl site (O_3SiO-H) [2] respectively.

It has also been suggested that atomic level stress plays a role in the radiation induced damage process of a-SiO_2 [11-13]. Devine and Arndt [12,13] have recently provided strong evidence that this is the case by observing large defect enhancements on plastically densified fused silicas over undensified silicates. But, to date, there has not been a concrete relationship established between the aforementioned point defects and a specific strained silicate structure. In this study we provide evidence that suggests that strained cyclic trisiloxanes (3-membered rings, an n-membered ring has n-silicon tetrahedra connected by bridging oxygens) are also precursor structures to E' centers and oxygen hole centers (OHC's) [14]. We have used Raman scattering combined with previous ^{29}Si nuclear magnetic resonance (NMR) studies [15] to identify these strained silicate structures.

Prominent features in the Raman spectra of silicate gels are illustrated in Fig. 1. It is generally believed [15-20] that the sharp Raman, 608 cm^{-1}, D_2 band results from oxygen ring breathing vibrations of highly regular, planar, strained, cyclotrisiloxanes

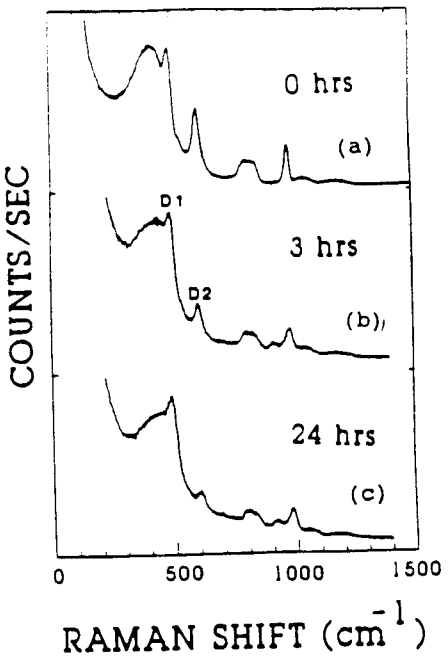

Figure 1 Raman spectra of sol-gel silicates exposed to water vapor for the various times (a) 0 hrs, (b) 3 hrs, and (c) 24 hrs.

(3-membered rings) with Si-O-Si angles ø = 137°. Molecular orbital calculations [20] of 3-membered ring structures indicate that the reduction of the Si-O-Si bond angle, ø, is accompanied by a reduction in the tetrahedral angle (from 109.5° to 103°) and an increase in the Si-O bond length (from 1.626 to 1.646Å). The average structure of a-SiO_2 is believed to consist mainly of puckered, unstrained, 5-8 membered rings with an average ø = 149° [21]. Diffraction studies [22] clearly indicate that regular forms of SiO_2 contain a wide range of Si-O-Si intertetrahedral bond angles. Bond angle (energy) calculations [23] indicate that strained bonds also exist in regular forms of silica due to bond angle variations from 149°; these sites may also be precursor sites to radiation induced defects.

To establish a relationship between radiation induced point defects and strained silicate structures we have irradiated high surface area sol-gel silicates with varying relative intensities of the Raman D_2 band. We chose to investigate the radiation effects on high surface area gels since they exhibit the largest concentration of strained rings, and are thus, an ideal system to investigate the response of strained silicate species to ionizing radiation. However, we believe that our observations are relevant to other high surface area silicates and to a wide range of fused silicas since the D_2 Raman band is present in virtually all forms of a-SiO_2, i.e., fused silica [16], thermally grown SiO_2 films on Si [24]. Essentially all of the experimental features of the D_2 band in the silica gels are identical to those found in other forms of a-SiO_2 [18]; the only difference is that the concentrations of these rings in the dehydroxylated gels are significantly larger.

The evidence regarding the structural origin of the D_2 band found in conventional fused silica and high surface area silica gels is quite compelling. (1) The relative intensity of D_2 increases with glass fictive temperature [19] with an activation energy that agrees with molecular orbital calculations for the heat of formation of 3-membered structures [20] and with that found by differential scanning calorimetry measurements [18] in sol-gel glasses.

(2) Galeener et al. [17] calculated the force constants needed to vibrationally decouple these "defect" bands from the continuous random network, thereby, explaining the narrow lines as well as the lack of silicon motion. (3) Brinker et al. [15] have performed ^{29}Si NMR and Raman scattering studies of high surface area silica gels demonstrating that the 608 cm^{-1} D_2 band is related to reduced Si-O-Si bond angles. The correlation of the ^{29}Si chemical shift and the Si-O-Si bond angle, ø, indicated that the structures responsible for D_2 have ø = 137° consistent with the formation of strained 3-membered rings [15,18] according to:

$$O_3Si\text{-}OH + HO\text{-}SiO_3 - O_3Si\text{-}O\text{-}SiO_3 + H_2O \quad (1)$$

We use high surface area silica gels prepared in an identical manner as in the NMR studies to establish the relationship between siloxane bond strain and radiolysis in this study. The high surface area silica gels (surface area 850 m^2/g) were prepared using a two-step acid-base hydrolysis procedure described in Ref. 18. After drying at 60°C the gels were heated at 1°C/min to 400°C in air, and held at 400°C for 2 hrs to oxidize the organics. The samples were then annealed at 1°C/min to 650°C, held at that temperature for 60 hrs in vacuum (10^{-7} Torr), cooled to room temperature, and sealed in glass test tubes under vacuum. During the gamma irradiations (^{60}Co), ESR, and Raman scattering measurements the gels were maintained under rigorously dry conditions. Another set of experiments were performed on gels exposed to 100% relative humidity at room temperature for either 3, 12 or 24 hrs; after exposure to water vapor the gels were gamma irradiated.

The ESR measurements were made at room temperature for the E' centers and at either room temperature or 120K for

the OHC's. The spectra for the E' centers (OHC's) were taken using a microwave power of 5 μW (5 mW). Because of the interference of the E' center with the OHC, we used the amplitude of the positive maximum-negative minimum of the OHC spectrum as an indication of the relative behavior of the defect density. By comparing the spectra to a calibrated spin standard (strong pitch) spin concentrations were determined.

Exposure of the silicate gels to water vapor for increasing times results in a monotonic decrease of the Raman D_2 band as illustrated in Fig. 1. The Raman data was not normalized in this figure and the Rayleigh wing was not subtracted. The extent of hydrolysis on the D_2 band was previously examined by normalizing to the 430 cm^{-1} band [25]. This hydrolysis result has been explained by Brinker et al. [18] and is consistent with the work of Michalske and Bunker [26] dealing with strain enhanced reactivity of Si-O bonds. We believe that the water vapor is simply hydroxylating strained Si-O bonds thereby releasing the strain according to the reverse of reaction 1. Since these gels were originally synthesized in an aqueous environment, and have never been heated above 650°C, it is unlikely that measurable quantities of oxygen vacancies are present in the dehydroxylated gels, and that exposure to water vapor will produce a measurable reduction in oxygen vacancies. For example, Galeener [24] has shown that for conventional a-SiO_2 the number of E' precursors (presumably oxygen vacancies) decreases with glass fictive temperature as does the D_2 band. Thus for glasses never heated above 650°C, the number of pre-existing oxygen vacancies should be very small. Therefore, oxygen vacancies and their possible destruction/creation by water vapor/dehydroxylation should not greatly contribute to our results. Examining the high surface area silica gels simply enables us to study the relationship between the strained rings and the corresponding point defects generated in a more straightforward manner. In contrast, this would be extremely difficult in other forms of a-SiO_2 in which the concentrations of these rings are so smaller, so other precursors of radiation damage centers may dominant.

In Fig. 2 we illustrate ESR spectra of E' centers in gamma irradiated (220 MRad) silicate gels with different D_2 concentrations. Fig. 2 (a, b, and c) corresponds to the samples shown in Fig. 1 (a, b, and c) respectively. For example, the sample used in Fig. 2(a) has the largest D_2 concentration; the sample used in Fig. 2(c) has the smallest D_2 concentration. As demonstrated, the irradiated gels with the largest D_2 concentration exhibit the largest concentration of E' centers,

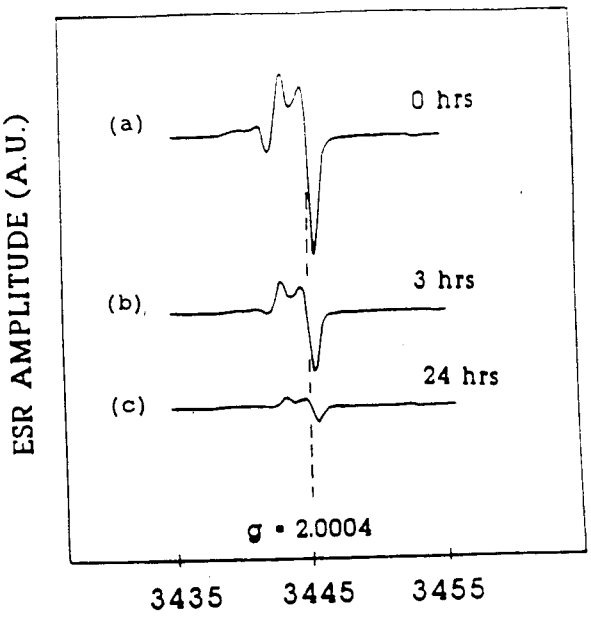

Figure 2 ESR spectra of E' centers in irradiated silicate gels exposed to water vapor for the various times (a) 0 hrs, (b) 3 hrs, and (c) 24 hrs. All samples were irradiated to 220 MRad; all spectrometer settings and sample masses where identical.

8 X 10^{15} E' centers/gram.

Figure 3 illustrates the relative E' concentration as a function of irradiation dose for silicate gels with two different D_2 concentrations. (The sample with the larger D_2 intensity was not exposed to water vapor; the silica gel with the smaller D_2 intensity was exposed to water vapor for 12 hrs.) Note that the relative E' concentration is greater (especially at higher doses) in the silicate gel with the largest D_2 concentration.

In Fig. 4 we illustrate the relative concentration of the OHC's vs. irradiation dose for the same samples illustrated in Fig. 3. As shown, the concentration of OHC's is also significantly greater in the silicate gels with the largest D_2 concentrations. By comparing Figs. 3 and 4 one can see that the rate of generation of E' centers and OHC's is nearly identical, as also found by Devine and Arndt [12] in irradiated plastically densified Suprasil W1. The maximum concentration of OHC's in Fig. 4 is 7 X10^{15}/gram; however, it is difficult to extract a precise value (even at 120K) due to the interference of the E' center as mentioned earlier. The concentrations of the E' centers and OHC's are not very large in comparison to regular fused

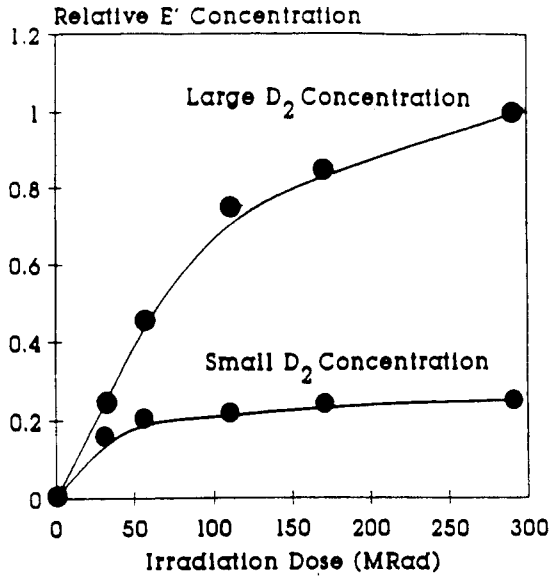

Figure 3 Relative E' concentration vs. irradiation dose for silicate gels with different D_2 concentrations.

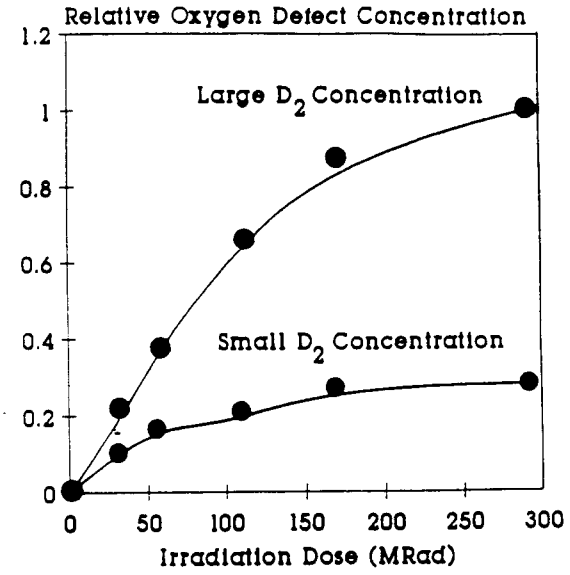

Figure 4 Relative paramagnetic oxygen center concentration vs. irradiation dose for silicate gels with different D_2 concentrations. The samples used are the same as those used in Figure 3.

silica; we believe that this is because (1) the 3-membered rings are not under a lot of strain, and the strain is local in nature, (2) the very low temperature of the gels [24] and (3) the effects we are observing are primarily surface related. Nonetheless, the rings are strained enough that there are marked differences in the response of the gels with different concentrations of them.

Our results cannot be explained by the notion that we are destroying precursors to the NBOHC in the gels exposed to water vapor. SiOH groups are the most generally accepted precursor to the NBOHC; thus, exposure of the gels to water vapor, which causes the formation of SiOH according to the reverse of reaction (1), might be expected to increase the OHC density after irradiation. Our results show an opposite trend: exposure to water vapor causes a reduction in the OHC density after irradiation. Thus, SiOH must not predominate OHC precursors in this case. The close correspondence of the OHC and E' densities with dose suggest a different mechanism in which E' and OHC's are created by the same mechanism.

Figures 1 through 4 show that the concentration of radiation induced point defects is greater when the relative concentration of the D_2 species is the greatest. Assuming that bond strain due to the small rings increases radiation sensitivity, we believe that this observation suggests evidence for a new fundamental precursor to both E' and paramagnetic oxygen centers involving strained Si-O bonds.

Since we do not observe any broadening or distortion of the E' spectrum due to dipole-dipole interactions the E' centers and OHC's must be at least 15Å apart. Therefore, it is unlikely that an E' center and a OHC are nearest neighbors as expected for the simple reaction.

$$h\nu + O_3Si\text{-}O\text{-}SiO_3 \longrightarrow \cdot SiO_3 + \cdot O\text{-}SiO_3$$

The process mechanism is undoubtedly more complicated.

In summary, we have been able to provide evidence that suggests that strained three membered rings can be precursors to E' centers and OHC's. This observation may be of considerable importance since it provides for the first time some evidence for a relationship between a specific strained silicate structure and radiation induced paramagnetic point defects in a-SiO_2.

REFERENCES

1) Ionizing Radiation Effects in MOS Devices and Circuits, eds. T-P. Ma and P.V. Dressendorfer, (Wiley, N.Y., 1989).

2) M. Stapelbroek, D.L. Griscom, E.J. Friebele and G.H. Sigel, J. Non-Cryst. Solids, 32, 313 (1979).

3) D.L. Griscom and E.J. Friebele, Phys. Rev. B24, 4896 (1981).
4) R.H. Silsbee, J. Appl. Phys., 32, 1456 (1961).
5) D.L. Griscom, E.J. Friebele and G.H. Sigel, Solid State Commun., 15, 479 (1974).
6) E.J. Friebele, D.L. Griscom, M. Stapelbroek and R.A. Weeks, Phys. Rev. Lett., 42, 1346 (1979).
7) F.J. Feigl, W.B. Fowler and K.L. Yip, Solid State Commun., 14, 225 (1974).
8) J. Robertson, J. Phys. C, 17, L221 (1984).
9) A.H. Edwards, W.B. Fowler and F.J. Feigl, Phys. Rev. B37, 9000 (1988).
10) P.M. Lenahan and P.V. Dressendorfer, J. Appl. Phys., 55, 3495 (1984).
11) F.J. Grunthaner and P.J. Grunthaner, Mat. Sci. Rep., 1, 69 (1986).
12) R.A.B. Devine and J. Arndt, Phys. Rev. B39, 5132 (1989)
13) R.A.B. Devine, Nucl. Instrum. Meth., B46, 244 (1990).
14) We are unable to specify if the OHC's are peroxy radicals, NBOC's or H-O-O· centers since the g tensor of these three point defects are similar. ^{17}O isotope experiments are needed to prove the identity of our OHC's. D.L. Griscom and C.J. Brinker found this to be especially true in sol-gel glasses, Diff. and Defect Data, 53-54, 213 (1987) and J. Non-Cryst. Solids, 92, 295 (1987).
15) C.J. Brinker, R.J. Kirkpatrick, D.R. Tallant, B.C. Bunker and B. Montez, J. Non-Cryst. Solids, 99, 418 (1988)
16) F.L Galeener, Sol. State Commun., 44, 1037 (1982).
17) F.L. Galeener, R.A. Barrio, E. Martinez, and R.J. Elliot, Phys. Rev. Lett., 53, 2429 (1984).
18) C.J. Brinker, D.R. Tallant, E.P. Roth and C.S. Ashley, J. Non-Cryst. Solids, 82, 117 (1986).
19) A.E. Geissberger and F.L. Galeener, Phys. Rev. B28, 3266 (1983).
20) M. O'Keeffe and G.V. Gibbs, J. Chem. Phys., 81, 876 (1984)
21) R.J. Bell and P. Dean, Phil. Mag., 25, 1381 (1972).
22) R.L. Mozzi and B.E. Warren, J. Appl. Cryst., 2, 164 (1969).
23) P. Ordejon and F. Yndurdin, Phys. Rev. B43, 4552 (1991).
24) F.L. Galeener, J. Non Cryst. Solids, 71, 373 (1985).
25) C.J. Brinker, B.C. Bunker, D.R. Tallant and K.J. Ward, J.deChemie Physique, 83, 851 (1986).
26) T.A. Michalske and B.C. Bunker, J. Appl. Phys., 56, 2686 (1984).

Journal of Non-Crystalline Solids 136 (1991) 151–162
North-Holland

JOURNAL OF
NON-CRYSTALLINE SOLIDS

Experimental evidence for two fundamentally different E′ precursors in amorphous silicon dioxide

William L. Warren
Sandia National Laboratories, Ceramics Division, Albuquerque, NM 87185, USA

Patrick M. Lenahan
The Pennsylvania State University, University Park, PA 16802, USA

C. Jeffrey Brinker
Sandia National Laboratories Inorganic Materials Chemistry Division, Albuquerque, NM 87185, USA

Received 7 May 1991
Revised manuscript received 2 July 1991

E′ centers (trivalent silicons) in two silicate systems, thermally grown SiO_2 films on silicon and high surface area bulk sol–gel silicates, have been investigated. In the thermally grown silicon dioxide films, earlier work is extended by demonstrating that the hole trapping process is reversible; no complex structural rearrangement occurs at the hole trapping site (E′ centers) after subsequent electron capture. This provides further evidence that these thermal oxide E′ centers are oxygen vacancies as originally proposed by Feigl, Fowler and Yip. Also investigated is the radiation-induced generation of paramagnetic centers in high surface area sol–gel silicates containing various concentrations of the Raman active 608 cm^{-1} D_2 band attributed to strained cyclic trisiloxanes (three-membered rings). The results suggest a correlation between the concentration of the strained three-membered rings and the concentration of radiation-induced E′ and paramagnetic oxygen centers, thus providing the first substantive evidence of the relationship between a *specific strained siloxane structure* and radiation damage in amorphous silicon dioxide. These results suggest the existence for (1) two different fundamental E′ precursors and (2) a relationship between atomic level stress and the radiation damage process in amorphous silicon dioxide.

1. Introduction

The effects of ionizing radiation on amorphous silicon dioxide have been extensively investigated for over thirty years [1–6]. Ionizing radiation degrades the insulating layers of metal oxide semiconductor field effect transistors (MOSFETs) [4–6] and impairs the transmission properties of low loss optical fibers [7,8]. Thus, a detailed understanding of the mechanisms and structural origins of the radiation damage process in amorphous silicon dioxide (a-SiO_2) is of considerable interest.

Electron spin resonance (ESR) is generally recognized as a sensitive probe of atomic scale defect structure in a-SiO_2. Extensive ESR studies have been performed on crystalline quartz [2,9] and bulk a-SiO_2 [7,8,10] subjected to various forms of irradiation (X-rays, gamma rays and neutrons). These investigations have identified several intrinsic point defects: E′ centers, peroxy radicals and non-bridging oxygen hole centers (NBOHC). The E′ center is an unpaired electron on a silicon bonded to three oxygen atoms [9,10]; it is the most extensively investigated point defect in a-SiO_2. One theoretical model [11–14] identifies the E′ center precursor as an oxygen vacancy ($O_3{\equiv}Si{-}Si{\equiv}O_3$). The positive charge state of the oxygen vacancy E′ centers in gamma irradiated and vacuum ultraviolet irradiated thermally grown

silicon dioxide films on silicon was experimentally established by a number of workers [15–22].

The peroxy radical ($\cdot O-O-Si\equiv O_3$) and NBOHC ($\cdot O-Si\equiv O_3$) have been identified as two intrinsic paramagnetic oxygen centers that predominate in 'dry' (low water, < 5 ppm OH) and 'wet' (high water) silicas, respectively [7,23–25]. The precursors for the peroxy radical and NBOHC are believed to be an oxygen surplus site ($O_3\equiv Si-O-O-Si\equiv O_3$) [23] and a hydroxyl site ($O_3\equiv SiO-H$) [24], respectively.

Unfortunately, ESR does not always provide information concerning precursor structures of defects since they may be diamagnetic. Other experimental tools in conjunction with ESR are usually needed to obtain information regarding the nature of a defect's precursors [2,26,27]. In this investigation, we have investigated E' centers in two amorphous silica systems – thermally grown silicon dioxide films on silicon and high surface area bulk silicate gels; we find evidence for two fundamentally different E' precursors: (1) oxygen vacancies and (2) structures involving strained silicon–oxygen bonds. To obtain this information, ESR in conjunction with other experimental techniques were used.

First, we further investigate the hole trapping process in thermal oxides on silicon using ESR, capacitance vs. voltage (CV) measurements and a series of electron and hole injection sequences. Examining the dynamic behavior of E' centers [28], we find that the E' center can be cycled back and forth repeatedly from positively charged to neutral to positively charged without detectably altering the ESR signature. This result, we believe, is completely consistent with the theoretical model of the E' center proposed by Feigl, Fowler and Yip (FFY), the oxygen vacancy model [11–14].

Second, we investigated the generation of paramagnetic centers in high surface area sol–gel silicates. Based on the results of ESR, Raman scattering, and ^{29}Si magic angle spinning nuclear magnetic resonance (MAS-NMR) experiments, we present evidence for a new fundamental E' and oxygen hole center (unpaired spin on an oxygen atom) precursor involving strained silicon–oxygen bonds. For years it has been suggested that atomic level stress plays a role in the radiation induced damage process in a-SiO_2 [29–32]. Devine and Arndt [31,32] have provided the first experimental evidence that this is the case by observing large enhancements of defect concentrations in plastically densified silicates over undensified ones. No relationship has been established between paramagnetic point defects generated by ionizing radiation and a *specific* strained silicate structure to our knowledge. This study provides evidence that suggests that strained cyclic trisiloxanes (three-membered rings – an n-membered ring has n silicon tetrahedra connected by n bridging oxygens) are also precursors to E' centers as well as oxygen hole centers (OHC).

We have used Raman scattering combined with earlier ^{29}Si MAS-NMR studies [33] to identify these strained silicate structures. The Raman vibrational band of interest in this study is the 608 cm^{-1} D_2 band. A model consistent with the data for this D_2 line is oxygen ring breathing vibrations of highly regular, planar, strained, cyclotrisiloxanes (three-membered rings) with Si–O–Si angles $\phi = 137°$ [33–39]. Molecular orbital calculations of three-membered ring structures indicate that the reduction of the Si–O–Si bond angle, ϕ, is accompanied by a reduction in the tetrahedral angle (from 109.5° to 103°) and an increase in the Si–O bond length (from 1.626 to 1.646 Å) [38]. By contrast, the average structure of amorphous silicon dioxide is believed to consist mainly of puckered, unstrained, 5–8-membered rings with average $\phi = 149°$ [40,41]. However diffraction studies clearly indicate that regular a-SiO_2 does contain a wide range of Si–O–Si intertetrahedral bond angles [42]. Bond angle (energy) calculations [43,44] indicate that strained bonds also exist in regular vitreous silica due to a distribution of bond angles around 149°. It may be the strained sites in regular forms of silica are also precursor sites to radiation induced paramagnetic defects.

We chose to investigate the radiation effects on high surface area gels since they exhibit the largest concentration of strained rings and are, thus, an ideal system to investigate the response of strained silicate species to ionizing radiation. However, we believe that our observations are

relevant to other high surface area silicates and to a wide range of fused silicas since the Raman D_2 band is present in all known forms of a-SiO_2, i.e., leached alkali silicate glasses, conventional fused silica, flame pyrolyzed $SiCl_4$ (e.g., Cab-O-Sil®), optical fibers and chemical vapor deposited dielectrics on Si. Essentially, all of the experimental features of the D_2 band in the silica gels are identical to those found in other forms of a-SiO_2; the only difference is that the concentrations of these rings in the high surface area dehydroxylated gels are significantly larger, because the formation of three-membered rings appears to be the preferable way to terminate the dehydroxylated silica surface [45].

Examining the high surface area silica gels simply enables us to study the relationship between the strained rings and the corresponding point defects generated in a more straightforward manner; by contrast, this would be extremely difficult in other forms of a-SiO_2 where the concentrations of these rings are so much smaller, that other radiation damage paramagnetic center precursors will most likely dominant.

First, we discuss our thermal oxide results that further demonstrate the E′ precursor to be consistent with the oxygen vacancy model of FFY. Then, we present our results on the silicate gels that suggest that the E′ precursor can also be a strained cyclic trisiloxane.

2. Experimental details – thermal oxide structures

The thermal oxides used in this study were steam grown at 1050°C on p-type (100 Ω cm) silicon with a (111) surface orientation. The oxide thickness was measured to be 1200 Å by ellipsometry, and the Si substrate thickness was 20 mils.

The ESR measurements were made using a TE_{104} double resonant cavity; a weak pitch standard was used to calculate the concentration of E′ centers. When making ESR measurements, care was taken to avoid microwave cavity loading by aligning the samples in the cavity with the c-Si (111) interface plane perpendicular to the external magnetic field (this aligns the sample conjointly with the microwave magnetic field). Using fairly resistive Si substrates, and only two (4.0 × 20 mm) wafer slices also helped avoid microwave cavity loading. CV measurements (1 MHz) were made using a Boonton capacitance bridge and a Hg probe. The mid-gap shifts in the CV curves were used to calculate the number of holes trapped (or annihilated). By comparing the number of E′ centers and the amount of space charge in the oxide (CV), the charge state of the E′ center can be determined. We estimate that the absolute spin concentrations are accurate to at least a factor of two, the relative spin concentrations are accurate to about 10%.

To flood the oxide selectively with holes, we exposed it to vacuum ultraviolet (VUV) photons. The bare oxide structures were first exposed to positive corona ions [46] which applied a relatively (±15%) uniform potential of +25 V across the oxide. The samples were then placed in a vacuum (10^{-4} Torr) and exposed to 10.2 eV photons from a 50 W deuterium lamp. Since the bandgap of SiO_2 is about 9 eV, these photons create electron/hole pairs in the top 100 Å or so of the oxide. Under the action of a positive 'gate' bias, the holes are driven to the Si/SiO_2 interface; the electrons simply recombine with the positively charged corona ions. This procedure was repeated five times to increase our signal to noise ratio. Etch back experiments indicate that the positive charge is located near the Si/SiO_2 interface in accord with earlier works [17,47].

To flood the oxide selectively with electrons unbiased oxide structures were subjected to less energetic photons (< 5.5 eV photons) from a 100 W mercury lamp. This ultraviolet (UV) illumination photoemits electrons from the silicon valence band into the silicon dioxide conduction band.

3. Oxygen vacancy E′ centers

The results of our multiple cycling of electrons and holes into thermal oxide structures are illustrated in figs. 1 and 2. In fig. 1, we illustrate our CV and ESR measurements of thermal oxides subjected to hole and electron injection sequences. Figure 2 shows the concentrations of E′

centers and space charge in the oxide as a function of illumination (injection) history. In fig. 1(a), we show the virgin CV and ESR measurements. Next the samples were flooded with holes as described earlier. As seen by the negative shift in the CV curve of fig. 1(b), hole trapping has occurred. From the ESR measurements (figs. 1(b) and 2), E′ centers were also created. The concentration of E′ centers is located close to the Si/SiO_2 interface as observed in earlier studies [15–18]. The E′ center is identified by its double humped lineshape and zero-crossing $g = 2.0005$. The g factor is defined as $g = h\nu/\beta H$, where h is Planck's constant, ν is the microwave frequency, β is the Bohr magneton and H is the magnetic field at which resonance occurs.

Next, the samples were subjected to UV illumination (the oxide was flooded with electrons). After about 10 h of electron injection, we again made CV and ESR measurements (figs. 1(c) and 2). We find that most of the E′ centers and trapped holes have been annihilated.

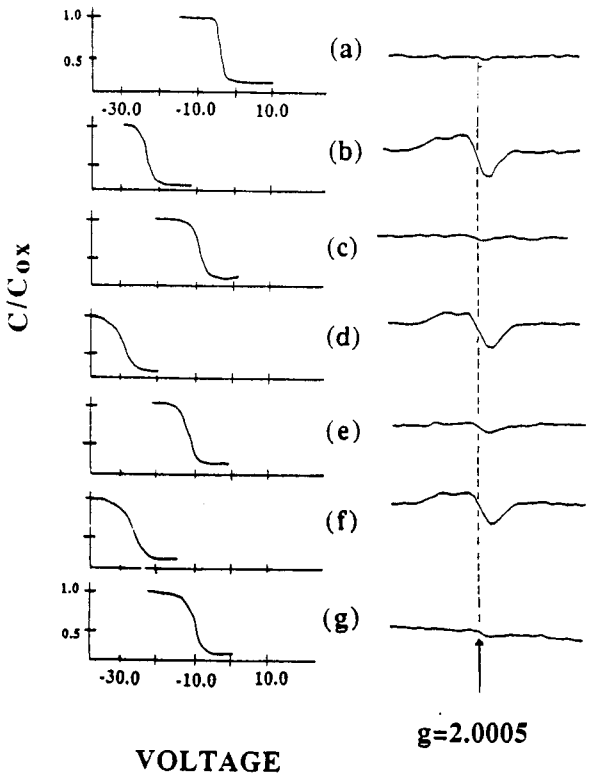

Fig. 1. CV curves and ESR traces for various electron and hole injection sequences: (a) virgin, (b) hole injection, (c) electron injection, (d) hole injection, (e) electron injection, (f) hole injection, and (g) electron injection.

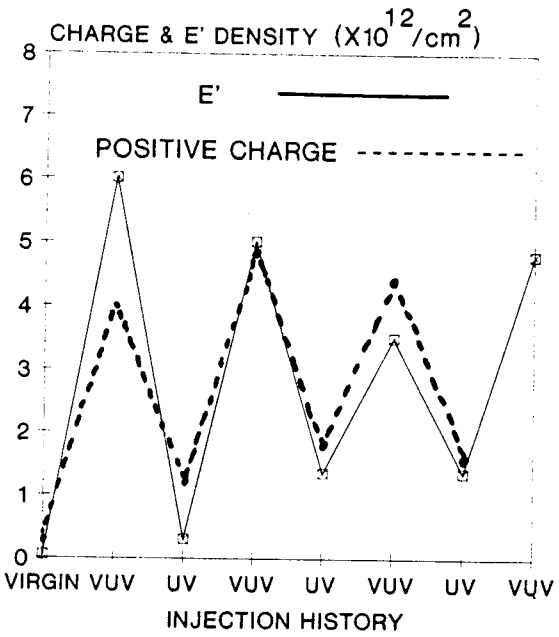

Fig. 2. Densities of trapped holes and E′ centers in a thermal oxide subjected to various electron and hole injection sequences. The absolute error in the spin resonance measurements is a factor of two and relative error is about 10%. The estimated error in the concentration of trapped charge is 10%.

At this point the cycling behavior of the E′ center was investigated, i.e., we subject the samples to exactly the same hole and electron flooding procedure used in the first steps of the experiment. Our results are consistent with the oxygen vacancy model for the E′ center [11–14]. The oxygen vacancy model of FFY is illustrated in fig. 3. Upon hole capture, an asymmetric relaxation occurs. In their model the unpaired electron is localized at one of the silicon sites, rather than shared by both. The other silicon is positively charged and decreases its energy by relaxing, approximately, into the plane of its three remaining oxygen neighbors, forming sp^2 hybrids. The FFY model agrees quite well with the ^{29}Si E′ hyperfine data of Silsbee [9] in quartz and Griscom et al. [10] in bulk amorphous silica; these hyperfine studies showed that the unpaired elec-

tron is highly localized on one silicon atom. (However, as we shall show, this is not an unambiguous identification of precursor structure.) The positive charge state of the oxygen vacancy E' center was established by others on thin thermal oxide films [15–19,21,22]; this state is also consistent with this work.

After trapping the hole, the positively charged E' centers are a Coulombically attractive trap for electrons. We would expect that with electron injection into the oxide, these positively charged centers would readily capture the electrons, 're-forming' the neutral oxygen vacancy as illustrated in fig. 3 (bottom part). As shown in fig. 1(c), this is consistent with our observations.

Now, if the neutral oxygen vacancy is truly reformed, then upon hole injection we should again observe the generation of E' centers and positive charge. As illustrated in fig. 1(d), again this sequence is observed.

It is possible that the variation in the E' concentration following each hole flooding sequence (fig. 2) most likely results from the nature of the corona ions. The corona ion bias can vary by ±15% during each VUV illumination, which will vary the concentration of holes injected into the oxide by ±15%. (The procedure was repeated five times for each datapoint.) With a varying hole flux, the E' density may vary.

In order to further demonstrate that the E' center is positively charged when paramagnetic,

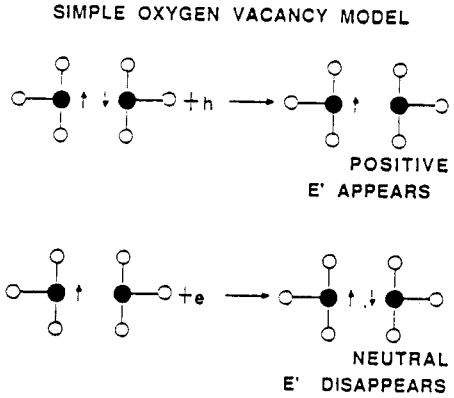

Fig. 3. Schematic illustration of the hole trapping process followed by subsequent electron capture in the oxygen vacancy model.

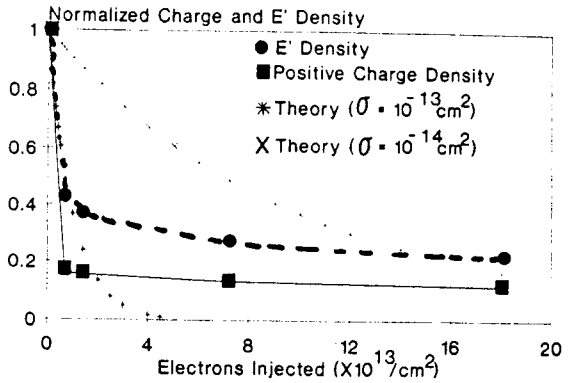

Fig. 4. Decay of the E' center and the positive charge vs. the areal concentration of electrons photoinjected. The theoretical decay rate for defects with capture cross-sections of 1×10^{-13} cm^2 and 1×10^{-14} cm^2 are also plotted using eq. (2). The lines drawn through the experimental points are meant only as a guide. The decay rates are indicative of a Coulombically attractive trap.

we have calculated the capture cross-section for annihilating the E' center by electrons. The thermal oxides were flooded with holes as described above (resulting in the generation of E' centers and positive charge), and subsequently flooded with a known number of electrons. To estimate the number of electrons injected, a positive voltage on the oxide surface was applied using corona ions. This voltage was measured using a Kelvin probe and an electrostatic voltmeter. By measuring the decay in the corona ion bias during UV illumination, the number of electrons photoinjected into the oxide can be calculated from $C_{ox}V = Q$. Figure 4 presents our results. Assuming that the positively charged E' centers are annihilated by electron capture, and assign a capture cross-section, σ, to this center, the E' annihilation may be described by first order trapping kinetics [48,49],

$$dE'/dt = -\sigma E'(dn_e/dt), \qquad (1)$$

where E' is the volume density of E' centers and n_e is the number of electrons injected into the oxide per cm^2. Integrating, we obtain

$$E' = E'_{VUV}\exp(-\sigma n_e), \qquad (2)$$

where E'_{VUV} is the maximum E' concentration following VUV illumination (hole flooding).

Figure 4 plots the normalized E' and positive charge density versus the concentration of electrons injected into the oxide, n_e. Again the numbers of positive charge and of E' centers exhibit similar trends. Figure 4 also plots the expected decay in the E' density assuming that the capture cross-section is either $\sigma = 1 \times 10^{-13}$ cm^2 or 1×10^{-14} cm^2 using eq. (2). Even though a single capture cross-section could not be fit to our data, the range of capture cross-sections is close to that for a Coulombically attractive (positively charged) trap [49].

At this time, we would like to further argue that the E' centers in our experiments are generated by hole capturing events at pre-existing oxygen vacancies. Our results cannot be interpreted by an oxygen displacement or by some sort of precursor transformation that may occur during a non-radiative decay of excitons (from a laser [50,51]). Because an electric field was applied during the illuminations, the photo-generated electron/hole pairs are separated, inhibiting exciton formation, and the subsequent generation of permanent oxygen vacancies that may occur due to their non-radiative decay [51].

Even though the cycling experiments are consistent with the FFY oxygen vacancy model, and the E' center is a deep hole trap in these MOS thermal oxides, it cannot generally be concluded that E' centers are always responsible for the positive charge in a thermal oxide. There are examples in which this is not the case, i.e., thermal oxides subjected to high electric fields [52–54] or the negative bias temperature instability [55]. Likewise, recent hole flooding work by Yokogawa et al. [56] shows that the E' center is not the nature of the hole trap in their thermal oxides.

4. Experimental details – sol–gel silicates

The high surface area silicate gels (surface area 850 m^2/g) were prepared using a two-step acid–base hydrolysis procedure described in ref. [57]. After gelation at room temperature, the solvent (ethanol) was evaporated at 60°C. The gels were then heated at 1°C/min to 400°C in air and held at 400°C for 2 h to oxidize organics. The samples were then annealed at 1°C/min to 650°C, held at this temperature for 60 h in vacuum (10^{-7} Torr), cooled to room temperature, and sealed in glass test tubes under vacuum. Previous ^{29}Si MAS-NMR and Raman spectroscopic studies indicated that after heating to 650°C the gels contained over 2.2 cyclic trisiloxanes/nm^2 of surface [45] and exhibited a very intense 608 cm^{-1} Raman active vibration, labeled D_2 [58].

During gamma irradiations (^{60}Co) and ESR measurements, the gels were maintained under dry conditions. A second set of experiments was performed on the gels after exposure to 100% relative humidity at room temperature for either 1, 3, 12 or 24 h. The ESR measurements were made at room temperature for the E' centers and 120 K or room temperature for the OHCs. The spectra for the E' centers (OHCs) were taken using a microwave power of 5 μW (5 mW) and a modulation amplitude of 0.2 G (2.5 G). Because of the interference of the E' center with the OHC, we used the amplitude of the positive maximum-negative minimum of the OHC spectrum as an indication of the relative numbers of the defect. By comparing the spectra to a calibrated spin standard (strong pitch) spin concentrations were determined using a TE_{104} cavity. The absolute spin concentrations are accurate to about a factor of two.

Before presenting our ESR and Raman scattering results on the silicate gels, we discuss evidence regarding the structural origin of the Raman active 608 cm^{-1} D_2 band. Our conclusions regarding the precursor of the E' center in some silicate gels are based upon Galeener's 'generally' accepted model [33–39] (see ref. [59] for a differing interpretation) of the D_2 band, namely, oxygen ring-breathing vibrations of a highly regular, planar, strained, cyclotrisiloxanes.

5. D_2 band in silicates

Prominent features in the Raman spectra of silicate gels are illustrated in fig. 5. The spectra consist of narrow bands at 490 and 608 cm^{-1} and broad features at 430, 800, 1065 and 1200 cm^{-1}. The broad features can be understood in terms of

the vibrations of a continuous random network model [60,61]. The narrow bands at 490 and 608 cm^{-1} could not be explained by that model.

The evidence relating the structural origin of the D_2 band found in conventional fused silica and high surface area silica gels to cyclic trisiloxanes (three-membered rings) is by now quite compelling. For instance, Brinker et al. [33] have performed ^{29}Si nuclear magnetic resonance and Raman scattering studies of high surface area silica gels demonstrating that the 608 cm^{-1} D_2 band is related to reduced Si–O–Si bond angles. The correlation [62] of the ^{29}Si chemical shift and the Si–O–Si bond angle, ϕ, indicated that the structures responsible for D_2 have $\phi = 137°$ consistent with the formation of three-membered rings according to reaction (3):

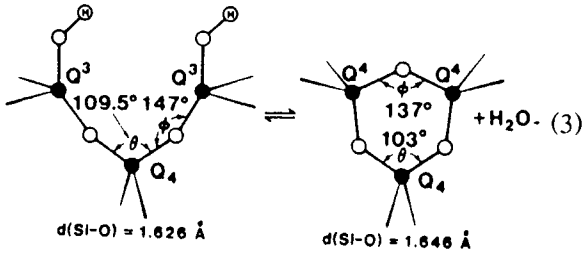

Hydrolysis of the rings according to the reverse of reaction (3) was shown to increase the average Si–O–Si bond angle to 147° (eliminate strain) and severly reduce the D_2 band to a level comparable to well annealed conventional a-SiO_2 [33].

6. Sol–gel silicate results

Exposure of the silicate gels to water vapor for increasing times at room temperature results in a monotonic decrease of the Raman D_2 band, as illustrated in fig. 5. This hydrolysis result has been explained by Brinker and co-workers [33,37] and is consistent with the work of Michalske and Bunker [63] dealing with strain enhanced reactivity of Si–O bonds.

Figure 6 shows the ESR spectra of E′ centers in gamma irradiated (220 MRad) silicate gels with differing D_2 concentrations. Figure 6 (a)–(c) correspond to the samples shown in fig. 5 (a)–(c), respectively. For example, the sample used in fig.

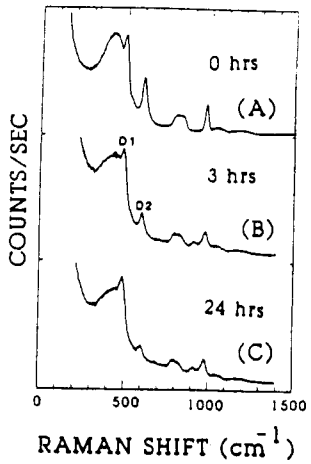

Fig. 5. Raman spectra of sol-gel silicates exposed to water vapor for various times: (a) 0 h, (b) 3 h and (c) 24 h.

6(a) has the largest D_2 concentration; the sample used in fig. 6(c) has the smallest D_2 concentration. As fig. 6 demonstrates, the irradiated silicate gels with the largest D_2 concentration have the largest concentration of E′ centers (this is especially evident at high irradiation doses); the gels with the smallest D_2 concentration have the smallest concentration of E′ centers.

Figure 7 illustrates the relative E′ concentration as a function of irradiation dose for silicate

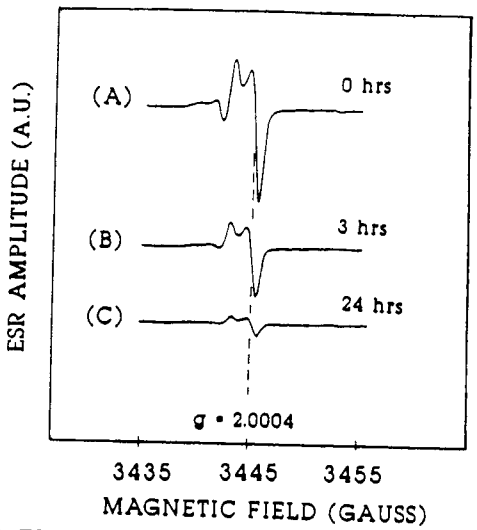

Fig. 6. ESR spectra of E′ centers in irradiated silicate gels exposed to water vapor for various times: (a) 0 h, (b) 3 h and (c) 24 h. All samples were subjected to 220 MRad.

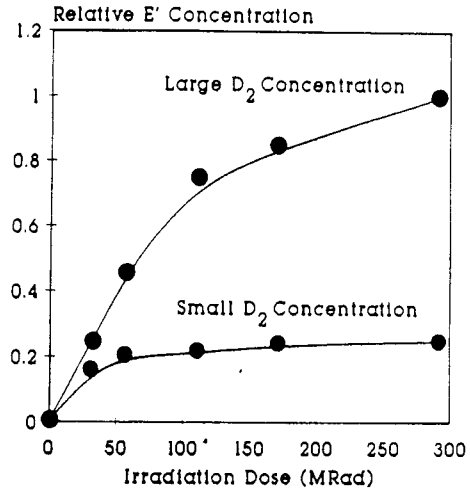

Fig. 7. Relative E′ concentration as a function of irradiation dose for silicate gels with different D_2 concentrations. The lines drawn are meant only as a guide to the eye.

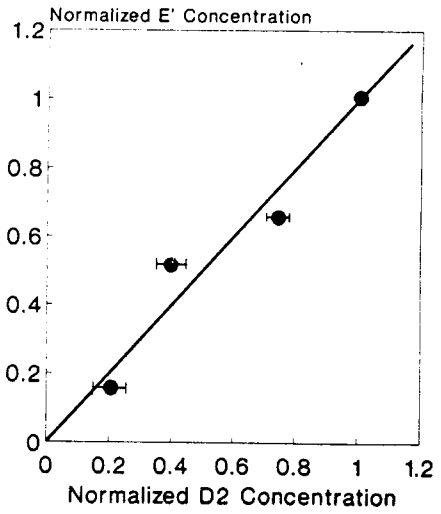

Fig. 8. Plot of the relative D_2 intensity vs. the relative E′ concentration for silica gels exposed to water vapor for 0 h, 1 h, 3 h and 24 h and subsequently irradiated to 220 MRad. The D_2 intensity was calculated using the psuedo-first order rate constant of $5.2+10^{-3}$/min given in ref. [64]. The relative error in E′ is 10%. The line drawn simply represents the situation assuming a 1:1 correlation between D_2 and E′.

gels with differing D_2 concentrations. (The sample with the larger D_2 intensity was not exposed to water vapor; the silica gel with the smaller D_2 intensity was exposed to water vapor for 12 h.) The concentration of E′ centers in the sample with the largest D_2 concentration after 290 MRad is 7×10^{15}/g.

In fig. 8, we plot the normalized D_2 concentration vs. the normalized E′ concentration. The D_2 peak in the gel not exposed to H_2O vapor was normalized to one. The four samples correspond to silicate gels exposed to water vapor for 0 h, 1 h, 3 h and 24 h. We calculate the normalized D_2 intensity using the psuedo first order rate equation for the hydrolysis of three-membered rings exposed to water vapor [64], i.e., the rate constant is $5.2\ (\pm 0.5) \times 10^{-3}$/min. As can be seen, there appears to be correlation between the D_2 species and the number of radiation induced E′ centers.

Figure 9 illustrates the relative concentration of OHCs [65] vs. irradiation dose for the samples for which data is shown fig. 7. As shown, the concentration of OHCs is also greater in the silicate gels with the largest D_2 concentration. The concentration of OHCs is approximately 7×10^{15}/g. The concentrations of E′ centers and OHCs are not very large in comparison to bulk vitreous a-SiO_2; this may result because the gels are prepared at very low temperatures and have extremely high surface areas compared to bulk a-SiO_2. In these different forms of silica, different paramagnetic precursors are likely to predominant.

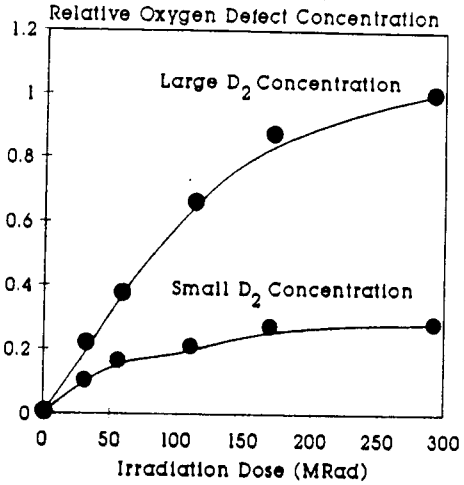

Fig. 9. Relative oxygen hole center concentration vs. irradiation dose of silicate gels with different D_2 concentrations. The samples used were the same as those used in fig. 7. The lines drawn are provided simply as a guide to the eye.

Figures 6–9 show that the concentration of radiation induced point defects is greater when the relative concentration of Raman D_2 species is greatest. Assuming that bond strain due to the small rings increases radiation sensitivity, this observation may provide evidence for a new fundamental precursor to both the E' center and OHCs [65] involving strained Si–O bonds.

7. Discussion

7.1. Alternative models

At this point, we discuss some alternative explanations of our data. For instance, it could be argued that the water vapor exposures not only decrease the concentration of three-membered rings, but also the concentration of oxygen vacancies which are known to be precursors to the E' center. In this case, the correlation between the D_2 concentrations and the gamma irradiated E' and OHC concentrations would be casual, not causal, i.e., upon exposure to water vapor, the D_2 band and E' and OHC precursors may be removed by separate parallel reactions albeit with virtually identical rates. We discuss the consequences/significance of this in the following paragraphs.

First, since these gels were originally synthesized from well defined $Si(OC_2H_5)_4$ molecules in an aqueous environment and have never been heated above 650°C, it is unlikely that measurable quantities of oxygen vacancies are present in dehydroxylated gels, and therefore that exposure to water vapor will produce a measurable reduction of them. For example, Galeener [66] has shown that for conventional a-SiO_2 the number of E' precursors (presumably oxygen vacancies) decreases with glass fictive temperature as does the D_2 band. Thus, for glasses never heated above 650°C, the number of pre-existing oxygen vacancies should be very small. Therefore, oxygen vacancies and their possible destruction/creation by water vapor/dehydroxylation should not greatly contribute to our results. By contrast, the concentration of strained bonds in the dehydroxylated gels is much larger than that in a-SiO_2 due to the high concentrations of three-membered rings. The predominant effect of water vapor in this case is simply the hydrolysis of strained Si–O bonds according to the reverse of reaction (3).

Second, further evidence of a causal relationship between strained three-membered rings and gamma irradiated E' generation is that both the strained siloxane bonds and the E' (and OHC) precursors are located in close proximity to the surface and exhibit virtually identical responses to water vapor exposure. The diffusion constant of water in a-SiO_2 is $< 5 \times 10^{-20}$ cm^2/s at room temperature [67]; therefore, water can diffuse only about 6 Å in 24 h at room temperature, requiring both the strained siloxane bonds and the E' (and OHC) precursors to be located within this surface affected region. Further, fig. 7 shows approximately a 1 : 1 dependence of the change in E' concentration with change in strained cyclotrisiloxanes (D_2) upon exposure to water vapor. We suggest that for the strained siloxane bonds and the E' precursor to be located near the silica surface and to exhibit practically identical responses to water vapor exposure indicates that the strained siloxane bonds and E' precursors are one and the same.

Third, in several instances [68,69] SiOH, rather than oxygen vacancies, have been suggested as precursors to the E' center. Devine [68] suggested that SiOH precursors might explain the significant increase in the E' defect creation in gamma irradiated undensified and densified wet silica (Suprasil 1) as compared with dry silica (Suprasil W1). Our results clearly show the opposite trend, namely, exposure of comparatively dry gels to water vapor creates SiOH groups according to the reverse of reaction (3), yet after gamma irradiation fewer E' centers were generated. We do not mean to overemphasize this suggested precursor model to the E' center, since it may pertain in only limited cases; nonetheless, it supports the idea that exposing the gels to water vapor does nessecarily destroy supposed E' precursors.

Fourth, Stapelbroek, Griscom and co-workers have shown that SiOH is the most likely the precursor to the NBOHC [7,24,25]. Therefore, exposure of the gels to water vapor, which causes

the formation of SiOH according to the reverse of reaction (3), might be expected to increase the OHC concentration after irradiation. Our results show an opposite trend: exposure to water vapor causes a reduction in the OHC concentration after gamma irradiation as illustrated in fig. 9. Thus, SiOH must not be the predominant OHC precursor in this case. The close correspondence of the OHC and E′ concentration with dose suggests that the E′ and OHCs are created by the same mechanism.

Although the arguments put forth are not unambiguous proofs in and of themselves, they suggest that the dominant E′ and OHC precursors in the dehydroxylated gels are strained siloxane bonds contained in three-membered rings and that the E′ and OHC form by the rupture of strained silicon–oxygen bonds.

Since we do not observe any broadening or distortion of the E′ spectrum due to dipole–dipole interactions (which one would expect for two unpaired spins in close proximity), the E′ centers and OHC, once generated, must separate to a distance of at least 15 Å. Therefore, it is unlikely that an E′ center and OHC are nearest neighbors as expected for the simple reaction,

$$h\nu + O_3{\equiv}Si{-}O{-}Si{\equiv}O_3 \text{---} O_3{\equiv}Si\cdot + \cdot O{-}Si{\equiv}O_3. \quad (4)$$

The process is undoubtedly more complicated. They may be created as such but other processes cause their ultimate separation.

7.2. ^{29}Si hyperfine interactions

In fig. 10 we illustrate the ^{29}Si E′ hyperfine structure of irradiated (a) Suprasil 1 and (b) silicate gels that have a large D_2 concentration. The ^{29}Si E′ hyperfine structure of Suprasil 1 is shown for comparison only. (The ^{29}Si E′ hyperfine spectra of Suprasil 1 has been reported previously by Griscom et al. [10].)

Hyperfine interactions result from the interaction of an unpaired electron with a nucleus with a magnetic moment. Since ^{29}Si has a spin $I = 1/2$, a two-line ESR spectrum results as shown in fig. 10. The hyperfine lines in fig. 10(a) and (b) were

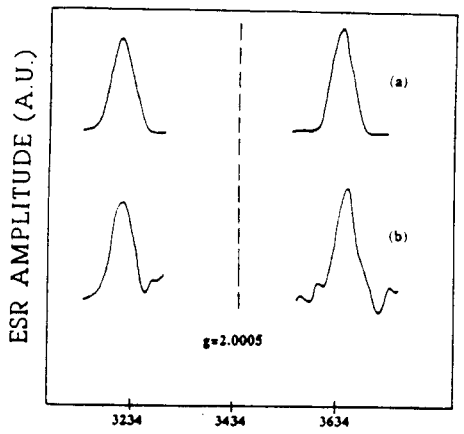

Fig. 10. ^{29}Si E′ hyperfine spectra of (a) Suprasil 1 and (b) a high surface area sol–gel silicate with a large D_2 concentration.

observed in an out of phase second harmonic detection mode at relatively high microwave power (30 mW). Under these conditions, it has been found that the detected signal represents the absorption of the spectrum (approximately) rather than the second derivative of the spectrum [26]. (^{29}Si is only 4.7% abundant.) This detection scheme has been used by a number of authors with success [26,70,71].

From an observation of fig. 10(a) and (b), it is quite obvious that the ^{29}Si hyperfine spectra are identical, within errors of measurements, for the gamma irradiated sol–gel silicate with a large concentration of D_2 species and the Suprasil 1. (As expected, the ^{29}Si hyperfine spectra of our Suprasil 1 sample is identical to that reported by Griscom et al. [10].) From a computer analysis of the ^{29}Si hyperfine spectra, Griscom et al. [10] were able to show that the unpaired electron is highly localized on an sp^3 hybridized orbital on a silicon bonded to three oxygens. The E′ center in the silicate gel with a large concentration of strained silicon–oxygen bonds can be described in this way.

It should be stressed that the Raman spectra of Suprasil 1 (extensively illustrated in the literature [72,73]) exhibit a significantly smaller Raman D_2 band intensity compared with the high surface area silica gels; therefore, it seems unlikely that

strained Si–O bonds, at least in a three-membered ring, are the predominant E′ precursors in Suprasil 1. (As discussed above, strained Si–O bonds also exist in regular forms of silica; thus, it could be argued that the strained sites in regular silica also serve as precursors to radiation induced defects as we have argued for the three-membered rings.) Nonetheless, the ^{29}Si E′ hyperfine spectra are essentially identical for the Suprasil 1 and the sol–gel silicates with large D_2 concentrations. The rupture of a strained bond may release most of the strain, allowing the E′ center to relax back to its 'equilibrium' configuration. This observation may indicate that the strain of the three-membered ring is somewhat localized, once the ring is ruptured the strain is released. (The hydrolysis of the strained Si–O–Si bond also causes the total reduction of stress [33].) It is quite interesting that the work of Devine and Arndt [70] found that the ^{29}Si hyperfine spectrum is dependent on silica densification. It is possible that their densified silica is under a greater strain and is not local in nature since the E′ center does not relax back to equilibrium. These observations may also be explained by assuming that the surface can relax more easily than the bulk. These results demonstrate that the ^{29}Si E′ hyperfine spectra do not necessarily lead to an unambiguous identification of E′ precursor structure. It can, however, provide information regarding E′ defect structure, as shown in other studies [9,10].

8. Conclusions

We have provided experimental evidence for two fundamentally different E′ precursors in amorphous silicon dioxide – namely, oxygen vacancies and strained cyclotrisiloxanes (three-membered rings). In thermally grown silicon dioxide films, we have been able to provide further evidence that E′ precursors are oxygen vacancies, and that the oxygen vacancy E′ center is positively charged when ESR active.

In another silicate system, i.e., high surface area silica gels, we find that the concentrations of both E′ centers and OHCs increase with the concentration of strained three-membered rings, and that the E′ and OHC generation exhibit quite similar dose dependences. The normalized E′ concentration is proportional to the normalized concentration of three-membered rings and both the E′ and the strained siloxane bonds are located in close proximity to the silica surface. Collectively this evidence is consistent with the hypothesis that strained siloxane bonds are precursors to both E′ centers and OHCs. With the various kinds of E′ centers, as also discussed by Griscom [26], it becomes quite apparent that defect analysis in amorphous silicon dioxide is complicated.

The authors would like to thank C.S. Ashley (SNL) and S.T. Reed (SNL) for sample preparation, as well as D.L. Griscom (NRL), R.A.B. Devine (CNET), and E.H. Poindexter (ETDL) for many useful discussions during the course of this work. They would also like to thank D.L. Tallant (SNL) for the Raman data. This work was supported in part by Sandia National Laboratories under contract number DE-AC04-76-DP0078 and by the Defense Nuclear Agency under contract number DNA001-86-C-0055.

References

[1] E.W.J. Mitchell and E.G.S. Paige, Philos. Mag. 8 (1956) 1085.
[2] R.A. Weeks, J. Appl. Phys. 27 (1956) 1376.
[3] R.A. Weeks and C.M. Nelson, J. Am. Ceram. Soc. 43 (1960) 399.
[4] H.L. Hughes and R.R. Giroux, Electronics 37 (1964) 58.
[5] J.R. Schwank, D.M. Fleetwood, P.S. Winokur, P.V. Dressendorfer, D.C. Turpin and D.T. Sanders, IEEE Trans. Nucl. Sci. NS-34 (1987) 1152.
[6] For a complete discussion list of references dealing with the ionizing radiation effects in MOS devices please see: T.-P. Ma and P.V. Dressendorfer, eds., Ionizing Radiation Effects in MOS Devices Circuits (Wiley, New York, 1989).
[7] D.L. Griscom, J. Non-Cryst. Solids 73 (1985) 51.
[8] D.L. Griscom and E.J. Friebele, Rad. Eff. 65 (1982) 63.
[9] R.H. Silsbee, J. Appl. Phys. 32 (1961) 1459.
[10] D.L. Griscom, E.J. Friebele and G.H. Sigel, Solid State Commun. 15 (1974) 479.
[11] F.J. Feigl, W.B. Fowler and K.L. Yip, Solid State Commun. 14 (1974) 225.
[12] K.L. Yip and W.B. Fowler, Phys. Rev. B11 (1975) 2327.
[13] J.K. Rudra and W.B. Fowler, Phys. Rev. B35 (1987) 8223.

[14] A.H. Edwards, W.B. Fowler and F.J. Feigl, Phys. Rev. B37 (1988) 9000.
[15] P.M. Lenahan and P.V. Dressendorfer, IEEE Trans. Nucl. Sci. NS-29 (1982) 1459.
[16] P.M. Lenahan and P.V. Dressendorfer, J. Appl. Phys. 55 (1984) 3495.
[17] H.S. Witham and P.M. Lenahan, Appl. Phys. Lett. 51 (1987) 1007.
[18] Y.Y. Kim and P.M. Lenahan, J. Appl. Phys. 64 (1988) 3551.
[19] A. Kalinsky, J.P. Ellul, E.H. Poindexter, P.J. Caplan, R.A. Lux and A.R. Boothroyd, J. Appl. Phys. 67 (1990) 7359.
[20] R.A.B. Devine, J. Appl. Phys. 66 (1989) 4702.
[21] W.E. Carlos, Nucl. Instr. and Meth. B1 (1984) 383.
[22] T. Takahashi, B.B. Triplett, K. Yokogawa and T. Sugano, Appl. Phys. Lett. 51 (1987) 1334.
[23] E.J. Friebele, D.L. Griscom, M. Stapelbroek, and R.A. Weeks, Phys. Rev. Lett. 42 (1979) 1346.
[24] M. Stapelbroek, D.L. Griscom, E.J. Friebele and G.H. Sigel Jr., J. Non-Cryst. Solids 32 (1979) 313.
[25] D.L. Griscom and E.J. Friebele, Phys. Rev. B24 (1981) 4896.
[26] D.L. Griscom, Nucl. Instr. and Meth. B1 (1984) 481.
[27] H. Imai, K. Arai, H. Imagawa, H. Hosona and Y. Abe, Phys. Rev. B38 (1988) 12772.
[28] The dynamic behavior of the E' center by annealing/reirradiation was addressed by R.A.B. Devine and C. Fiori, J. Appl. Phys. 58 (1985) 3368.
[29] A.G. Revesz, IEEE Trans. Nucl. Sci. NS-24 (1977) 2102.
[30] F.J. Grunthaner and P.J. Grunthaner, Mater. Sci. Rep. 1 (1986) 69.
[31] R.A.B. Devine and J. Arndt, Phys. Rev. B39 (1989) 5132.
[32] R.A.B. Devine, Nucl. Instr. and Meth. B46 (1990) 244.
[33] C.J. Brinker, R.J. Kirkpatrick, D.R. Tallant, B.C. Bunker and B. Montez, J. Non-Cryst. Solids 99 (1988) 418.
[34] F.L. Galeener, Solid State Commun. 44 (1982) 1037.
[35] F.L. Galeener, J. Non-Cryst. Solids 49 (1982) 53.
[36] F.L. Galeener, R.A. Barrio, E. Martinez and R.J. Elliot, Phys. Rev. Lett. 53 (1984) 2429.
[37] C.J. Brinker, D.R. Tallant, E.P. Roth and C.S. Ashley, J. Non-Cryst. Solids 82 (1986) 117.
[38] M. O'Keeffe and G.V. Gibbs, J. Chem. Phys. 81 (1984) 876.
[39] A.E. Geissberger and F.J. Galeener, Phys. Rev. B28 (1983) 3266.
[40] R.J. Bell and P. Dean, Philos. Mag. 25 (1972) 1381.
[41] A. Wright and J. Erwin Desa, Phys. Chem. Glass 19 (1978) 140.
[42] R.L. Mozzi and B.E. Warren, J. Appl. Cryst. 2 (1969) 164.
[43] G.V. Gibbs, Am. Mineral. 67 (1982) 421.
[44] P. Ordejon and F. Yndurdin, Phys. Rev. B43 (1991) 4552.
[45] C.J. Brinker, R.K. Brow, D.R. Tallant and R.J. Kirkpatrick, J. Non-Cryst. Solids 120 (1990) 26.
[46] Z.A. Weinberg, D.L. Matthies, W.C. Johnson and M.A. Lampert, Rev. Sci. Instrum. 46 (1975) 201.
[47] R.J. Powell and G.F. Derbenwick, IEEE Trans. Nucl. Sci. NS-18 (1971) 99.
[48] T.H. Ning, J. Appl. Phys. 47 (1976) 3203.
[49] D.J. DiMaria, Z.A. Weinberg and J.M. Aitken, J. Appl. Phys. 48 (1977) 898.
[50] R.A.B. Devine, C. Fiori and J. Robertson, in: Defects in Glasses, eds. F.L. Galeener, D.L. Griscom and M.J. Weber (Materials Research Society, Pittsburgh, PA, 1986) p. 177.
[51] T.-E. Tsai, D.L. Griscom and E.J. Friebele, Phys. Rev. Lett. 61 (1988) 444.
[52] W.L. Warren and P.M. Lenahan, Appl. Phys. Lett. 49 (1986) 1296.
[53] W.L. Warren and P.M. Lenahan, IEEE Trans. Nucl. Sci. NS-34 (1987) 1355.
[54] L.P. Trombetta, G.J. Gerardi, D.J. DiMaria and E. Tierney, J. Appl. Phys. 64 (1988) 2434.
[55] G.J. Gerardi, E.H. Poindexter, P.J. Caplan, M. Harmatz, W.R. Buchwald and N.M. Johnson, J. Electrochem. Soc. 136 (1989) 2609.
[56] K. Yokogawa, Y. Yajima, T. Mizutani, S. Nishimatsu and K. Suzuki, Jpn. J. Appl. Phys. 29 (1990) 2265.
[57] C.J. Brinker, K.D. Keefer, D.W. Schaefer, R.A. Assink, B.D. Kay and C.S. Ashley, J. Non-Cryst. Solids 63 (1984) 45.
[58] J.B. Bates, R.W. Hendricks and L.B. Shaffer, J. Chem. Phys. 61 (1974) 4163.
[59] J.C. Phillips, J. Non-Cryst. Solids 63 (1984) 347.
[60] P.N. Sen and M.F. Thorpe, Phys. Rev. B15 (1978) 4030.
[61] F.L. Galeener, Phys. Rev. B19 (1979) 4292.
[62] R. Oestrieke, W.H. Yang, R.J. Kirkpatrick, R.L. Hervig A. Navrotsky and B. Montez, Geochim. Cosmochim. Acta 51 (1987) 2199.
[63] T.A. Michalske and B.C. Bunker, J. Appl. Phys. 56 (1984) 2686.
[64] C.J. Brinker, B.C. Bunker, D.R. Tallant and K.J. Ward, J. Chem. Phys. (Paris) 83 (1986) 851.
[65] We are unable to tell at this time if the paramagnetic oxygen centers are peroxy radicals or nonbridging oxygen center since the g tensors of these two point defects are similar and the interference of the E' resonance. ^{17}O isotope experiments are needed to identify the nature of these oxygen centers. D.L. Griscom and C.J. Brinker found this to be especially true in sol–gel glasses, Diff. Defect Data 53–54 (1987) 213 and J. Non-Cryst. Solids 92 (1987) 295.
[66] F.L. Galeener, J. Non-Cryst. Solids 71 (1985) 373.
[67] S.K. Ghandhi, VLSI Fabrication Principles (Wiley, New York, 1983) p. 375.
[68] R.A.B. Devine, Phys. Rev. B35 (1987) 9783.
[69] R.L. Pffefer, J. Appl. Phys. 57 (1985) 5176.
[70] R.A.B. Devine and J. Arndt, Phys. Rev. B35 (1987) 9376.
[71] T-E. Tsai and D.L. Griscom, J. Non-Cryst. Solids 91 (1988) 170.
[72] G.E. Walrafen and J. Stone, Appl. Spectrosc. 29 (1975) 337.
[73] R.H. Stone and G.E. Walrafen, J. Chem. Phys. 64 (1976) 2623.

SIMOX Publications
June 1, 1989 - May 31, 1992

J.F. Conley, P.M. Lenahan, and P. Roitman, "Electron Spin Resonance Study of Trapping Centers in SIMOX Buried Oxides", Paper presented at INFOS'91, Liverpool, England, April 1991, Proceedings of 1991 INFOS Conference, W. Eccleston editor, William Hilger, Bristol, 259 (1991)

J.F. Conley, P.M. Lenahan and P. Roitman, "Electron Spin Resonance Study of E' Trapping Centers in SIMOX Buried Oxides" IEEE Trans. NS-38, 1247(1991)

J.F. Conley, P.M. Lenahan and P. Roitman, "Electron Spin Resonance of Separation by Implanted Oxygen Oxides: Evidence for Structural Change and a Deep Electron Trap, Appl. Phys. Lett. 60, 2889 (1992)

Paper presented at INFOS '91, Liverpool, April 1991
Contributed Papers, Section 6

Electron spin resonance study of trapping centers in SIMOX buried oxides

John F. Conley and P. M. Lenahan
The Pennsylvania State University, University Park, PA 16802

P. Roitman
National Institute of Standards and Technology, Gaithersburg, MD

ABSTRACT: We combine electron spin resonance and capacitance versus voltage measurements to study E' centers in a variety of SIMOX buried oxides. The oxides had all been annealed above 1300°C. Our results clearly show that E' centers play an important role in the trapping behavior of these oxides.

1. INTRODUCTION

Silicon-on-insulator (SOI) promises many advantages over conventional silicon technology. These advantages include total isolation, high speed, high packing density, low power consumption, and radiation hardness.

Among the many SOI technologies, separation by implanted oxygen (SIMOX) has emerged as the leading method for the formation of the buried oxide (BOX). In SIMOX, a high dose of oxygen ions ($>10^{18}$ cm^2) at a high energy (>100 keV) is implanted deep into silicon to form the BOX layer. Initially, the process resulted in a BOX with many oxide precipitates near its surface (1). However, high temperature ($T \gtrsim 1300°C$) annealing allows for the dissolution of these oxide "islands" into the BOX by Ostwald ripening (2). Since the SIMOX process is so different from conventional thermal growth, the resulting oxides may exhibit radically different charge trapping behavior. Indeed, much study of the BOX is needed before the potential advantages of SIMOX technologies can be fully exploited with regard to radiation hardness.

Charge trapping in SIMOX due to irradiation was recently studied by Boesch et al. (3). Boesch et al. concluded that efficient trapping of radiation induced holes exists in the bulk of the oxide and that initial trapping and subsequent thermal detrapping of electrons also takes place in the BOX. However, they did not deal with the structure of these charge trapping centers.

During the past four years, several groups have investigated SIMOX oxides with ESR.(4-7). Nearly all of these investigators have dealt with paramagnetic centers at precipitate surfaces. (These precipitates can be eliminated by a high temperature anneal (4)). However, in SIMOX oxides subjected to x-irradiation, Stahlbush, et al. (6) found an ESR signal similar to that of an E' center. A very recent study of Stesmans et al. (7) also involved gamma irradiation; they observed several ESR defects, including E' centers. In these earlier studies the authors did not directly correlate their ESR results to charge trapping in the oxides.

In this study, we use electron spin resonance (ESR) and capacitance versus voltage (CV) measurements along with vacuum ultraviolet (hc/λ = 10.2 ev) and ultraviolet (hc/λ = 5 ev) irradiation sequences to explore the role of E' trapping centers in SIMOX buried oxides. (The E' center is a silicon back-bonded to three oxygens (8-11). In thermally grown oxide films, it is the dominant deep hole trap and is a hole trapped in an oxygen vacancy (10-12). It has a zero crossing g-value of 2.0005.) There is experimental evidence for neutral E'

defects in PECVD oxides (13). In this study, we present experimental evidence which links E' centers to charge trapping in SIMOX oxides.

2. EXPERIMENTAL PROCEDURE

The SIMOX buried oxides studied were approximately 4000Å thick and received an anneal at 1300°C or 1325°C for five hours in 99.5% argon 0.5% oxygen or eight hours in 99.5% nitrogen 0.5% oxygen. Before any measurements were made, a surface oxide and the top layer of silicon were removed by etches in HF and KOH (HF attacks only SiO_2 and KOH attacks only Si).

Our electron spin resonance (ESR) measurements were conducted at room temperature on an IBM ER-200 X-band spectrometer. A TE104 "double" resonant cavity was used with a calibrated "weak-pitch" standard so that accurate determinations of both relative and absolute number of spins could be obtained. (Relative spin-concentration measurements are estimated to be accurate to ±10% while absolute spin-concentration measurements are accurate to a factor of two. Capacitance versus voltage (CV) measurements were taken at room temperature using a 1-MHz Boonton capacitance bridge and a mercury probe. The density of space charge was determined from shifts in the CV curve.

3. IRRADIATION

E' centers were generated by exposing (bare) BOX to vacuum ultraviolet light (VUV) from a deuterium lamp. In some cases, an LiF filter was used, and the oxides were illuminated briefly while positively biased. The filter passes only photons with $hc/\lambda<10.2eV$. Most of these photons are absorbed in the top 100Å of the oxide where they create electron hole pairs. The positive bias drives holes across the oxide while electrons are swept out. In other cases, the oxides were VUV illuminated without the filter ($hc/\lambda \lesssim 10.2eV$) and unbiased for an extended period (~ 20 hours).

Ultraviolet illumination (UV) from a sub-SiO_2 bandgap ($hc/\lambda<5.5eV$) mercury-xenon lamp was also used in combination with positive bias. The UV illumination results in the internal photoemission of electrons from the Si. The positive bias drives electrons across the oxide.

Biasing was performed by depositing low-energy ions created by corona discharge (14) onto the samples. (These ions have essentially thermal kinetic energy.) Corona charging allowed the generation of a uniform electric field over the large surface area samples (~1 cm^2) required for ESR measurements. The surface potential was measured with a Kelvin probe electrostatic voltmeter.

4. RESULTS

We exposed a variety of SIMOX buried oxides to 20 hours of vacuum ultraviolet (VUV) light from a 50 watt deuterium lamp. The behavior of all samples was qualitatively the same. A strong E' signal is generated by the VUV illumination. No other signals are visible. A broad scan around the "free electron" g = 2.002 is illustrated in Figure 1. (The g is defined by $h\nu/\beta H$, where h is Planck's constant, ν is the microwave frequency, β is the Bohr magneton and H is the magnetic field at which resonance occurs. Table 1 illustrates E' concentrations for a variety of SIMOX films. In all of the oxides, a high density (≃1 x $10^{18}/cm^3$) of E' centers were generated. (A 20 hour exposure was sufficient to "saturate" the spin densities.)

Etch back experiments (shown in Figure 2) on both and argon and the nitrogen annealed samples show that the E' centers generated by VUV irradiation without bias are distributed throughout the oxide.

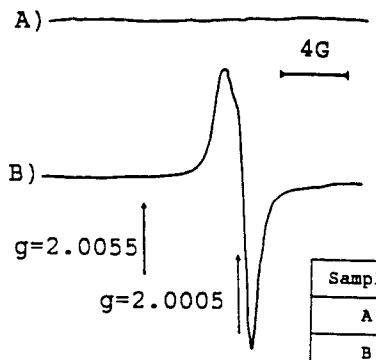

Figure 1: A broad ESR trace before (A) and after (B) exposure to VUV: illumination. A strong E' signal appears at g=2.0005. No "amorphous silicon" signal appears at g=2.0055.

Sample	Anneal Ambient	Implant	Spin Density(cm^{-3})
A	Ar/0.5% O_2 1325 C	Single	$0.7x10^{18}$
B	N_2/0.5% O_2 1325 C	Single	$1.4x10^{18}$
C	Ar/0.5% O_2 1315 C	Single	$1.0x10^{18}$
D	Ar/0.5% O_2 1315 C	Double	$0.35x10^{18}$

Table 1: E' concentrations for a variety of SIMOX films.

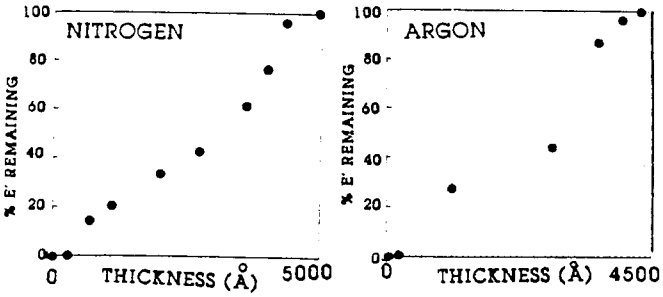

Figure 2: Etchback experiments illustrate the distribution of E' centers throughout the VUV illuminated SIMOX oxides.

Capacitance versus voltage measurements on the VUV illuminated oxides indicate virtually no buildup of net positive space charge within the oxide (~1 volt with respect to the preillumination curve). This result indicates that the E' centers are either electrically neutral or compensated by an equally high number of negatively charged centers. In order to test these possibilities, we exposed the VUV irradiated oxides to ultraviolet light ($hc/\lambda \lesssim 5eV$) from a 100 watt mercury xenon lamp while the oxide surface was positively charged. Oxides were charged with corona ions to about 80 volts (measured with a Kelvin probe). Oxides were then briefly (~ seconds) exposed to UV light from a mercury xenon lamp. A few seconds of UV light reduced the corona potential to ~10% of the original value, indicating electron injection into the oxide. The total electron injection fluence was roughly determined from CV = Q. The process was repeated until an injected electron fluence of about $\approx 2 \times 10^{14}$ electrons/cm^2 was achieved.

Results of the electron photoinjection are shown in Figure 3. The E' density is decreased by about half (from about $13 \times 10^{12}/cm^2$ to about $7 \times 10^{12}/cm^2$). CV measurements on the devices indicate shifts of about 10 volts -- corresponding to a change in space charge of about $\sim 10^{12}/cm^2$, assuming uniform charge capture throughout the insulator. Clearly, a significant fraction (at least half) of the E' centers can capture electrons with a relatively large capture cross section.

To further test the relationship between oxide charge and E' centers, we exposed these same SIMOX oxides (previously exposed to 20 hours VUV without bias and UV electron injection) to VUV with positive bias. We applied a corona potential of about 100V,

measured with a Kelvin probe electrostatic voltmeter. Then we exposed the oxide to 10.2 eV photons from a deuterium lamp. Most of the electron hole pairs are generated in the top ~100Å of the oxide. The positive bias floods the oxide with holes. The process was repeated until an injected hole fluence of about 1 x 10^{14} holes/cm^2 was achieved.

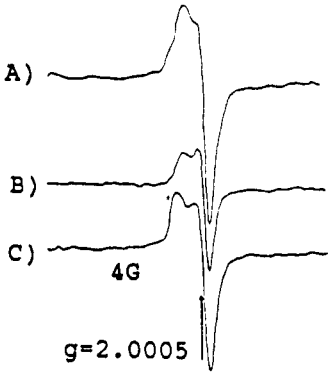

Figure 3: ESR traces of a SIMOX oxide (A of Table 1). (A) after VUV illumination, (B) after VUV illumination and injection of ~2x10^{14} electrons/cm^2, and (C) after VUV illumination, electron injection, and the injection of ~1x10^{14} holes/cm^2.

The result of this process is also shown in Figure 3. The E' density increased to almost the value before the electron injection process. Notice that the line shape of the curve has been changed slightly. This result is also qualitatively consistent with a paramagnetic E' structure corresponding to a hole trapped in an oxygen vacancy. However, coupled with the (pre-charge injection) results of high E' densities (~1 x 10^{18}/cm^3) and CV traces within a few volts of the origin, it suggests that the charged E' centers may be compensated by negatively charged centers.

We conclude that E' centers play an important role in SIMOX oxide trapping. E' precursors are present in high density in the SIMOX oxides explored in this study. Large changes in E' density are induced by injecting electrons or holes into VUV illuminated oxides; this shows that a high percentage of the centers are efficient traps. CV measurements show low amounts of net space charge; this suggests a compensating trap mechanism. The electronic properties of SIMOX oxides are more complex than those of thermal oxides on silicon.

REFERENCES

1. J. Stoemenos, C. Jasaud, M. Bruel, and J. Margail, J. Chryst. Growth 73, 546 (1985).
2. C. Jaussaud, J. Stoemenos, J. Margail, M. Dupuy, B. Blanchard, and M. Bruel, Appl. Phys. Lett 46, 1046 (1985).
3. H. E. Boesch, Jr., T. L. Yuglar, L. R. Hite, and W. E. Bailey, IEEE Trans NS 37, 1982 (1990).
4. R. G. Barklie, A. Hobbs, P. L. F. Hemmet, and K. Reesor, J. Phys. C. 19, 6417 (1986).
5. T. Makino and J. Takahashi, Appl. Phys. Lett 50, 267 (1987).
6. R. E. Stahlbush, W. E. Carlos, and J. M. Prokes, IEEE Trans NS 34, 1680 (1987).
7. A. Stesmans, R. A. B. Devine, A. Revesz, and H. Hughes, IEEE Trans NS 37, 2008 (1990).
8. R. A. Weeks, J. Appl. Phys. 27, 1376 (1956).
9. D. L. Griscom, Phys Rev. B 22, 4192 (1980).
10. P. M. Lenahan and P. V. Dressendorfer, IEEE Trans NS 30, 4602 (1983).
11. P. M. Lenahan and P. V. Dressendorfer, J. Appl. Phys. 55, 3495 (1984).
12. H. S. Witham and P. M. Lenahan, Appl. Phys. Lett 51, 1007 (1987).
13. H. L. Warren, P. M. Lenahan, B. Robinson, and I. H. Sathis, Appl. Phys. Lett 53, 482 (1988).
14. Z. A. Weinberg, W. C. Johnson, and M. A. Lampert, J. Appl. Phys. 47, 248 (1976).

ELECTRON SPIN RESONANCE STUDY OF E' TRAPPING CENTERS IN SIMOX BURIED OXIDES

John F. Conley and P. M. Lenahan
Department of Engineering Science
The Pennsylvania State University
University Park, PA 16802

and

P. Roitman
National Institute of Standards and Technology
Gaithersburg, MD 20899

Abstract

We combine electron spin resonance and capacitance versus voltage measurements with vacuum ultraviolet and ultraviolet illumination sequences to study E' centers in a variety of SIMOX buried oxides. The oxides had all been annealed above 1300°C. Our results clearly show that E' centers play an important, probably dominating role in the trapping behavior of these oxides. This role is considerably different from the role that E' centers play in thermal oxides.

Introduction

Silicon-on-insulator (SOI) promises many advantages over conventional silicon technology. These advantages include total isolation, high speed, high packing density, low power consumption, and transient radiation hardness. In order to accurately assess the potential of SOI in harsh environments, it is important that we develop a fundamental understanding of the radiation response of the buried oxide (BOX). Radiation damage can include (among other things) trapping of charge carriers in the buried oxide (BOX). This trapped charge can create back-channel leakage paths in partially depleted devices and affect threshold voltages in fully depleted devices. These problems must be addressed before full use can be made of SOI's rad hard advantages.

Among the many SOI technologies, separation by implanted oxygen (SIMOX) has emerged as the leading method for the formation of the BOX. In SIMOX, a high dose of oxygen ions ($>10^{18}/\ cm^2$) at a high energy (>100 keV) is implanted deep into silicon to form the BOX layer. Initially, the process results in a BOX with many oxide precipitates near its surface [1]. However, high temperature (T>1300°C) annealing allows for the dissolution of these oxide "islands" into the BOX by Ostwald ripening [2].

Since the SIMOX process is so different from conventional thermal oxide growth, the resulting oxides may exhibit radically different charge trapping behavior. A complete understanding of the charge trapping mechanisms in SIMOX buried oxide may be required to optimally harden SIMOX and effectively exploit the potential radiation resistant advantages of SIMOX. A path to future exploitation of SIMOX may be found through intensive study of charge trapping mechanisms in the SIMOX buried oxide.

Charge trapping in the BOX due to irradiation was recently studied by Boesch et al. [3]. Boesch et al. concluded that efficient trapping of radiation induced holes takes place in the bulk of the oxide and that initial trapping and subsequent thermal detrapping of electrons also takes place in the BOX. However, they did not deal with the structure of these charge trapping centers.

During the past five years, other groups have investigated SIMOX oxides with ESR.[4-7] Nearly all of these investigators have dealt with paramagnetic centers at precipitate surfaces. (These precipitates are eliminated by a high temperature anneal [5]). However, in SIMOX oxides subjected to x-irradiation, Stahlbush, et al. [6] found an ESR signal similar to that of an E' center. (The E' center is a silicon back-bonded to three oxygens. [8-11]) A very recent study of Stesmans et al. [7] involved both unirradiated and gamma irradiated samples; they observed several ESR defects, including E' centers and "amorphous silicon" centers. In none of these earlier studies did the authors directly correlate their ESR results to charge trapping in the oxides.

We have recently begun a study [12, 13] in which we use electron spin resonance (ESR) and capacitance versus voltage (CV) measurements along with vacuum ultraviolet ($hc/\lambda \leq 10.2$ ev) and ultraviolet ($hc/\lambda \leq 5$ ev) irradiation sequences to

0018-9499/91/$01.00 ©1991 IEEE

explore the role of E' trapping centers in SIMOX buried oxides. We had earlier demonstrated [13] that E' centers can be generated in SIMOX BOX in high concentration, that these centers are distributed in an essentially uniform density across the oxide, and that high E' densities can be generated without the simultaneous generation of comparable density of net positive charge in the BOX. In this paper we considerably extend those preliminary results. In thermally grown oxide films, E' centers are primarily holes trapped in oxygen vacancies [14-16] and are the dominant deep hole trap. There is experimental evidence for neutral E' defects in some PECVD oxides [17].

We present experimental evidence that E' centers are present in very large densities ($1x10^{18}/cm^3$), are important electrical defects in SIMOX oxides, and behave somewhat differently than E's found in thermal oxides. Our results indicate that E' centers plays a very important role in SIMOX oxide charge trapping.

Experimental Details

The SIMOX buried oxides studied were approximately 400 nm thick and received a 1325°C anneal (sufficient for the removal of all SiO_2 precipitates)[2] for either five hours in 99.5% argon 0.5% oxygen or eight hours in 99.5% nitrogen 0.5% oxygen. Before any measurements were made, a surface oxide and the top layer of silicon were removed by etches in HF and KOH (HF attacks only SiO_2 and KOH attacks only Si). A thermally grown oxide annealed for 5 hours in 95.5% argon and 0.5% oxygen at 1325°C and a soft thermal oxide (270nm grown at 1000°C) were also used.

Our electron spin resonance (ESR) measurements were conducted at room temperature on a state of the art commercial X-band spectrometer with a TE_{104} "double" resonant cavity and a calibrated "weak-pitch" spin standard (permitting relative spin-concentration measurements estimated to be accurate to ±10% and absolute spin-concentration measurements accurate to a factor of two). CV measurements were taken at room temperature using a 1-MHz Boonton capacitance bridge and a mercury probe. The density of radiation induced space charge was determined from shifts in high frequency CV curves.

E' centers were generated by exposing (bare) buried oxides to vacuum ultraviolet light (VUV) from a 50 watt deuterium lamp in a vacuum.[12,13] In some cases, a 10.2 eV notch filter was used; in these cases the oxides were illuminated briefly while positively biased.[13] The filter passes only photons with hc/λ = 10.2 eV. Most of these photons are absorbed in the top 10 nm of the oxide where they create electron hole pairs. The positive bias drives holes across the oxide (hole injection) while electrons are swept out. In other cases, the oxides were VUV illuminated without the filter ($hc/\lambda \leq 10.2$ eV) and unbiased for an extended period (≈ 20 hours). Exposing the samples to this extended illumination creates extremely high densities of E' centers. [13] The E' signal amplitude appears to be reaching a maximum, a "saturated" value after the 20 hour illumination. We tentatively assume that this extended illumination renders all or most of the E' precursor centers paramagnetic (ESR active).

Ultraviolet illumination (UV) from a sub-SiO_2 bandgap ($hc/\lambda \leq 5$ eV) mercury-xenon lamp was used in combination with positive bias. The UV illumination results in the internal photoemission of electrons from the Si into the oxide. The positive bias drives electrons across the oxide (electron injection).

Biasing was performed by depositing low-energy ions created by corona discharge [14] onto the samples. (These ions have essentially thermal kinetic energy.) Corona charging allowed the generation of a uniform electric field over the large surface area samples (≈ 1 cm^2) required for ESR measurements. Surface potentials were measured with a Kelvin probe electrostatic voltmeter.

Experimental Results

We exposed a variety of SIMOX buried oxides to 20 hours of vacuum ultraviolet (VUV) light from a 50 watt deuterium lamp. The behavior of all samples was qualitatively and semiquantitatively the same. Figure 1 illustrates the result. Pre illumination curve 1a shows no paramagnetic signals. However, post VUV illumination curve 1b shows generation of a strong E' signal at g = 2.0005. (The g value is defined by $h\nu/\beta H$, where h is Planck's constant, ν is the microwave frequency, β is the Bohr magneton and H is the magnetic field at which resonance occurs.) In all of the SIMOX oxides, a high density (≈ 1 x $10^{18}/cm^3$) of E' centers was generated.

These E' densities are much higher than those reported by A. Stesmans et al.[7] This difference may be due to differences in irradiation conditions. In the Stesmans et al. work oxides were gamma irradiated (~6 to 20 Mrad). Our 20 hour VUV illumination may be sufficient to "saturate" nearly all of the BOX E' precursors. (E' concentrations for a variety of SIMOX films are shown in Table 1.)

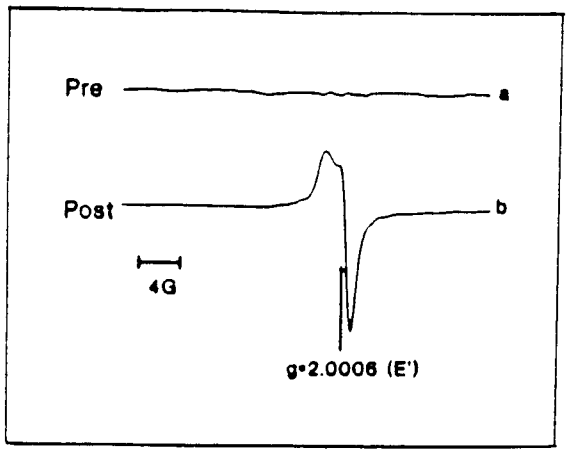

Figure 1: A broad ESR trace before (a) and after (b) exposure to VUV illumination. A large ($\approx 10^{18}/cm^3$) E' signal appears at g=2.0005.

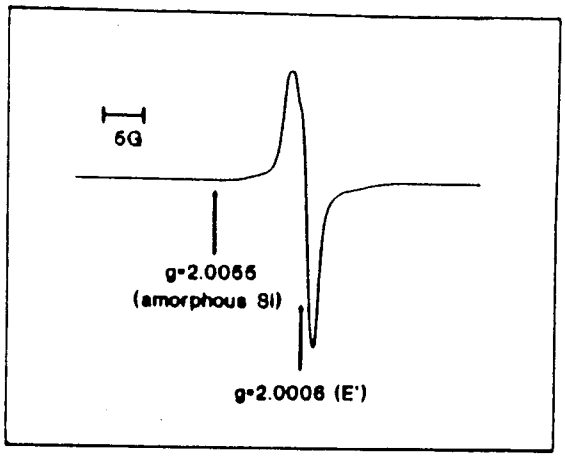

Figure 2: Wide scan search for other paramagnetic centers in a SIMOX oxide exposed to VUV illumination. The spectrometer was sent to optimize the sensitivity to the "amorphous silicon" signal at g=2.0055. (High microwave power and high magnetic field modulation). Only the E' signal is visible; the "amorphous silicon" signal does not appear.

Table 1: E' spin densities of various SIMOX oxides exposed to 20 hours VUV illumination without bias.

Sample	Anneal Ambient	Implant	Spin Density (cm-3)
A	99.5% Ar/0.5% O_2 1325°C	Single	$0.7x10^{18}$
B	99.5%N_2/0.5% O_2 1325°C	Single	$1.4x10^{18}$
C	99.5% Ar/0.5% O_2 1315°C	Single	$1.0x10^{18}$
D	99.5% Ar/0.5% O_2 1315°C	Double	$0.35x10^{18}$

Figure 2 illustrates a slightly broader ESR scan centered around the "free electron" g = 2.002. The spectrometer settings of this scan were set to optimize sensitivity for the "amorphous silicon" signal which Stesmans et al.observed in large densities in both unirradiated and irradiated SIMOX BOX samples. (The E' signal g = 2.0006 is somewhat distorted in Figure 2 because the spectrometer settings were optimized for a broader ESR signal.) The sensitivity limit for the "amorphous silicon" signal is about $\simeq 1x10^{11}/cm^2$, considerably lower than the $\sim 1x10^{14}/cm^2$ signal reported by Stesmans et al. Our results strongly indicate that the "amorphous silicon" defects do not play a significant role in SIMOX oxide trapping. E' centers, however, do.

In order to determine the distribution of these E' centers, an etchback experiment was performed. The results of this etchback are shown in Figure 3. The E' centers are distributed throughout the buried oxide in SIMOX. This is very different from distribution in thermal oxides irradiated under positive gate bias; in that case, E' centers are generally found only close to the Si/SiO_2 interface.[15]

CV measurements were made in an attempt to correlate the E' centers presence with charge trapping behavior. Typical results are shown in Figure 4. CV measurements show virtually no buildup of net positive space charge within the VUV illuminated oxides (≈ 1 volt CV shift with respect to the preillumination curve). This result indicates one of two possibilities: that the E' centers are either (1)

electrically neutral or (2) positively charged and compensated by an equally high number of negatively charged centers. In order to test these possibilities, we performed a series of charge injection experiments. First, we injected electrons by exposing the VUV irradiated oxides to ultraviolet light (hc/ $\lambda \leq 5$ eV) from a 100 watt mercury xenon lamp while the oxide surface was positively biased. The oxides were first charged with corona ions to about 80 volts (measured with a Kelvin probe); the oxides were then briefly ($\approx$ seconds) exposed to UV light This illumination reduced the corona potential to $\approx$ 10% of the original value. (The electrons injected into the oxide recombined with positively charged corona ions at the oxide surface.) The process was repeated until a total injected electron fluence of about $\approx 2 \times 10^{14}$ electrons/cm^2 (roughly determined from CV=Q)was achieved.

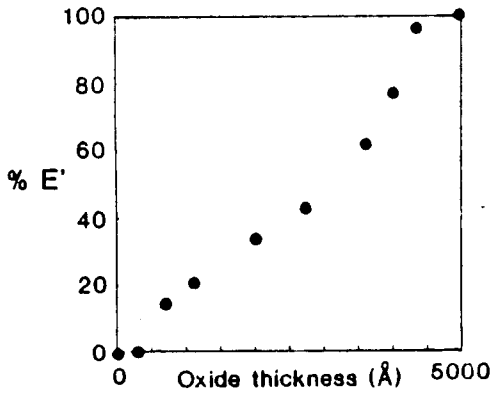

Figure 3: Etchback experiments illustrate the distribution of E' centers throughout the VUV illuminated SIMOX oxides.

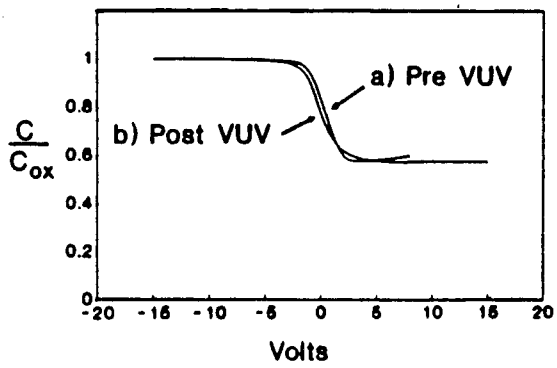

Figure 4: CV traces taken on the samples shown in Figure 1. Traces taken before and after VUV illumination show very little CV shift accompanying the large increase in E' concentration.

Figure 5 shows that the E' density is diminished by about half (from about (5a) 13 x 10^{12}/cm^2 to about (5b) 7 x 10^{12}/cm^2). CV measurements on the devices reveal shifts of about 10 volts -- corresponding to a change in space charge of about 1.5 x 10^{12}/cm^2, assuming uniform charge capture throughout the insulator. (Etchback experiments in Figure 3 support this.) Clearly, a significant fraction (at least about half) of the E' centers can capture electrons with a relatively large capture cross section. (A large electron capture cross section favors a positively charged E' center.) However, the change in spin density and space charge density are not equal. The spin density is not equal to charge density either before or after charge injection. Even allowing for worst case experimental error (=a factor of two) the numbers differ by at least an additional factor of two. In thermal oxides, the numbers track very well [14-16]. Our results suggest that there may be some neutral E' centers and clearly demonstrate that E' centers play a more complex role in SIMOX oxides than in thermally grown SiO_2 films.

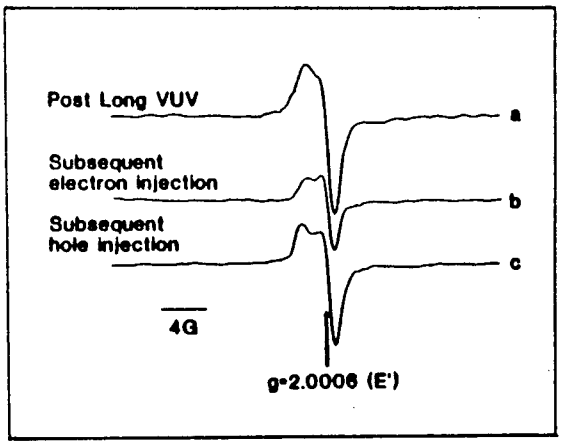

Figure 5: ESR traces of a SIMOX oxide (A of Table 1). (a) after VUV illumination, (b) after VUV illumination and injection of ~2x10^{14} electrons/cm^2, and (c) after VUV illumination, electron injection, and the injection of ~1x10^{14} holes/cm^2.

To further test the relationship between oxide charge and E' centers, we injected holes into the oxide. We exposed these same SIMOX oxides (previously exposed to 20 hours VUV without bias and UV electron injection) to VUV with positive bias. Oxides were charged to a potential of about 100V and then exposed to 10.2 eV photons from the deuterium lamp. The VUV illumination generates electron hole pairs primarily in the top $\approx$ 10 nm of the oxide and the positive bias floods the oxide with

holes. The process was repeated until an injected hole fluence of about $1x10^{14}$ holes/cm^2 was achieved.

As shown in Figure 5c, the hole injection resulted in an increase in the paramagnetic E' density to nearly the quantity before the electron injection process. Notice that the line shape of the curve has been changed slightly. We were unable to obtain good CV curves for the samples after hole injection. We were thus unable to obtain accurate numbers for space charge density. This result is again qualitatively consistent with a paramagnetic E' structure corresponding to a hole trapped in an oxygen vacancy. This result, coupled with the (pre-charge injection) results of high E' densities (~1 x 10^{18}/cm^3) and CV small shifts, suggests that the charged E' centers may be compensated by negatively charged centers.

In order to make a more direct comparison between SIMOX thermal oxides and to examine the effects of the high temperature (>1300°C) anneal, we identically exposed two differently processed thermal oxides and a SIMOX oxide to 20 hours of VUV irradiation. In Figure 6 we show the ESR spectra of two thermal oxides (one grown at 1325°C and the other grown at 1100°C) which were exposed to the same 20 hour VUV exposure that generated the large E' signal in the SIMOX. (The 1325°C "high temperature" oxide was grown to a thickness of 110 nm in an ambient identical to that used in the anneal of some of the SIMOX samples: 0.5% oxygen and 99.5% argon. The second thermal was grown in steam at 1100°C to a thickness of 270 nm. Figure 6c shows the large (~10^{18} spins/cm^3) E' resonance generated in the SIMOX sample. The resonance is weaker in the 6b "high temperature" processed thermal (~10^{17}/cm^3) and much weaker in the 6a soft thermal (<10^{17}/cm^3). Once again, no other signals are visible and pre-illumination curves show no signals. The results show a huge quantitative difference in the number of E's in SIMOX and both thermals. The fact that the high temperature processed thermal has significantly more spins than the lower temperature oxide suggests that the same high temperature that enables the dissolution of the precipitates may also aid in the creation of E' precursors. However, the high temperature thermal oxide was grown in an ambient identical to that of the SIMOX anneal. Although the high temperature thermal exhibits a much higher E' density than the lower temperature thermal it's E' density is still considerably lower than the density of the SIMOX sample. This observation suggests that the high E' precursor density can not be entirely explained in terms of the high temperature anneal.

We conclude that E' centers play an extremely important role in SIMOX oxide charge trapping. We draw this conclusion from several experimental observations: (1) E' precursors are present in high density in the SIMOX oxides explored in this study ~$1x10^{18}$/cm^3. (2) large changes in E' density are induced by injecting electrons or holes into VUV illuminated oxides; this clearly demonstrates that a high percentage of the centers are efficient electrical traps. Since a comparison of CV measurements and ESR measurements show less than perfect correlation between net space charge density and spin density, our results suggest a compensating trap and possibly some neutral paramagnetic E' centers. Finally, many more paramagnetic E' centers were generated in the SIMOX samples than in the thermal oxides revealing a great quantitative difference. Our observations clearly demonstrate that SIMOX oxide charge trapping mechanisms are somewhat different and more complex than those in thermal oxides on silicon (Earlier work on thermal oxides indicates a close correlation between E' concentration and the density of trapped positive charge. [14-16] Although a complete understanding of the SIMOX trapping centers will require far more study, our work clearly establishes that E' center precursors are abundant and electrically active in SIMOX oxides. They clearly play an extremely significant role in the electronic properties of these dielectric films.

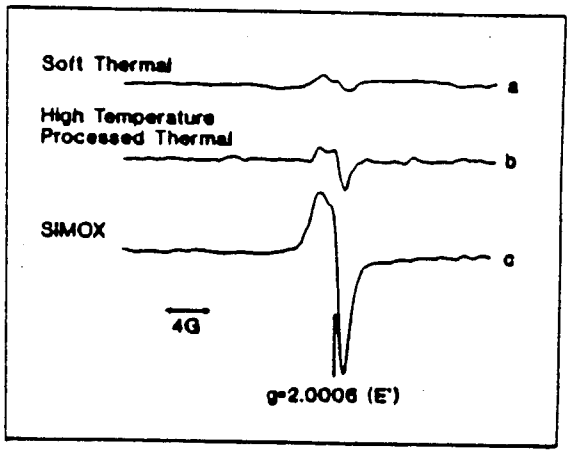

Figure 6: ESR traces of (a) soft thermal oxide, (b) high temperature annealed thermal oxide, and (c) SIMOX buried oxide identically exposed to 20 hours VUV illumination without bias. E' traces adjusted for oxide volume.

REFERENCES

[1]. J. Stoemenos, C. Jasaud, M. Bruel, and J. Margail, "New Conditions for Synthesizing SOI Structures by High Dose Oxygen Implantation," J. Crst. Growth 73, 546 (1985).

[2]. C. Jaussaud, J. Stoemenos, J. Margail, M. Dupuy, B. Blanchard, and M. Bruel, "Microstructure of Silicon Implanted with High Dose Oxygen Ions," Appl. Phys. Lett 46, 1064 (1985).

[3]. H. E. Boesch, Jr., T. L. Taylor, L. R. Hite, and W. E. Bailey, "Time-Dependent Hole and Electron Trapping Effects in SIMOX Buried Oxides," IEEE Trans NS 37, 1982 (1990).

[4]. R. G. Barklie, A. Hobbs, P. L. F. Hemmet, and K. Reesor, "EPR of Defects in Silicon-on-Insulator Structures Formed by Ion Implantation: I. 0^+ Implantation," J. Phys. C. 19, 6417 (1986).

[5]. T. Makino and J. Takahashi, "Electron Spin Resonance Studies on Buried Oxide Silicon-on-Insulator," Appl. Phys. Lett 50, 267 (1987).

[6]. R. E. Stahlbush, W. E. Carlos, and J. M. Prokes, "Radiation- and Processing-Induced Effects in SIMOX: A Spectroscopic Study," IEEE Trans NS 34, 1680 (1987).

[7]. A. Stesmans, R. A. B. Devine, A. Revesz, and H. Hughes, "Irradiation-Induced ESR Active Defects in SIMOX Structures," IEEE Trans NS 37, 2008 (1990).

[8]. R. A. Weeks, "Paramagnetic Resonance of Lattice Defects in Irradiated Quartz," J. Appl. Phys. 27, 1376 (1956).

[9]. R. H. Silsbee, "Electron Spin Resonance in Neutron-Irradiated Quarts," J. Appl. Phys., 32, 1459 (1961).

[10]. F. J. Feigl, W. B. Fowler and K. L. Yip, "Oxygen Vacancy Model for the E' Center in SiO_2, Solid State Commun.," 14, 225, (1974).

[11]. D. L. Griscom, "E' Center in Glassy SiO_2: ^{17}O, and 'Very Weak' Superhyperfine Structure," Phys Rev. B 22, 4192 (1980).

[12]. J. F. Conley, P. M. Lenahan and P. Roitman, "Direct Experimental Evidence for a Dominant Hole Trapping Center in SIMOX Oxides," Proc. IEEE SOS/SOI Technology Conf. (1991).

[13]. J. F. Conley, P. M. Lenahan and P. Roitman, "Electron Spin Resonance Study of Trapping Centers in SIMOX Buried Oxides,"Proceeding of the Insulating Films on Semiconductors (INFOS) Conference, W. Eccleston, editor, Institute of Physics, Liverpool, London, April (1991)

[14]. P. M. Lenahan and P. V. Dressendorfer, "Microstructural Variations in Radiation Hard and Soft Oxides Observed Through Electron Spin Resonance," IEEE Trans NS 30, 4602 (1983).

[15]. P. M. Lenahan and P. V. Dressendorfer, "Hole Traps and Trivalent Silicon Centers in Metal/Oxide/Silicon Devices," J. Appl. Phys. 55, 3495 (1984).

[16] H. S. Witham and P. M. Lenahan, "Nature of E' Deep Hole Trap in Metal-Oxide-Semiconductor Oxide," Appl. Phys. Lett 51, 1007 (1987).

[17]. W. L. Warren, P. M. Lenahan, B. Robinson, and I. H. Stathis, "Neutral E' Centers in Microwave Downstream Plasma Enhanced Chemical-Vapor-Deposited Silicon Dioxide," Appl. Phys. Lett 53, 482 (1988).

[18]. Z. A. Weinberg, W. C. Johnson, and M. A. Lampert, "High Field Transport in SiO_2 on Silicon Induced By Corona Charging of the Unmetallized Surface," J. Appl. Phys. 47, 248 (1976).

Electron spin resonance of separation by implanted oxygen oxides: Evidence for structural change and a deep electron trap

J. F. Conley, Jr. and P. M. Lenahan
Pennsylvania State University, University Park, Pennsylvania 16802

P. Roitman
National Institute of Standards and Technology, Gaithersburg, Maryland

(Received 27 December 1991; accepted for publication 2 April 1992)

We present direct evidence for deep electron traps and structural changes in separation by implanted oxygen (SIMOX) buried oxides and evidence that some positively charged E' centers are compensated by negatively charged centers in SIMOX oxides.

Separation by implantation of oxygen (SIMOX) is the leading technology for silicon-on-insulator (SOI), a device fabrication method with great promise for use in satellites and ultralarge scale integration. SIMOX buried oxides contain trapping centers that may play a significant role in the operation of devices utilizing this technology. We study trapping centers in SIMOX buried oxides with a combination of electrical measurements and electron spin resonance (ESR).[1]

Combining ESR and capacitance vs voltage (CV) measurements, we recently found that very high densities ($\sim 10^{18}/\text{cm}^3$) of paramagnetic (ESR active) point defects called E' centers are generated in SIMOX buried oxides exposed to vacuum ultraviolet (VUV) irradiation ($hc/\lambda > 10.2$ eV).[2-5] This indicated the presence of a very high density of E' precursors in the buried oxides. The E' center is an unpaired spin on a silicon bonded to three oxygens; the E' ESR spectrum has a zero crossing $g \sim 2.0005$. We searched for other ESR spectra in the vicinity of $g = 2.000$ but have not yet been able to detect other signals including the "amorphous silicon" signal reported by Stessmans, Revesz, and Devine.[6]

The creation of high densities of E' centers was accompanied by virtually no net space charge in the buried oxide.[3-5,7] This absence of net space charge in the presence of a large E' density suggests two possibilities:[3-5,7] (1) that the E' centers are neutral, or (2) that the E' centers are positively charged (E' centers are the dominant deep hole trap in thermal oxides)[8] and compensated by negatively charged centers.[3-5,7] To test these possibilities and determine whether or not SIMOX E' centers are electrically active, we performed a series of charge injection experiments.[2-5,7] Injection of electrons into VUV illuminated oxides reduced E' amplitude; injection of holes into the oxides increased E' amplitude.[4,5,7] Both of these results demonstrate that SIMOX E' centers are electrically active and that at least some of them are positively charged when paramagnetic. However, in these experiments we consistently observed an E' density greater than total charge density.[4,5,7] The fact that the trapped charge density is considerably lower than the presumably positive E' center density leads one to suspect some form of electrically compensating mechanism to account for the discrepancy.

In this letter, we determine more directly the effects of electron and hole injection on the buried oxide and provide very strong evidence for compensating positive and negative charge. We also provide evidence for structural changes and the creation of a deep electron trap as a result of VUV illumination.

The samples used in this study include $P\langle 100\rangle$ 405 nm single implant and $N\langle 100\rangle$ 385 nm multiple implant SIMOX oxide samples. Both single and multiple implant samples received a 5 h anneal in 99.5% argon and 0.5% oxygen at 1315 °C. All samples received a total oxygen dose of $1.8\times 10^{18}/\text{cm}^3$ at an energy of 200 keV, a current of 34 mA, and an implant temperature of 640 °C. A residual oxide and the top layer of silicon were removed by subsequent etches in HF and then KOH at room temperature. The behaviors of the multiple and single implant oxides were qualitatively the same though not identical.

We made X-band ESR measurements at room temperature using a TE_{104} "double" resonant cavity and a "weak-pitch" spin standard. Relative spin-concentration measurements are accurate to $\pm 10\%$ with an absolute accuracy of a factor of two. High frequency CV measurements were taken at room temperature using a mercury probe. Net oxide space charge density was determined from CV curve shifts. (Etchback experiments indicate charge trapping throughout the oxides).

E' centers were generated by exposing (bare) buried oxides to VUV light from a 50 W deuterium lamp in a vacuum. In some cases, a filter passing only 10.2 eV photons was used; in these cases the oxides were illuminated briefly under positive bias. Biasing was performed by depositing low-energy ions created by corona discharge[9] onto the samples. Surface potentials were measured with a Kelvin probe electrostatic voltmeter. [Most of these 10.2 eV photons are absorbed in the top 100 Å of the oxide where they create electron hole pairs.[10,11] The positive bias drives holes across the oxide (hole injection) while sweeping electrons out.] In other cases, the oxides were VUV illuminated unbiased without the filter ($hc/\lambda < 10.2$ eV) for an extended period (~ 40 h). Exposing the samples to this "extended" VUV illumination generates extremely high densities of paramagnetic E' centers ($\sim 10^{18}/\text{cm}^3$).

Ultraviolet illumination (UV) from a sub-SiO_2 band gap ($hc/\lambda = 5.5$ eV) mercury-xenon lamp was also used in combination with positive corona bias. The UV illumination results in the internal photoemission of electrons from

 0003-6951/92/232889-03$03.00

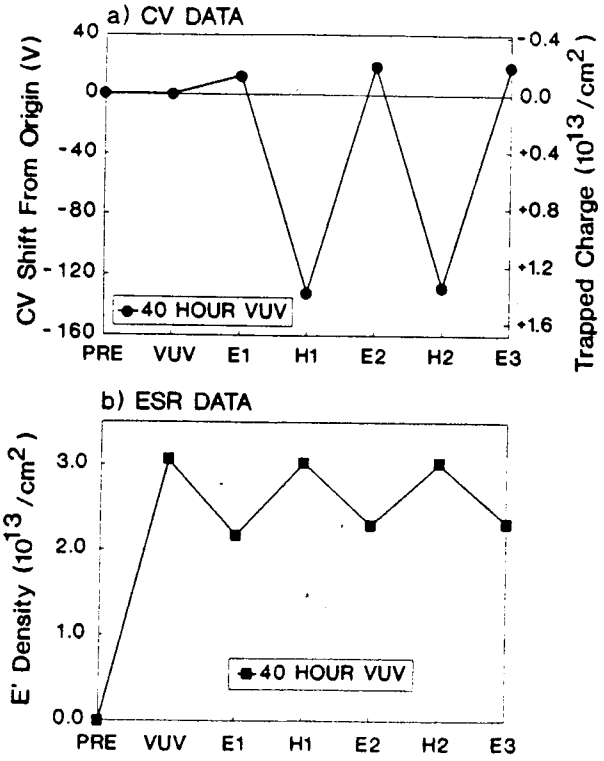

FIG. 1. Effects of electron (E) and hole (H) injection on (a) space charge density (CV) and (b) spin density (ESR) measurements of VUV illuminated buried oxides.

the Si. The positive bias drives electrons across the buried oxide (electron injection).

Figure 1 shows quantitative results of electron/hole charge cycling on VUV irradiated single implant SIMOX oxides. Consistent with earlier work,[3-5,7] the 40 h of VUV illumination results in a large E' signal [Fig. 1(b)] with little or no net space charge [Fig. 1(a)]. About 5×10^{13}/cm^2 electrons and holes were then alternately injected into the VUV irradiated oxide. The CV results in Fig. 1(a) show that, after the initial electron injection, the amount of net trapped charge cycles with almost perfect repeatability with about 1.5×10^{13} charges captured on each subsequent injection. (Note that the positive shifts indicate electron capture.)

Figure 1(b) allows a comparison of ESR E' spin density data with CV charge density data in Fig. 1(a). Beginning with the initial electron injection, the E' magnitude cycles back and forth, changing about 8×10^{12} spins per cycle. This matches our CV data within a factor of two and shows that paramagnetic E' centers are capturing electrons and diamagnetic E' centers are capturing holes with a large capture cross section ($\sim10^{-13}$ cm^2). The fact that CV measurement of space charge and ESR measurements of spin density do not "match" after the initial electron injection suggests that some structural change may be occurring at the trapping sites. To determine whether or not this is the case, we explore the effects of electron and hole injection on unilluminated (no VUV) oxides.

Figures 2(a) and 2(b) show the effects of electron and hole injection into unirradiated multiple implant buried

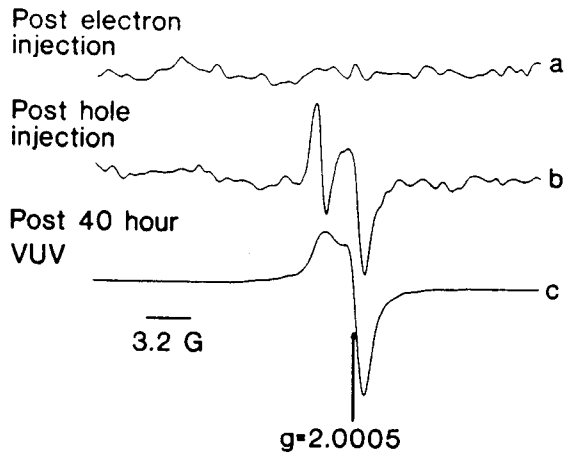

FIG. 2. ESR traces of SIMOX oxide (a) after the injection of about 10^{14} electrons/cm^2, (b) after the injection of about 10^{14} holes/cm^2, and (c) after exposure to 40 h of VUV illumination. In all traces, sample size and geometry were identical. Spectrometer settings were identical in traces (a) and (b) but gain was reduced in trace (c).

oxides. No paramagnetic signals could be observed in the oxides prior to charge injection. Photoinjection of 5×10^{13} electrons/cm^2 into an unilluminated sample does not generate a measurable E' signal. CV measurements indicate virtually no net space charge; very few electrons are trapped. Injection of 5×10^{13} holes/cm^2 into the unirradiated buried oxide generates a fairly strong E' signal (5×10^{16} spins/cm^3) and a large (-170 V) negative CV shift. Electron injection *does not* result in the generation of paramagnetic E' centers; hole injection *does* generate E' centers. This strongly indicates that at least some of the E' centers are positively charged when paramagnetic. The peculiar line shape [compare to Fig. 2(c)] of the hole injection induced E' suggests a different local environment than that experienced by the "extended VUV" generated E'. Note also the absence of electron trapping in the unirradiated oxide. In VUV irradiated oxides (Fig. 1), injection of the same number of electrons resulted in a substantial buildup of negative space charge. This indicates that VUV irradiation causes some sort of structural change that results in a deep electron trap.

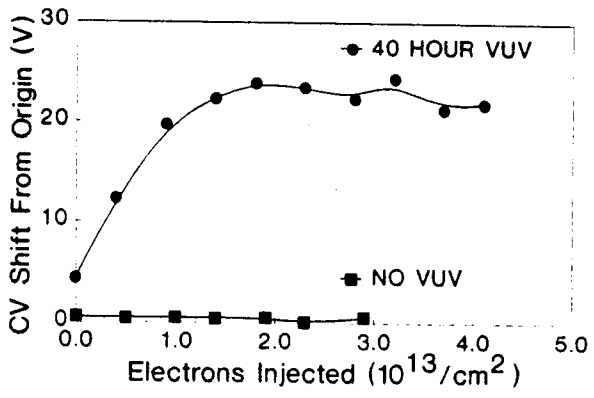

FIG. 3. Shown here are CV shifts of a VUV irradiated oxide and an unirradiated oxide subjected to similar electron injection. Substantial electron trapping occurs in the VUV irradiated samples while little or no trapping occurs in the unirradiated sample.

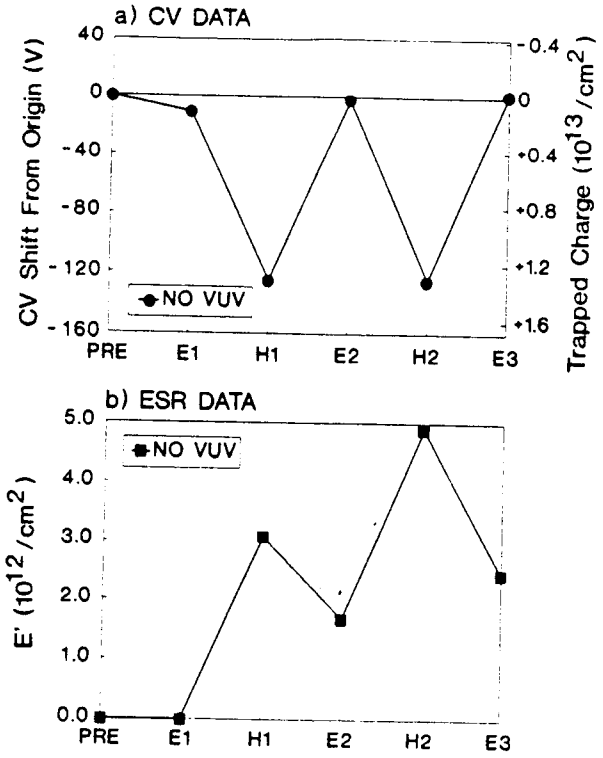

FIG. 4. Effects of electron (E) and hole (H) injection on (a) space charge density (CV) and (b) spin density (ESR) measurements of unilluminated buried oxides.

A comparison of irradiated and unirradiated oxides demonstrates electron trap generation quite directly. Figure 3 allows a comparison of charge trapping in VUV illuminated and unilluminated multiple implant SIMOX oxides subjected to electron injection. Substantial electron trapping ($>10^{12}$/cm^2) occurs in the VUV irradiated sample but not in the unirradiated sample. (Etchback studies show the net negative charge to be distributed in an approximately uniform manner throughout the oxide.) VUV illumination directly results in the creation of a deep electron trap. (This electron trapping phenomenon is different from that recently reported by Boesch *et al.*,[12] who demonstrated the presence of quite shallow electron traps in SIMOX oxides.)

Figure 4 shows the effects of alternately injecting electrons and holes into unirradiated single implant oxides. Once again, the charge cycles repeatably ($\approx 1.3\times10^{13}$/cm^2 charges/cycle) after the initial electron injection. However, the ESR results do not closely match the electrical measurements. Although the amount of trapped charge cycles repeatably, the number of paramagnetic E' centers grows by a substantial amount after each hole injection. This strongly suggests structural change in the oxide.

In summary, we present evidence for structural change and observe the creation of deep electron traps in SIMOX buried oxides. We demonstrate that a significant fraction of paramagnetic E' centers are positively charged, although some may be neutral. A negatively charged defect compensates for the positive charge in at least some E' sites. Since the appearance of deep electron traps coincides with the appearance of paramagnetic E' centers, a link between E' centers and the deep electron traps is strongly suggested.

Note added in proof. After submission of this letter, we became aware of backgate threshold measurements of Ouisse *et al.* [13] on SIMOX transistors which suggest the presence of deep electron traps and a radiation induced enhancement in their density or cross section.

This work has been supported in part by the Defense Nuclear Agency and the Office of Naval Research (Grant No. N00014-89-J-2022).

[1] A. Abrigam and B. Bleaney, in *Electron Paramagnetic Resonance of Transition Ions* (Oxford University Press, Oxford, 1970).
[2] J. F. Conley, P. M. Lenahan, and P. Roitman, *Procceedings of the 1990 IEEE SOS/SOI Technology Conference* (IEEE, New York, 1990), R164.
[3] J. F. Conley, P. M. Lenahan, and P. Roitman, Bull. Amer. Phys. Soc. **36**, 620 (1991).
[4] J. F. Conley, P. M. Lenahan, and P. Roitman, *Proceedings of the Insulating Films on Semiconductors (INFOS) Conference*, Liverpool, April, 1991, edited by W. Eccleston (Hilger, Bristol, 1991), p. 259.
[5] J. F. Conley, P. M. Lenahan, and P. Roitman, IEEE Trans. Nucl. Sci. **38**, 1247 (1991).
[6] A. Stesmans, R. A. B. Devine, A. Revesz, and H. Hughes, IEEE Trans. Nucl. Sci. **37**, 2008 (1990).
[7] J. F. Conley, P. M. Lenahan, and P. Roitman, *Proceedings of the IEEE SOI Technology Conference, 1991* (IEEE, New York, 1991), p. 12.
[8] P. M. Lenahan and P. V. Dressendorfer, J. Appl. Phys. **55**, 3495 (1984).
[9] Z. A. Weinberg, W. C. Johnson, and M. A. Lampert, J. Appl. Phys. **47**, 248 (1976).
[10] P. S. Winokur and M. M. Sokoloski, Appl. Phys. Lett. **28**, 627 (1976).
[11] R. J. Powell and G. F. Derbenwick, IEEE Trans. Nucl. Sci. **18**, 99 (1971).
[12] H. E. Boesch, Jr., T. L. Taylor, L. R. Hite, and W. E. Bailey, IEEE Trans. Nucl. Sci. **37**, 1982 (1990).
[13] T. Ouisse, S. Christoloveanu, and G. Borel, IEEE Electron. Devices Lett. **12**, 312 (1991).

Nitrided Oxide and Reoxidized Nitrided Oxide Publications

I.A. Chaiyesena, P.M. Lenahan, and G.J. Dunn, "Identification of a Paramagnetic Nitrogen Dangling Bond Defect in Nitrided Silicon Dioxide Films on Silicon", Appl. Phys. Letter 58, 2141 (1991)

I.A. Chaiyesena, P.M. Lenahan, and G.J. Dunn, Electron Spin Resonance Investigation of the Trapping in Reoxidized Nitrided Silicon Dioxide" to be published in The Journal of Applied Physics, July 15, 1992

Identification of a paramagnetic nitrogen dangling bond defect in nitrided silicon dioxide films on silicon

I. A. Chaiyasena and P. M. Lenahan
The Pennsylvania State University, University Park, Pennsylvania 16802

G. J. Dunn
Lincoln Laboratory, Massachusetts Institute of Technology, Lexington, Massachusetts 02173

(Received 8 November 1990; accepted for publication 16 February 1991)

We report the first observation of a nitrogen dangling bond center in nitrided thermally grown silicon dioxide films on silicon. Interpretation of the ^{14}N hyperfine parameters indicates that the unpaired electron wave function is strongly localized on the central nitrogen and that the wave function is highly p in character.

Implementation of nitrided oxide as the gate dielectric in metal-oxide-semiconductor field-effect transistors (MOSFETs) has been shown to significantly improve resistance to channel hot-carrier degradation.[1-3] Lifetime improvements of many orders of magnitude (versus conventional oxide devices) have been demonstrated. This is due to the virtually complete suppression of interface state generation, which dominates oxide n-MOSFET degradation under static bias stress.[4] Hot-carrier degradation in nitrided oxide devices, both n-channel[1] and p-channel,[3] is due predominantly to electron trapping on nitridation-induced electron traps.[5]

In this letter we report the first observation of a nitridation-induced point defect in nitrided thermal oxide films on silicon. The point defect involves an unpaired spin on a bridging nitrogen atom. High densities ($\sim 10^{13}/cm^2$) are rendered paramagnetic by exposing the nitrided oxide films to vacuum ultraviolet (VUV) illumination ($hc/\lambda \lesssim 10.2$ eV) from a 50 W deuterium lamp. These paramagnetic centers are not detectable in ordinary oxides or in reoxidized nitrided oxides subjected to identical VUV illumination. Since it is well established that the nitridation process creates substantial densities of electron traps and that subsequent reoxidation considerably diminishes the densities of these traps, our observations suggest that these centers play an important role in electron trapping. Our observations provide the first direct experimental evidence regarding changes in the structure of point defects in nitrided and reoxidized nitrided oxides.

The nitrided oxide films used in this study were prepared by thermal nitridation of silicon dioxide films on high-resistivity ($\rho \sim 50$–$100\ \Omega$ cm) n-type silicon with (100) surface orientation. Before oxidation, a sacrificial oxidation and etch was performed. Oxides 945 Å thick were grown in dry oxygen at 1000 °C; after oxidation the wafers were given a 10 min anneal in nitrogen at 1000 °C. Thermal nitridation of some of the oxides was carried out in pure ammonia (NH_3) at 1100 °C for 30 min; after nitridation, the wafers were given an additional 10 min 1000 °C nitrogen anneal. Nitridation did not significantly alter the dielectric thickness. Some nitrided oxides were subjected to reoxidation in dry oxygen at 1100 °C for 60 min resulting in a reoxidized nitrided oxide thickness of 952 Å. Nitridation results in the incorporation of nitrogen and hydrogen into the films.[6-8] Reoxidation reduces the concentration of these elements.[6-8] Samples used in these experiments consisted of 4×20 mm^2 bars cut from the wafers with the (110) direction corresponding to the long side. The sample edges were etched in a buffered HF solution to eliminate any resonance signals caused by mechanical damage in the edge regions. (The flat surfaces of the samples were masked during the etch.)

Electron spin resonance (ESR) measurements were performed using a Bruker ER-200 series X-band spectrometer with a TE_{104} "double" cavity. Absolute spin concentration measurements were obtained by comparing unsaturated absorption spectra from the sample with those of a calibrated weak pitch standard. We estimate that the accuracy of our spin concentration measurements is better than a factor of 2 in absolute number and within $\pm 10\%$ in relative number. High-frequency (1 MHz) capacitance versus voltage measurements were made on samples treated identically to those used for ESR. A mercury probe provided a temporary gate contact to the surfaces of the films.

Samples were exposed to vacuum ultraviolet light using a McPherson model 632 deuterium lamp ($hc/\lambda \lesssim 10.2$ eV with an intense peak at 10.2 eV). ESR results for identical (12 h) illuminations (identical sample size and spectrometer settings) are illustrated in Fig. 1. Zero crossing g values are indicated at the bottom of the figure. The g value is defined as $g = h\nu/\beta H$, where h is Planck's constant, ν is microwave frequency, β is the Bohr magneton, and H is the magnetic field. Traces (a), (b), and (c) were taken on oxides, nitrided oxides, and reoxidized nitrided oxides, respectively. A weak E' resonance ($g = 2.0004$) and a somewhat stronger P_{b0} resonance ($g = 2.0059$) appear in oxide trace (a). The E' center is an unpaired electron on a silicon bonded to three oxygens,[9,10] almost certainly a hole trapped in an oxygen vacancy.[10,11] The P_{b0} center is a silicon bonded to three other silicons at the Si/SiO_2 interface.[12] P_b centers are the dominant interface defect centers in MOS devices.[12-14]

Trace (b) was taken on a nitrided oxide; a broad three peaked spectrum is clearly evident. Within experimental error, the line shape is independent of signal amplitude. Within experimental error, the line shape is also independent of sample orientation with respect to magnetic field

 0003-6951/91/192141-03$02.00

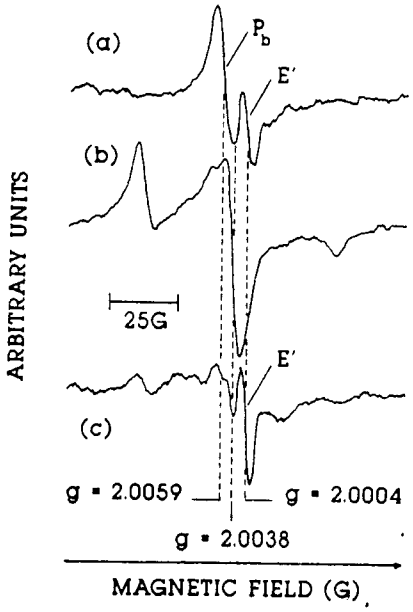

FIG. 1. ESR traces taken on VUV illuminated (a) silicon/silicon dioxide structures, (b) silicon/nitrided oxide structures, and (c) silicon/reoxidized nitrided oxide structures. Spectrometer settings, sample size and geometries, and magnetic field orientation (perpendicular to the Si/SiO_2 interface) are identical in all three traces. Only trace (b) exhibits a strong three peaked signal which is indicative of a bridging nitrogen center.

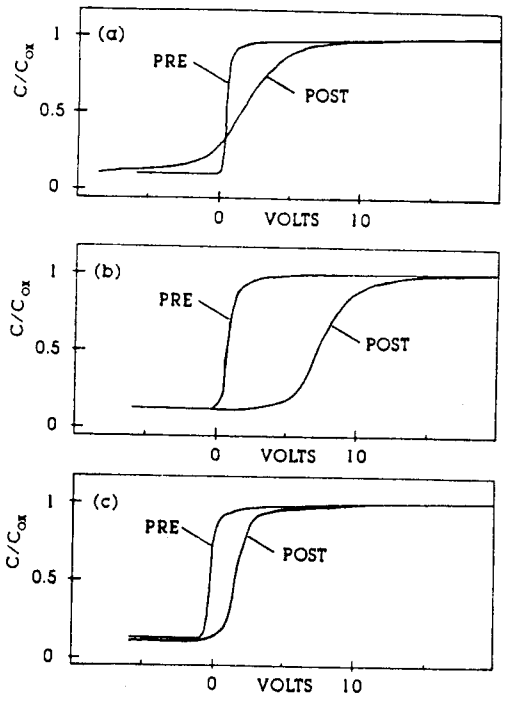

FIG. 2. Capacitance vs voltage (CV) curves taken on samples before and after VUV illumination: (a) silicon/silicon dioxide structures, (b) silicon/nitrided oxide structures, and (c) silicon/reoxidized nitrided oxide structures.

direction. [The P_{b0} trace of Fig. 1(a) *is* orientation dependent since its unpaired spins reside in orbitals which point along (111) directions of the silicon substrate. Defects in the amorphous insulator yield an orientation independent line shape.] A three line ESR spectrum is characteristic of a near 100% abundant nuclear spin of unity. These films contain significant amounts of four elements: hydrogen (nuclear spin of 1/2), silicon (95% spin zero nucleus, 5% spin 1/2 nucleus), oxygen (nuclear spin zero), and nitrogen (99.6% abundant nuclear spin of unity). We may conclude with virtual certainty that the ESR spectrum involves an unpaired spin associated with a nitrogen atom.

Trace (c) of the reoxidized samples shows a greatly reduced (barely visible) nitrogen center as well as a weak E' signal.

The spectrum of trace 1(b) (nitrided oxide) is quite similar to an ESR spectrum first observed by Mackey *et al.*[15] in sodium silicate glasses containing significant amounts of nitrogen. It is also *somewhat* similar to an ESR spectrum recently reported by Warren *et al.*[16] in silicon nitride films. As discussed by Mackey *et al.*[15] and Warren *et al.*[16] line shapes of this form are clearly indicative of unpaired electrons highly localized ($\sim$70%) on the central nitrogen with an electron wave function which is almost entirely p in character. As Mackey *et al.* were first to point out, following the earlier arguments of Walsh,[17] such wave functions are almost certainly due to a bridging nitrogen center. (A bridging nitrogen center consists of an unpaired spin on a nitrogen atom which is bonded to only two other atoms; whether the two atoms are silicons or oxygens is not certain.) The ESR trace of Fig. 1(b) indicates a spin density of approximately $1.2\times10^{13}/cm^2$.

In Fig. 2 we compare pre- and post-illumination capacitance versus voltage (CV) measurements using samples illuminated in a manner identical to that utilized in the measurements of Fig. 1. Traces (a) of the ordinary oxide demonstrate that the post-illumination curve is "stretched out" considerably with respect to the unilluminated control—a qualitative indication of interface state generation. The post-illumination CV curve is also shifted to slightly more negative voltage, indicating a small amount of positive charge buildup. Traces (b) of the nitrided oxide show that the post-illumination curve is shifted substantially towards a positive voltage, indicating electron trapping. Traces (c) of the reoxidized nitrided oxide show that the post-illumination curve is neither "stretched out" nor shifted significantly, indicating very little interface state generation and little charge buildup.

Etchback measurements demonstrate that the paramagnetic centers are distributed throughout the dielectric and that the concentration is strongly peaked near the surface. A similar distribution of nitrogen has been noted in earlier Auger studies of nitrided oxide films;[6–8] however, this similarity could be coincidental. This distribution of paramagnetic centers may match that of pre-existing precursors or may arise because the photon absorption (at least near $hc/\lambda \simeq 10.2$ eV) is primarily near the insulator/air surface.

The high concentration of paramagnetic centers near the air/insulator surface makes a quantitative comparison of space-charge (CV) measurements and ESR measurements ambiguous.

In order to obtain some indication of the charge trapping properties of these centers, we have injected electrons

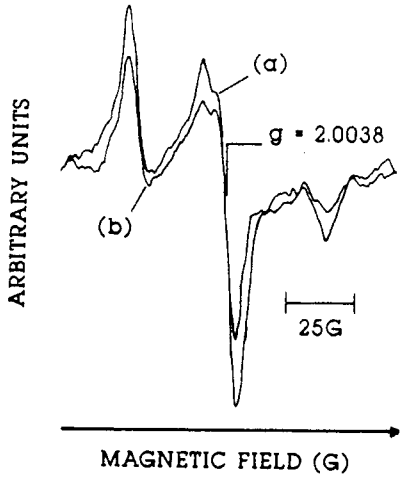

FIG. 3. ESR traces taken on VUV illuminated oxynitrides (a) before and (b) after electron injection. (Identical spectrometer settings.)

into VUV illuminated nitrided oxides using a corona biasing technique. We have applied a positive corona bias of approximately 20 V across the nitrided oxide films and then exposed the films to ultraviolet illumination from a 100 W mercury xenon lamp ($hc/\lambda \lesssim 5$ eV). After a few seconds of illumination, electrons photoinjected from the silicon neutralize the corona charge. (The corona ion potential is measured with a Kelvin probe electrostatic voltmeter.) We find that these brief exposures do not generate detectable spin densities in unbiased (previously unilluminated) samples. The process is repeated approximately 100 times for an injected electron flux of approximately $5\times10^{14}/\text{cm}^2$. As Fig. 3 shows, the electron injection process significantly reduces the paramagnetic nitrogen signal. Apparently the paramagnetic nitrogen centers are capturing electrons, and are rendered diamagnetic by electron capture. Although *CV* measurements after electron injection consistently indicate the presence of net negative charge in the oxide the high concentration of paramagnetic centers near the surface did not allow a quantitative comparison of space charge and ESR measurements.

In conclusion, we report the first observation of a nitridation-induced paramagnetic bridging nitrogen center in nitrided oxides; the unpaired spin resides primarily on the central nitrogen and the electron wave function is almost entirely *p* in character. The center is rendered paramagnetic by exposing the samples to vacuum ultraviolet light. The mechanism by which these centers are rendered paramagnetic is not yet clear, nor are the electronic properties of these centers convincingly established. However, we have made a number of observations which suggest that these centers play an important (probably dominant) role in electron trapping. Three observations are particularly significant. (1) VUV illumination creates both substantial trapped electron density and spin density only in the nitrided oxides. (2) The nitrogen defect is generated in large quantity only in the nitrided oxides; it is not present in significant numbers in thermal oxides or reoxidized nitrided oxides. This is consistent with the behavior of electron traps; nitrided oxides contain high densities of electron traps; reoxidized nitrided oxides and oxides contain small numbers of electron traps. (3) The spin density decreases approximately 30% when substantial numbers of electrons are injected into the oxide. We tentatively conclude that the nitrogen centers are rendered diamagnetic by electron capture. Experiments which may eventually provide a more conclusive identification of the electronic properties of this center are now in progress.

This work has been sponsored by the Office of Naval Research. We wish to acknowledge useful discussions with Dr. William L. Warren, Dr. Mark A. Jupina, and Dr. Peter Wyatt.

[1] G. J. Dunn and S. A. Scott, IEEE Trans. Electron Devices **37**, 1719 (1990).
[2] B. S. Doyle and G. J. Dunn, Electron Device Lett. (to be published).
[3] G. J. Dunn and J. T. Krick, IEEE Trans. Electron Devices **38**, 901 (1991).
[4] P. Heremans, R. Bellens, G. Groeseneken, and H. E. Maes, IEEE Trans. Electron. Devices **35**, 2194 (1988).
[5] F. L. Terry, P. W. Wyatt, M. L. Naiman, B. P. Mathur, C. T. Kirk, and S. D. Senturia, J. Appl. Phys. **57**, 2036 (1985).
[6] F. H. P. M. Habraken, A. E. T. Kuiper, Y. Tamminga, and J. B. Theeten, J. Appl. Phys. **53**, 6996 (1982).
[7] S. S. Wong, S. H. Kwon, H. R. Grinolds, and W. G. Oldham, in *Proceedings of the Symposium on Silicon Nitride Thin Insulating Films*, edited by V. J. Kapoor and H. J. Stein (Electrochemical Society, Pennington, NJ, 1983), Vol. 83-8, p. 346.
[8] H. Hori, W. Iwasaki, and K. Tsuji, IEEE Trans. Electron Devices **35**, 904 (1988).
[9] R. H. Silsbee, J. Appl. Phys. **32**, 1459 (1961).
[10] F. J. Feigl, W. B. Fowler, and K. L. Yip, Solid State Commun. **15**, 479 (1974).
[11] P. M. Lenahan and P. V. Dressendorfer, J. Appl. Phys. **55**, 3495 (1984).
[12] E. H. Poindexter, P. J. Caplan, B. E. Deal, and R. R. Razouk, J. Appl. Phys. **52**, 879 (1981).
[13] Y. Nishi, T. Tanaka, and A. Ohwada, J. Appl. Phys. **11**, 85 (1972).
[14] P. M. Lenahan and P. V. Dressendorfer, J. Appl. Phys. **54**, 1457 (1983).
[15] J. H. Mackey, J. W. Boss, and M. Kopp, Phys. Chem. Glasses **11**, 205 (1970).
[16] W. L. Warren, P. M. Lenahan, and S. E. Curry, Phys. Rev. Lett. **65**, 207 (1990).
[17] A. D. Walsh, J. Chem. Soc. **466**, 2260 (1953).

Electron spin resonance investigation of hole trapping in reoxidized nitrided silicon dioxide

I. A. Chaiyasena and P. M. Lenahan
Department of Engineering Science and Mechanics, The Pennsylvania State University, University Park, Pennsylvania 16802

G. J. Dunn
Lincoln Laboratory, Massachusetts Institute of Technology, Lexington, Massachusetts 02173

(Received 21 October 1991; accepted for publication 10 April 1992)

Radiation-induced hole trapping in reoxidized nitrided silicon dioxide (RNO) was studied with electron spin resonance spectroscopy. It is demonstrated that the dominant hole trap in RNO is not the well known E' center of conventional oxides. This finding confirms our earlier speculation, based on detrapping experiments, that the dominant hole trap in RNO is a species distinctly different from that in conventional oxide.

Metal-oxide-semiconductor field effect transistors (MOSFETs) which incorporate reoxidized nitrided oxide (RNO) as the gate dielectric can exhibit radiation hardness superior to conventional "hard" oxides.[1] Complete suppression of interface state generation and rapid annealing of trapped holes are characteristic of RNO. These attributes provide virtual immunity to ionizing radiation at relatively low dose rates, such as occurs in the natural space environment. However, at higher dose rates, hole trapping and consequent threshold voltage shift are important concerns.[1] In particular, RNO MOSFETs irradiated under negative gate bias can exhibit significant threshold shift due to the efficient trapping of holes near the gate/dielectric interface.[1,2]

In an earlier publication[1] we reported on the distinct annealing behavior of trapped holes in RNO. It is well known that holes trapped near the interface in conventional SiO_2 detrap by tunneling.[3] This mechanism is enhanced by positive applied bias, which lowers the trapezoidal tunneling barrier. In RNO, however, the detrapping of holes at either interface is enhanced by an applied field of either polarity. Similar annealing behaviors were observed for the near-gate and near-substrate trapped holes in RNO, suggesting that the same species of hole trap exists at both interfaces.[1,2] The very different annealing behaviors of trapped holes in RNO versus conventional oxide led us to speculate that the dominant hole trap in RNO may not be the well-known E' center, an oxygen-deficient silicon defect and the dominant hole trap in conventional silicon dioxide.[4,5] In this communication we report on a study to test that speculation.

At 37 nm RNO dielectric was grown on both sides of double-polished 50–100 Ω cm(100) silicon substrates by exposing the wafers to pure dry O_2 at 1000 °C for 36 min, pure NH_3 at 1100 °C for 15 min, and dry O_2 at 1100 °C for 30 min. N_2 purges of the furnace tube were performed between O_2 and NH_3 exposures. This process results in an RNO dielectric with a very high density of near-surface hole traps.[2] (The high density of hole traps yields only a relatively small threshold voltage shift since the traps are so close to the gate.) A negative bias (corresponding to a field of about -2 MV/cm) was applied to the bare RNO dielectric by the corona discharge technique.[6] The potential was evaluated with a commercial Kelvin probe electrostatic voltmeter. Then the samples were exposed to 10.2 eV vacuum ultraviolet (VUV) photons from a filtered deuterium lamp. Photons of this energy have an absorption coefficient of $\sim 10^6$ cm^{-1} in SiO_2; therefore, most of the radiation is absorbed in the top 10 nm of the dielectric surface. The negative corona bias sweeps the radiation-generated holes toward the dielectric surface. Relatively few holes are created in or transported through the substrate interface region of the dielectric.

The corona charging VUV illumination sequence was repeated about ten times. This resulted in high frequency capacitance versus voltage (C-V) curve flatband shifts of about -2.8 V. Virtually all of the C-V shift is eliminated by etching off, in dilute hydrofluoric acid, 8 nm of the irradiated dielectric, indicating, as anticipated, a high density ($\gtrsim 1.5\times 10^{13}$/cm^2) of trapped holes in the upper portion of the dielectric.

The irradiated samples (unetched) were then analyzed using electron spin resonance (ESR) spectroscopy to determine whether the hole traps in RNO are the same as those in conventional oxide, viz., the well-characterized E' center.[4,5] The E' center is an unpaired electron on a silicon bonded to three oxygen and is (in conventional oxides) a hole trapped in an oxygens vacancy. The center is readily identifiable from its narrow characteristic line shape and zero crossing g value of $g=2.0005$. (The g is defined $g=h\nu/\beta H$, where h is Planck's constant, ν is microwave frequency, β is the Bohr magneton, and H is the magnetic field at resonance.)

In Fig. 1 we show two ESR measurements taken at identical nonsaturating microwave power levels. All spectrometer settings were the same and sample geometries were virtually identical. Trace (a) is of a radiation hard oxide containing 10^{11}/cm^2 E' density, as determined by comparison with a calibrated weak pitch standard in a TE_{104} "double" cavity. The spin concentration is accurate

 0021-8979/92/140001-02$04.00

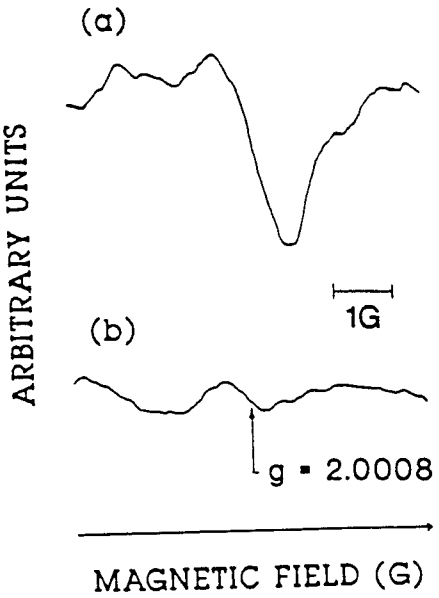

FIG. 1. ESR traces of an RNO and conventional oxide samples. Trace (a) is of a conventional radiation hard oxide sample containing 1×10^{11}/ cm^2 E' centers. Trace (b) is of an RNO sample containing $\geq 1.5 \times 10^{13}$/ cm^2 trapped positive charge within 8 nm of the air/RNO interface. The spectrometer settings are identical for both traces and sample geometries also essentially identical. The traces show that the RNO sample has $\leq 10^{10}$ E' centers/ cm^2.

to better than a factor of 2. The E' centers were generated by a synchrotron x-ray irradiation dose of 3000 mJ/ cm^2. Trace (b) is of an RNO sample with $\geq 1.5 \times 10^{13}$ trapped holes / cm^2 generated by the VUV illumination sequence described above.

Since both traces (a) and (b) were taken at nonsaturating microwave power levels, a comparison of the two traces indicates an RNO E' density of $\leq 1 \times 10^{10}$, three orders of magnitude less than the trapped hole density. This result conclusively demonstrates that the dominant near-gate hole trap in RNO is not the E' center, but an entirely new species.

In an earlier publication,[7] we noted that prolonged (12 h) VUV irradiation of RNO films can generate a weak E' center signal. Our new results do not contradict the earlier observations as the experimental conditions are quite different. The results of this letter involve brief (< 3 min) exposure to VUV illumination from a 10.2 eV filtered deuterium lamp. The earlier results involved (12 h) exposures of more intense unfiltered irradiation from the same deuterium lamp. We estimate that the 3 min exposure corresponds to roughly 10 Mrad of gamma irradiation. (This estimate is based on equivalent hole flux at the surface.) The 12 h exposure corresponds to an extremely heavy accumulated dose.

In summary, we have demonstrated that the dominant hole trap in reoxidized nitrided oxide is not the well known E' center of conventional SiO_2. This is consistent with earlier work[1] which indicated that RNO exhibits hole trapping rate and trapped hole annealing behavior very different from conventional thermal oxides. (We have not as yet been able to identify the defect or defects responsible for hole trapping in these dielectrics nor have we been able to rule out other detects as the principle hole trap.)

This work has been sponsored by the Office of Naval Research. We thank Dr. Peter Wyatt for useful discussions.

[1] G. J. Dunn and P. W. Wyatt, IEEE Trans. NS-36, 2161 (1989).
[2] G. J. Dunn, J. Appl. Phys. 65, 4879 (1989).
[3] T. R. Oldman, A. J. Lelis, and F. B. McLean, IEEE Trans. NS-33, 1203 (1986).
[4] P. M. Lenahan and P. V. Dressendorfer, J. Appl. Phys. 55, 3495 (1984).
[5] H. S. Witham and P. M. Lenahan, IEEE Trans. NS-34, 1147 (1987).
[6] Z. A. Weinberg, D. L. Matthies, W. C. Johnson, and M. A. Lampert, Rev. Sci. Instrum. 46, 201 (1975).
[7] I. A. Chaiyansena, P. M. Lenahan, and G. J. Dunn, Appl. Phys. Lett. 58, 2141 (1991).

APPENDIX A

The E' Center's Hyperfine Spectrum

The first observation of the E' center's hyperfine spectra in a thermal oxide, observed by SDR is shown in Figure 1. The difficulty in observing this spectra in a thermal oxide, even by SDR, is due to its greatly broadened linewidth. The hyperfine spectra was observed in an n-channel device with a (111) silicon substrate orientation. This device is described elsewhere in this report (see page 21) and was subjected to approximately 3 Mrad (SiO_2) of gamma irradiation. Using the standard hyperfine analysis of the E' center in the literature, [1] the percentage of s-character is 26% for an isotropic splitting (A_{iso}) of 471 G and the percentage of p-character is 61% assuming that the localization is 87%.

In an amorphous material, the separation of the hyperfine spectra yields a reliable number for A_{iso} (s-character), since it is measured directly by the separation of the hyperfine lines. However, the greatly broadened hyperfine spectra of the E' center provides a somewhat less reliable measurement of A_{aniso} (p-character) since some of the linewidth may not be due to the amount of p-character[1].

Recently, the hyperfine splitting of the E' center was measured as a function of density in bulk amorphous SiO_2 samples densified under pressure at high temperature.[2] Although A_{iso} is 410G the undensified oxides it was found to be as high as 457G in densified samples. Previous XPS (x-ray photoelectron spectroscopy) studies[3, 4] on oxidized wafers have found that the SiO_2 very near the Si/SiO_2 interface is more densified than bulk SiO_2. Therefore, this value of A_{iso} is consistent with an E' center being in a densified SiO_2 network very near the Si/SiO_2 interface.

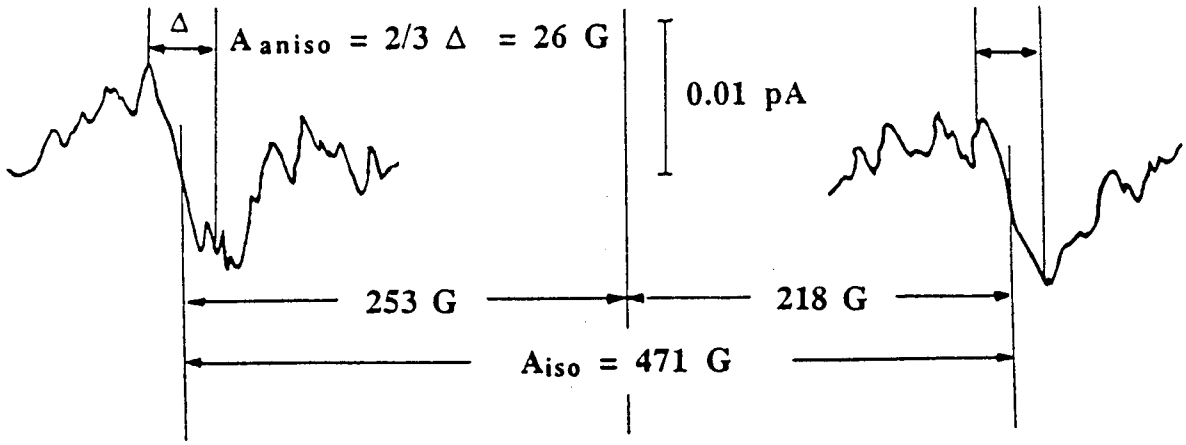

Figure 1 The ^{29}Si hyperfine spectrum of radiation induced E' centers in a MOSFET. The spectrum was obtained through spin dependent recombination. Although the signal to noise ratio is quite poor, the signals are clearly visible and allow for a fairly accurate measure of A_{iso}.

References

1. D. L. Griscom, E. J. Friebele, and G. H. Sigel, Solid State Commun., 15, 479 (1974).

2. R. A. B. Devine and J. Arndt, Phys. Rev., B-37, 6579 (1987).

3. F. J. Grunthaner, P. J. Grunthaner and J. Maserjian, IEEE Trans. Nucl. Sci., NS-29, 1462 (1982).

4. F. J. Grunthaner, B. F. Lewis, N. Zamani and J. Maserjian, IEEE Trans. Nucl. Sci., NS-27, 1640 (1980).